

# In situ production of hybrid N<sub>2</sub>O in dust-rich Antarctic ice

Lison Soussaintjean<sup>1</sup>, Jochen Schmitt<sup>1</sup>, Joël Savarino<sup>2</sup>, J. Andy Menking<sup>3,4</sup>, Edward J. Brook<sup>5</sup>, Barbara Seth<sup>1</sup>, Vladimir Lipenkov<sup>6</sup>, Thomas Röckmann<sup>7</sup>, Hubertus Fischer<sup>1</sup>

<sup>1</sup>Climate and Environmental Physics, Physics Institute and Oeschger Centre for Climate Change Research, University of Bern, Bern, 3012, Switzerland

<sup>2</sup>University Grenoble Alpes, CNRS, IRD, Grenoble INP, INRAE, IGE, Grenoble, 38000, France

<sup>3</sup>Australian Antarctic Program Partnership, Institute for Marine and Antarctic Studies, University of Tasmania, Hobart, Australia

<sup>4</sup>Environmental Research Unit Commonwealth Scientific and Industrial Research Organisation Aspendale, Victoria, Australia

<sup>5</sup>College of Earth, Ocean, and Atmospheric Sciences, Oregon State University, Corvallis, OR 97331, USA

<sup>6</sup>Climate and Environmental Research Laboratory, Arctic and Antarctic Research Institute, Saint Petersburg, 199397, Russia

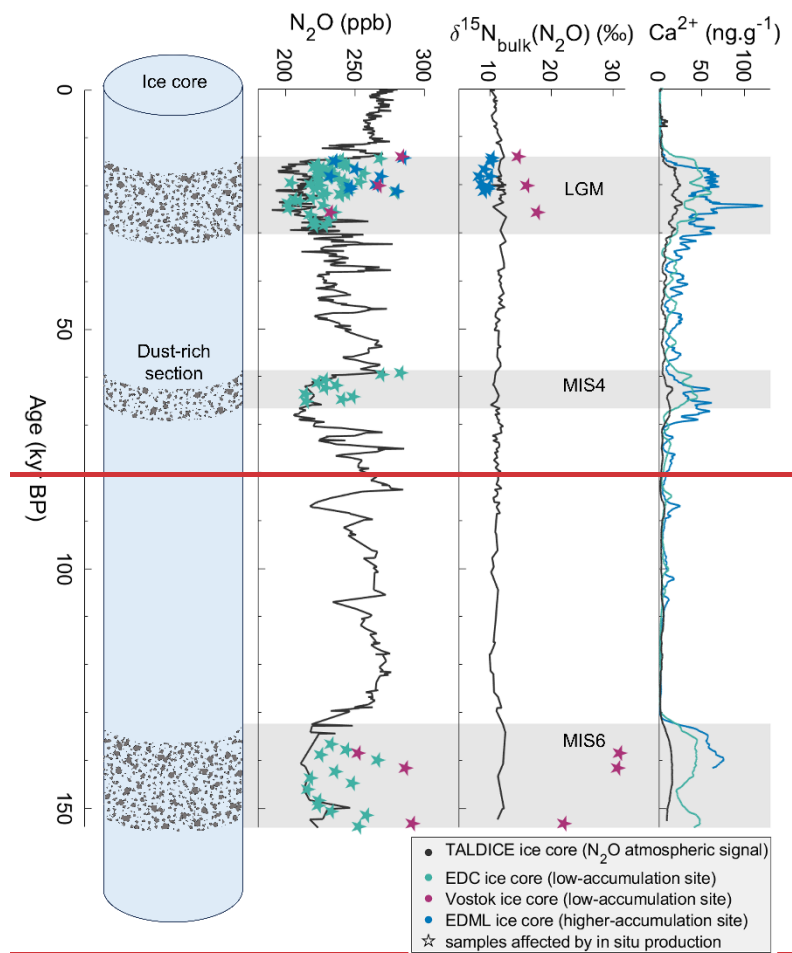
<sup>7</sup>Institute for Marine and Atmospheric research Utrecht (IMAU), Utrecht University, 3584CC Utrecht, the Netherlands

*Correspondence to:* Lison Soussaintjean (lison.soussaintjean@unibe.ch)

**Abstract.** Nitrous oxide (N<sub>2</sub>O) is a potent greenhouse gas involved in the destruction of stratospheric ozone. Past atmospheric mixing ratios of N<sub>2</sub>O are archived in ice cores; however, the presence of in situ N<sub>2</sub>O production in dust-rich Antarctic ice complicates their accurate reconstruction, especially during glacial periods. This production occurs in extremely cold ice and without sunlight. This study aims to understand the reaction producing N<sub>2</sub>O in Antarctic ice by identifying the precursors and the reaction pathway. We compared the oxygen and nitrogen bulk and position-specific isotope composition of in situ N<sub>2</sub>O in ice cores to the isotopic composition of nitrate (NO<sub>3</sub><sup>-</sup>), a possible precursor of N<sub>2</sub>O. The <sup>15</sup>N signature of NO<sub>3</sub><sup>-</sup> is fully transferred into the central N atom (N<sup>α</sup>) of in situ N<sub>2</sub>O, but it is not transferred into the terminal N atom (N<sup>β</sup>), resulting in a 50 % transfer of the <sup>15</sup>N signature of NO<sub>3</sub><sup>-</sup> into the bulk <sup>15</sup>N isotopic composition. These findings suggest that the in situ N<sub>2</sub>O production involves two different nitrogen precursors present in ice: the central N atom (N<sup>α</sup>) originates from NO<sub>3</sub><sup>-</sup> and the terminal N atom (N<sup>β</sup>) from a different precursor not yet identified. Oxygen isotope analysis shows that NO<sub>3</sub><sup>-</sup> cannot be the only reservoir for the O atom of in situ N<sub>2</sub>O. Temperature, pH, and absence of sunlight in Antarctic ice point to an abiotic N-nitrosation reaction. The limiting factor of the reaction is probably associated with mineral dust and might be Fe<sup>2+</sup>, reducing NO<sub>3</sub><sup>-</sup> to NO<sub>2</sub><sup>-</sup> or the precursor of the N<sup>β</sup> atom. The site preference (SP) values of in situ N<sub>2</sub>O are highly variable between different ice cores and depend on the bulk <sup>15</sup>N isotopic composition of N<sub>2</sub>O, itself depending on the <sup>15</sup>N isotopic composition of the NO<sub>3</sub><sup>-</sup> precursor. This finding is unexpected because SP is usually determined by the production pathway through symmetric reaction intermediates that mix the N atoms in α and β positions and average out their isotopic difference. In contrast, our results provide the first evidence of a hybrid N<sub>2</sub>O production pathway involving an asymmetric intermediate that preserves the distinct <sup>15</sup>N signatures of two different precursors – one

35 contributing to the  $N^{\alpha}$  atom and the other to the  $N^{\beta}$  atom. This finding has important implications: in this pathway, SP reflects the isotopic difference between the two precursors rather than the pathway itself, challenging how SP is commonly interpreted in environmental studies.

## 1 Introduction



40

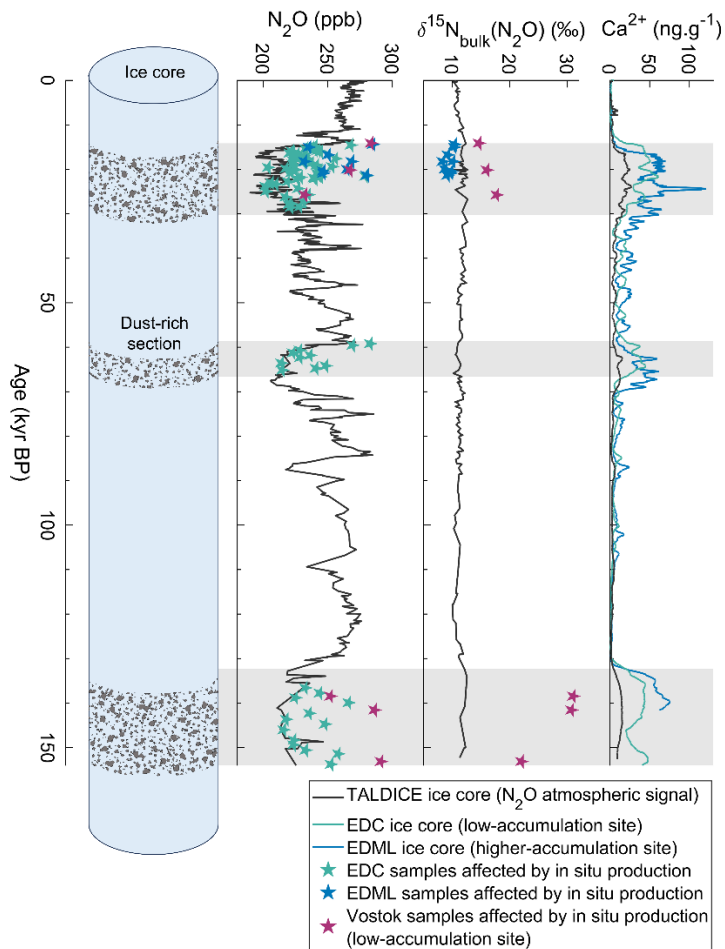


Figure 1.  $\text{N}_2\text{O}$  mixing ratio,  $\text{N}_2\text{O}$  bulk nitrogen isotopic composition, and  $\text{Ca}^{2+}$  concentrations that represent the mineral dust content, measured in the TALDICE (Schilt et al., 2010a), EDC (Schilt et al., 2010b), EDML (Fischer et al., 2019), and Vostok (Miteva et al., 2007) ice cores. Because of its low dust content, the TALDICE record in black is considered to represent the **best estimate of true** atmospheric  $\text{N}_2\text{O}$  levels (see Sect. 3.2.2). Stars correspond to samples affected by in situ production and represent the total  $\text{N}_2\text{O}$  measured, i.e., atmospheric  $\text{N}_2\text{O}$  **plus** in situ  $\text{N}_2\text{O}$ . Grey boxes mark the dust-rich sections of the EDC ice core corresponding to the Last Glacial Maximum (LGM), the Marine Isotope Stage (MIS) 4 and 6 cold periods.

Nitrous oxide ( $\text{N}_2\text{O}$ ) is a potent greenhouse gas whose global warming potential is 273 times higher than that of carbon dioxide ( $\text{CO}_2$ ) on a 100-year timescale (IPCC, 2021). As a result of the anthropogenic alteration of the nitrogen cycle (Gruber and Galloway, 2008), the  $\text{N}_2\text{O}$  atmospheric mixing ratio has risen by 23 % compared to pre-industrial levels (Rubino et al., 2019), reaching 338 ppb in December 2024 (Lan et al., 2025) and contributing around 6 % to the radiative forcing from long-lived greenhouse gases.  $\text{N}_2\text{O}$  is also the primary source of stratospheric nitrogen oxides ( $\text{NO}_x$ ) that destroy ozone (Ravishankara et al., 2009).

55 Soils and aquatic environments are the main sources of atmospheric N<sub>2</sub>O. Production of N<sub>2</sub>O occurs both during denitrification, the reduction of nitrate (NO<sub>3</sub><sup>-</sup>) to nitrite (NO<sub>2</sub><sup>-</sup>) and ultimately molecular nitrogen (N<sub>2</sub>), and as a by-product of nitrification, where ammonium (NH<sub>4</sub><sup>+</sup>) is oxidized to hydroxylamine (NH<sub>2</sub>OH) and then converted to NO<sub>2</sub><sup>-</sup> and NO<sub>3</sub><sup>-</sup> (Baggs, 2011; Bange, 2008). N<sub>2</sub>O is also produced during the reduction of NO<sub>2</sub><sup>-</sup> to N<sub>2</sub>O in nitrifier denitrification, where nitrifying microorganisms reduce NO<sub>2</sub><sup>-</sup> to N<sub>2</sub>O similarly to heterotrophic denitrifiers (Wrage-Mönnig et al., 2018). These reactions are performed by bacteria, archaea and fungi, but abiotic reactions have also been documented (Zhu-Barker et al., 2015). These include chemo-denitrification (Jones et al., 2015; Tischer et al., 2022), which is the reduction of NO<sub>3</sub><sup>-</sup> or NO<sub>2</sub><sup>-</sup> by Fe(II), and NH<sub>2</sub>OH oxidation by Fe(III) or Mn(IV).

The composition of the atmosphere in the past can be reconstructed by analyzing air trapped in polar and high-altitude ice cores. Ice cores are the only direct atmospheric archive and have provided continuous CO<sub>2</sub> and CH<sub>4</sub> records over the last 65 800,000 years covering eight glacial-interglacial cycles (Louergue et al., 2008; Lüthi et al., 2008) and a partial record of N<sub>2</sub>O (Schilt et al., 2010b). In addition to N<sub>2</sub>O mixing ratios, measurement of the stable isotopic composition of N<sub>2</sub>O is used for source attribution of N<sub>2</sub>O emissions. In the current state of the climate system, natural sources account for 57 % of total N<sub>2</sub>O emissions, while anthropogenic sources contribute the remaining 43 % (Tian et al., 2020). Natural sources are approximately 58 % emissions from soils, 38 % from marine ecosystems, and the remaining 4 % from lightning and atmospheric production (Tian et al., 2020). N<sub>2</sub>O emissions from both land and marine ecosystems may have varied in the past. Because sources differ in their isotopic signatures, past changes in terrestrial and marine emissions can be reconstructed using the isotopic composition of N<sub>2</sub>O archived in ice cores (Fischer et al., 2019; Menking et al., 2020; Schilt et al., 2014).

Beyond bulk isotope analyses ( $\delta^{15}\text{N}$  and  $\delta^{18}\text{O}$ ), position-specific measurements provide even more detailed insights into N<sub>2</sub>O production mechanisms. Because N<sub>2</sub>O is an asymmetric molecule, the nitrogen isotopic composition of the two N atoms can deviate from each other, and this difference can be measured separately at the central N atom (N<sup>α</sup>, bonded to oxygen) and the terminal N atom (N<sup>β</sup>). From these values, the site preference (SP =  $\delta^{15}\text{N}^{\alpha} - \delta^{15}\text{N}^{\beta}$ ) can be calculated. Because SP reflects intramolecular isotope partitioning during N-N bond formation, it is primarily controlled by the reaction mechanism and the structure of the last intermediate rather than by the isotopic composition of the precursor (Frame and Casciotti, 2010; Sutka et al., 2003, 2006; Toyoda et al., 2005). As a result, SP values are often characteristic of specific N<sub>2</sub>O formation pathways and can remain constant even when precursor  $\delta^{15}\text{N}$  values vary widely. In contrast to bulk  $\delta^{15}\text{N}$ , which integrates source and fractionation effects, SP provides mechanistic information on how N<sub>2</sub>O is formed and is therefore widely used to discriminate between N<sub>2</sub>O production pathways; SP values are typically negative for bacterial denitrification and positive for nitrification (Toyoda et al., 2017). Using this tool, Prokopiou et al. (2018) showed that SP values increased since preindustrial times, pointing to a relative shift from denitrification to nitrification, consistent with agricultural emissions playing a major role in the N<sub>2</sub>O increase. Similarly, Menking et al. (2025) demonstrated that the increase in N<sub>2</sub>O concentrations during the transition from the Last Glacial Maximum to the Holocene reflected contributions from both nitrification and denitrification, whereas the N<sub>2</sub>O decrease during the Younger Dryas was driven by reduced nitrification.

~~Furthermore, position-specific nitrogen isotope analysis provides an additional constraint for distinguishing N<sub>2</sub>O production pathways (Bernard et al., 2006; Menking et al., 2025; Prokopiou et al., 2017, 2018). This analysis consists of measuring  $\delta^{15}\text{N}$  of the central position N atom ( $\delta^{15}\text{N}^{\alpha}$ ) and the terminal position N atom ( $\delta^{15}\text{N}^{\beta}$ ) in N<sub>2</sub>O. The  $^{15}\text{N}$  site preference ( $SP = \delta^{15}\text{N}^{\alpha} - \delta^{15}\text{N}^{\beta}$ ) is considered to be independent of the  $\delta^{15}\text{N}$  signature of the nitrogen precursor (Frame and Caseiotti, 2010; Sutka et al., 2003, 2006; Toyoda et al., 2005).~~

However, the atmospheric signal of greenhouse gases archived in ice cores can be altered (Anklin et al., 1995; Delmas, 1993; Lee et al., 2020; Mühl et al., 2023). This is particularly true for N<sub>2</sub>O: the N<sub>2</sub>O mixing ratio in glacial period ice from Antarctica shows large scatter between nearby samples from the same core and different values between ice cores for the same age (Fig.1) (Flückiger et al., 2002; Sowers, 2001; Stauffer et al., 2003), which is inconsistent with the homogeneous global atmospheric mixing ratio of N<sub>2</sub>O resulting from its 123-year atmospheric lifetime (Prather et al., 2015) and the low-pass filtering of the atmospheric signal through the slow bubble enclosure process. Because these anomalies were observed for ice core analyses using two distinct gas extraction methods – wet extraction by melting (Schilt et al., 2010b) and dry extraction by grating the ice (Sowers, 2001) – it was concluded that N<sub>2</sub>O production occurred already in the ice sheet and not during the analysis. This “in situ production” or excess N<sub>2</sub>O in dust-rich sections of polar ice cores has two major consequences for the climatic interpretation. First, as the production process has not yet been identified, and the excess N<sub>2</sub>O has not yet been quantified, we do not have access to past atmospheric N<sub>2</sub>O mixing ratios during most past glacial periods (Schilt et al., 2010b), where high dust contents are found in the ice. Secondly, samples affected by in situ production deviate from the isotopic composition of atmospheric N<sub>2</sub>O (Fig.1), which ~~compromises~~~~precludes~~ source attribution (Fischer et al., 2019; Schilt et al., 2014). It is therefore necessary to understand the N<sub>2</sub>O production process(es) in the ice to systematically identify affected samples and thus avoid misinterpretation. Several detection methods were implemented to scrutinize the N<sub>2</sub>O record (Flückiger et al., 2004; Spahni et al., 2005), but they were only used to discard the samples likely to be affected. Understanding the production processes could potentially provide a reliable way of quantifying the fraction of N<sub>2</sub>O produced in situ and to correct the measured signal with the aim to obtain the past atmospheric signal.

This work also has relevance for nitrogen cycle processes in extreme environments. Very few studies have focused on N<sub>2</sub>O production under extreme conditions as those encountered in the Antarctic ice sheet, where temperatures reach down to -60 °C, pressures are enormous, and reaction time scales can be of the order of several thousand years. Priscu et al. (2008) measured very high N<sub>2</sub>O mixing ratios in a permanently ice-covered lake in the Dry Valleys, Antarctica, which they attributed to microbial nitrification. Investigating N<sub>2</sub>O production in Antarctic ice is an opportunity to explore whether microorganisms can be metabolically active at -60 °C. Although previous studies suggested potential N<sub>2</sub>O production by bacteria (Flückiger et al., 2002; Schilt et al., 2010b; Sowers, 2001), there is currently no evidence to support microbial activity in Antarctic ice as a source for in situ N<sub>2</sub>O. High microbial counts have only been found in a few of the Vostok ice core samples where in situ production was reported (Sowers, 2001). ~~Also, A~~ abiotic reactions may ~~also~~ cause N<sub>2</sub>O formation in polar ice. In the Dry Valleys, Antarctica, Samarkin et al. (2010) demonstrated abiotic N<sub>2</sub>O production by chemo-denitrification in the Don Juan Pond soils.

This study uses isotope analysis to characterize in situ N<sub>2</sub>O in various ice cores. The background of the study, the extreme environmental conditions in the polar environment, and the potential consequences for the reactions involved are presented in Sect. 2. ~~The background of the study and the extreme environmental conditions of the reactions involved are presented in Sect. 2.~~ Based on the strong enrichment in <sup>15</sup>N observed in some samples affected by in situ N<sub>2</sub>O production (Fig. 1), we hypothesize that NO<sub>3</sub><sup>-</sup>, which can also be highly enriched in <sup>15</sup>N in ice, is one of the nitrogen precursors for in situ N<sub>2</sub>O. To test this hypothesis, we measured the isotopic composition of N<sub>2</sub>O and NO<sub>3</sub><sup>-</sup> in the same ice core samples and calculated the isotopic signature of in situ N<sub>2</sub>O (Sects. 3 and 4). Position-specific nitrogen isotope analysis of N<sub>2</sub>O was carried out to further constrain the reaction pathway(s) involved. The potential mechanisms for in situ N<sub>2</sub>O production are discussed in Sect. 5.

~~We measured the isotopic composition of N<sub>2</sub>O in several ice cores and calculated the isotopic signature of in situ N<sub>2</sub>O (Sect. 3 and 4). The isotopic composition of NO<sub>3</sub><sup>-</sup> was also measured to identify potential precursors for the produced N<sub>2</sub>O. Position specific nitrogen isotope analysis of N<sub>2</sub>O was carried out to take a closer look into the reaction pathway(s). We discuss the potential reactions for in situ production of N<sub>2</sub>O in Sect. 5.~~

## 2 Background – Potential precursors and reaction rate of N<sub>2</sub>O production in polar ice

For both Greenland and Antarctic ice cores, N<sub>2</sub>O production is inferred in ice-core sections corresponding to glacial periods, while there is no in situ production apparent for the Holocene and other interglacial and interstadial periods (Flückiger et al., 2004; Schilt et al., 2010b). The chemical composition of the ice differs significantly between glacial and interglacial periods, particularly in terms of its mineral dust content. Dust concentrations are significantly higher during glacial periods than during interglacial periods (factor of 30-100) in Antarctic and Greenland ice cores (Fuhrer et al., 1999; Lambert et al., 2012). In fact, N<sub>2</sub>O excess production is only observed in dust-rich ice and, in Antarctica specifically, it increases with higher dust concentrations (Fig. 1). This points to a reaction involving at least one compound contained in or associated with the dust.

The excess N<sub>2</sub>O produced in Antarctic ice is on average 0.4 nmol N.kg<sup>-1</sup>. The main nitrogen compounds that are generally considered as N<sub>2</sub>O precursors are NO<sub>3</sub><sup>-</sup> and NH<sub>4</sub><sup>+</sup>. The typical concentrations of NO<sub>3</sub><sup>-</sup> and NH<sub>4</sub><sup>+</sup> in ice are above 320 nmol N.kg<sup>-1</sup> and 55 nmol N.kg<sup>-1</sup>, respectively (Kaufmann et al., 2010; Röthlisberger et al., 2000a), and therefore more than sufficient to produce the observed excess N<sub>2</sub>O. However, neither NO<sub>3</sub><sup>-</sup> nor NH<sub>4</sub><sup>+</sup> spontaneously react to N<sub>2</sub>O. These precursors need to be activated by a chemical or biochemical agent, such as iron II (Fe<sup>2+</sup>) (Zhu-Barker et al., 2015) or bacteria, respectively. Both Fe<sup>2+</sup> (Spolaor et al., 2012, 2013; Traversi et al., 2004) and bacteria (Miteva et al., 2016; Rohde et al., 2008; Sowers, 2001) were detected in polar ice.

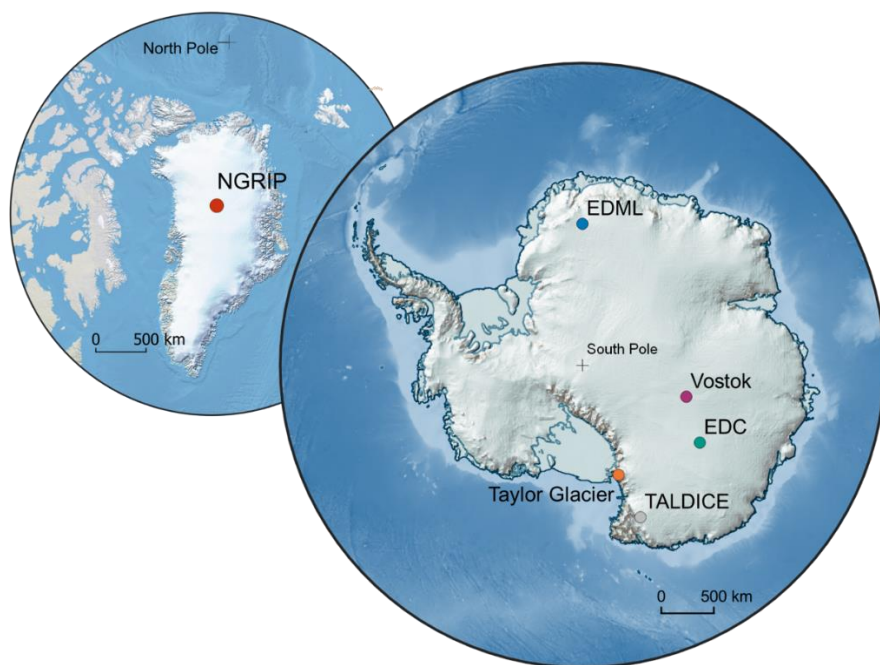
Previous research has shown that samples affected by in situ production exhibit isotopic deviations from the atmospheric signature that differ in both direction and magnitude across ice cores (Fischer et al., 2019; Menking et al., 2025; Schilt et al., 2014; Sowers, 2001). It has been observed that the <sup>15</sup>N signatures of total N<sub>2</sub>O – i.e. atmospheric plus in situ N<sub>2</sub>O – depend

on snow accumulation: sites with low accumulation show enrichment in  $^{15}\text{N}$  compared to the atmospheric signature (Sowers, 2001), while sites with higher accumulation show depletion in  $^{15}\text{N}$  (Fischer et al., 2019) (Fig. 1). A similar dependence of isotopic composition on accumulation rate is observed for  $\text{NO}_3^-$ . The accepted reason is that after deposition some of the  $\text{NO}_3^-$  undergoes photolysis in the photic zone, corresponding approximately to ~~ea.~~ the first meter of the surface snow. Kinetic isotope effects for photolysis favor the loss of the lighter isotopologues (i.e. containing  $^{14}\text{N}$ ), resulting in  $^{15}\text{N}$  enrichment of the remaining  $\text{NO}_3^-$  (Blunier et al., 2005; Frey et al., 2009). The fraction of photolyzed  $\text{NO}_3^-$  and the degree of isotopic enrichment depends on the time  $\text{NO}_3^-$  spends in the photic zone before it is archived in the ice by progressive burial. At low-accumulation sites, the duration within the photic zone is longer and a large fraction of  $\text{NO}_3^-$  is photolyzed leading to a highly  $^{15}\text{N}$ -enriched  $\text{NO}_3^-$  archived in the ice, reaching values of  $\delta^{15}\text{N}_{\text{bulk}} = 300 \text{ ‰}$  at Concordia (Erland, 2011; Erland et al., 2013). In ice core samples affected by in situ  $\text{N}_2\text{O}$  production, the presence of high  $\delta^{15}\text{N}_{\text{bulk}}$  values of  $\text{N}_2\text{O}$  along with  $^{15}\text{N}$ -enriched  $\text{NO}_3^-$  strongly suggests that in situ  $\text{N}_2\text{O}$  production uses N from  $\text{NO}_3^-$ . The isotopic composition of  $\text{NH}_4^+$  has never been measured in Antarctic ice cores, because large amounts of ice are required at the low  $\text{NH}_4^+$  concentrations, and the samples are highly sensitive to  $\text{NH}_3$  contamination (Lamothe et al., 2023). Although a low contamination protocol has been developed by Lamothe et al. (2023), it was used for samples with higher  $\text{NH}_4^+$  concentrations, where the blanks are small compared to the sample concentration. Nonetheless, the hypothesis of  $\text{NH}_4^+$  as an  $\text{N}_2\text{O}$  precursor is discussed in Sect. 5.1.

~~Regarding the reaction rate, t~~The production of  $\text{N}_2\text{O}$  might already start near the surface of the ice sheet, in the snow and firn, but most of the produced  $\text{N}_2\text{O}$  would be lost to the atmosphere via air exchange. In the diffusive zone of the firn column and below the air lock-in depth (Battle et al., 1996), exchange of the firn air with the atmosphere is limited or excluded and the produced  $\text{N}_2\text{O}$  is partly or fully preserved in the ice. To be able to observe in situ  $\text{N}_2\text{O}$  in ice cores, the production must continue close to or below the lock-in depth (located between 50 to 100 m, depending on the location and conditions of the ice sheet). For example, during the LGM at Vostok, Antarctica, the lock-in depth was around 94 m, and the age of the ice at this depth was 5200 years (Table 1). This means that at Vostok,  $\text{N}_2\text{O}$  was still produced several thousand years after the precursors were deposited onto the ice sheet. This observation shows that either it takes time for the precursors to come into contact, for example by diffusion in the ice or ice recrystallization, or that the reaction is very slow due to low temperatures. In the latter case, it would not be possible to reproduce such slow reaction kinetics in the laboratory. This observation also shows that the reaction does not need light.

### 3 Samples and Methods

#### 3.1 Ice core samples



185 **Figure 2. Location of the ice core drilling sites presented in this study. Maps created using the Quantarctica (Matsuoka et al., 2018) and QGreenland (Moon et al., 2023) QGIS data packages.**

To gain a comprehensive understanding of the  $N_2O$  production process(es) in diverse environmental settings, we analyzed ice core samples from different sites with different characteristics: variable dust contents, variable dust chemical compositions, variable snow accumulation rates and therefore isotopic signatures of  $NO_3^-$ , and variable drilling site  
190 temperatures. These characteristics are reported in Table 1. Calcium ( $Ca^{2+}$ ) concentrations are used as a proxy for dust content because they have been found to be correlated with mineral dust concentrations (Ruth et al., 2002). Figure 2 shows the location of the drilling sites.

We analyzed samples from five Antarctic ice cores: the Talos Dome Ice Core (TALDICE), the European Project for Ice Coring in Antarctica (EPICA) Dome C core (EDC), the EPICA Dronning Maud Land core (EDML), the Vostok ice core,  
195 and the main transect of the Taylor Glacier (TG) blue ice area. Additionally, we analyzed samples from one Greenland ice core, the North Greenland Ice Core Project ice core (NGRIP). The TALDICE ice core was selected for its low dust content (and ~~expected~~~~suspected~~ low degree of in situ  $N_2O$ ) compared to other Antarctic ice cores, the EDC and Vostok ice cores for their low snow accumulation rate, the EDML ice core for its relatively higher snow accumulation rate. The NGRIP ice core was analyzed to compare the isotopic signature of in situ  $N_2O$  in Greenland and Antarctic ice. ~~The five latter ice cores were~~

200 ~~obtained from deep drilling and are stratigraphically ordered, with recent layers at the surface of the ice sheet and older layers towards the bedrock. In contrast, the TG blue ice area exposes old ice — flowing from the Taylor Dome — at the surface due to local ice dynamics and ablation (Baggenstos et al., 2018). The TG ice core was sampled close to the surface along a transect where the horizontal stratigraphy is preserved, a so-called “horizontal core.” The age of the ice then varies with distance along this transect.~~

205 We measured the stable isotopic composition ( $\delta^{15}\text{N}_{\text{bulk}}$  and  $\delta^{18}\text{O}$ ) of  $\text{N}_2\text{O}$  in the TALDICE, EDC, EDML, Vostok, TG and NGRIP ice cores, and the stable isotopic composition ( $\delta^{15}\text{N}$  and  $\delta^{18}\text{O}$ ) of  $\text{NO}_3^-$  in all samples except NGRIP. We also carried out position-specific isotope analysis of the central ( $\delta^{15}\text{N}^\alpha$ ) and terminal ( $\delta^{15}\text{N}^\beta$ ) nitrogen atoms in  $\text{N}_2\text{O}$  in the Vostok and TG ice cores.

210 The samples date from either the Last Glacial Maximum (LGM) and glacial-interglacial transition (14 to 29 ka), Marine Isotope Stage 4 (MIS4, 57 to 71 ka), or Marine Isotope Stage 6 (MIS6, 130 to 191 ka), which are all dust-rich glacial periods and are therefore prone to in situ production of  $\text{N}_2\text{O}$ . We selected samples younger than 150 ka because the  $\text{N}_2\text{O}$  atmospheric baseline recorded in the dust-poor TALDICE ice core and used in our mass balance approach (see Sect. 3.2.2) does not extend to older periods.

**Table 1. Characteristics of the ice core drilling sites presented in this study.**

	<b>TG<sup>†</sup></b>	<b>Vostok</b>	<b>EDC</b>	<b>EDML</b>	<b>TALDICE</b>	<b>NGRIP</b>
<b>Latitude (°)</b>	-77.7598 <sup>b</sup>	-78.4642	-75.1000	-75.0019	-72.8302	75.1000
<b>Longitude (°)</b> <a href="https://add.scar.org/">https://add.scar.org/</a>	161.7212 <sup>b</sup>	106.8370	123.3326	0.0663	159.2004	-42.32
<b>Elevation (MSL)</b> <a href="https://add.scar.org/">(https://add.scar.org/)</a>	580	3488	3233	2892	2320 <sup>e</sup>	2917
<b>accumulation rate<sup>*a</sup> in ice equivalent per year (cm)</b>	0.8 <sup>b</sup>	1.2	1.4	3.7	4.5	6.3
<b>Age maximum<sup>a</sup> (ka)</b>	150	408	813	145	343 <sup>d</sup>	125
<b>Annual mean snow surface temperature<sup>*</sup> (°C)</b>	-46 <sup>†</sup>	-66 <sup>c</sup>	-60 <sup>e</sup>	-53 <sup>e</sup>	-44 <sup>e</sup>	-46 <sup>f</sup>
<b>Maximum depth where the <math>\text{N}_2\text{O}</math> production occurred (m)</b>	-	300	400	770	750	1600
<b>Temperature range of the ice where the production occurred (bore hole temperature) (°C)</b>	-	-56.6 - -55.2 <sup>g</sup>	-53.6 - -51.6 <sup>h</sup>	~ -40 <sup>i</sup>	-	-30 - -32 <sup>j</sup>

<b>Ice age – Gas age difference (<math>\Delta</math>age)<sup>*,a</sup> (yr)</b>	3350 <sup>b</sup>	5170	3960	1590	1000	890
<b>Air lock-in depth<sup>a</sup> (m)</b>	29 <sup>†</sup>	94	83	84	70	79
<b>Ca<sup>2+</sup> concentration* (ng.g<sup>-1</sup>) <u><sup>l</sup>) measured by continuous flow analysis (CFA)<sup>k</sup></u></b>	21±15 <sup>b</sup>	-	35±21 <sup>kl</sup>	47±37 <sup>lm</sup>	16±9 <sup>mm</sup>	292±187 <sup>no</sup>
<b><u>Fe concentration* (ng.g<sup>-1</sup>)</u> <u>[measurement technique]</u> <u>Fe<sup>2+*</sup></u> <u>Fe<sup>3+*</sup></u></b>	=	=	<u>~0.5<sup>p</sup> [CFA]</u> <u>~13<sup>p</sup> [ICP-SFMS]</u>	=	<u>~5<sup>q</sup> [CFA]</u> <u>~3<sup>q</sup> [CFA]</u> <u>~2<sup>q</sup> [CFA]</u>	=
<b>Dominant source of dust</b>	Southern South America (SSA) <sup>ot</sup>	SSA <sup>ps</sup>	SSA <sup>qt</sup>	SSA <sup>qt</sup>	SSA <sup>ru</sup>	East Asian deserts <sup>sv</sup>

215

<sup>†</sup>special case: horizontal core. LGM mean snow surface temperature estimated based on  $\delta^{18}\text{O}(\text{H}_2\text{O})$  data. LGM lock-in depth calculated using the Herron-Langway firn model with delta age and temperature inputs for the TG accumulation zone near Taylor Dome (Herron and Langway, 1980).

\*averaged over the period 15 – 30 ka

220 <sup>a</sup>Bouchet et al. (2023)

<sup>b</sup>Baggenstos et al. (2018)

<sup>c</sup>Buiron et al. (2011)

<sup>d</sup>Crotti et al. (2021)

<sup>e</sup>Markle and Steig (2022)

225 <sup>f</sup>Kindler et al. (2014)

<sup>g</sup>Salamatin et al. (1994)

<sup>h</sup>Ritz et al. (1982)

<sup>i</sup>~~Wilhelms et al.~~ Wilhelms et al. (2007)

<sup>j</sup>Tarasov and Peltier (2003)

230 <sup>k</sup>Röthlisberger et al. (2000b)

<sup>kl</sup>Lambert et al. (2012)

<sup>lm</sup>Fischer et al. (2007)

<sup>mm</sup>Schüpbach et al. (2014)

<sup>no</sup>Bigler (2004)

- 235 <sup>P</sup>Traversi et al. (2004)  
<sup>Q</sup>Spolaor et al. (2013)  
<sup>OR</sup>Aarons et al. (2017)  
<sup>PS</sup>Delmonte et al. (2004)  
<sup>QL</sup>Marino et al. (2009)  
240 <sup>RU</sup>Delmonte et al. (2010)  
<sup>RV</sup>Ruth et al. (2003)

## 3.2 N<sub>2</sub>O analysis

### 3.2.1 Measurement of N<sub>2</sub>O mixing ratio and isotopic composition

Prior to analysis, the samples were decontaminated by removing ~5 mm of the outer surface potentially affected by diffusion  
245 of modern air and chemical contaminants. Scraping was performed with a precleaned knife and wearing polyethylene gloves  
to minimize NO<sub>3</sub><sup>-</sup> contamination (see Sect. 3.3).

The mixing ratio and bulk isotopic composition of N<sub>2</sub>O were measured at the University of Bern, Switzerland, using the  
method described in detail in Schmitt et al. (2014). Briefly, the air was extracted by melting the ice core samples with  
infrared light in a glass vessel under high vacuum. Water vapor was removed from the air sample with a cold trap, CO<sub>2</sub> was  
250 removed using Ascarite™, and N<sub>2</sub>O, CH<sub>4</sub>, and other trace gases were separated from the bulk air components (N<sub>2</sub>, O<sub>2</sub>, and  
Ar) using a cold trap filled with activated carbon. N<sub>2</sub>O and CH<sub>4</sub> were then separated on a gas chromatography column, and  
N<sub>2</sub>O was analyzed with an IsoPrime isotope ratio mass spectrometer (IRMS). The results were converted to international  
isotope scales. ~~The air was extracted by melting the ice core samples, N<sub>2</sub>O was purified, analyzed by isotope ratio mass  
spectrometry (IRMS), and the results were converted to international isotope scales.~~ Isotopic compositions are expressed in δ  
255 values where  $\delta = \frac{R_{sample}}{R_{reference}} - 1$ , with R referring to <sup>15</sup>N/<sup>14</sup>N and <sup>18</sup>O/<sup>16</sup>O ratios. The international references are N<sub>2</sub> in air for  
nitrogen and Vienna Standard Mean Ocean Water (VSMOW) for oxygen. The analytical precision of N<sub>2</sub>O mixing ratio,  
δ<sup>15</sup>N<sub>bulk</sub> and δ<sup>18</sup>O values is 3 ppb, 0.3 ‰ and 0.4 ‰ respectively.

~~We analyzed the position-specific isotopic composition of N<sub>2</sub>O from ice core samples at Oregon State University following  
260 gas extraction, IRMS analysis, and data reduction methods described in detail in Menking et al. (2025). We analyzed the  
position-specific isotopic composition of N<sub>2</sub>O from ice core samples at Oregon State University following gas extraction,  
N<sub>2</sub>O purification, IRMS analysis, and data reduction methods described in detail in Menking et al. (2025). Briefly, the air  
was extracted by grating the ice core samples at -60°C to open the enclosed air bubbles (Bauska et al., 2016), i.e., using a so-  
called dry extraction device, without melting the ice. N<sub>2</sub>O was purified and pre-concentrated using a series of progressively  
265 smaller-volume cold traps and gas chromatography separation of the trapped N<sub>2</sub>O from residual CO<sub>2</sub>. Isotopic measurements  
were performed using a Thermo Delta V Plus IRMS, where m/z 44, 45, and 46 and m/z 30 and 31 were monitored~~

simultaneously for N<sub>2</sub>O isotopes and N<sub>2</sub>O fragment (NO) isotopes, respectively. (Bauska et al., 2016) The position-specific isotopic composition of N<sub>2</sub>O, i.e. δ<sup>15</sup>N<sup>α</sup> (central-position N atom), δ<sup>15</sup>N<sup>β</sup> (terminal-position N atom) and site preference (SP), is defined as:

$$\delta^{15}N_{bulk} = \frac{\delta^{15}N^{\alpha} + \delta^{15}N^{\beta}}{2} \frac{\delta^{15} + \delta^{15}N_{\beta}}{2} \quad (1)$$

$$SP = \delta^{15}N^{\alpha} - \delta^{15}N^{\beta} \frac{\delta^{15}N_{\alpha}}{\delta^{15}N_{\beta}} \quad (2)$$

The δ<sup>15</sup>N<sub>bulk</sub>, δ<sup>15</sup>N<sup>α</sup> and δ<sup>18</sup>O values were measured and the δ<sup>15</sup>N<sup>β</sup> and SP values were calculated using Eq. (1) and (2), respectively. The precision of the measurement is 3 ppb for N<sub>2</sub>O mixing ratio, ±0.4 ‰ for δ<sup>15</sup>N<sub>bulk</sub>, ±0.6 ‰ for δ<sup>15</sup>N<sup>α</sup>, ±0.8 ‰ for δ<sup>15</sup>N<sup>β</sup>, ±1.3 ‰ for SP, and ±0.6 ‰ for δ<sup>18</sup>O.

### 3.2.2 Calculation of the mixing ratio and bulk isotopic composition of the in situ N<sub>2</sub>O fraction

The N<sub>2</sub>O mixing ratio and isotopic composition that we measured represent the total N<sub>2</sub>O extracted from the ice cores, i.e., a mixture of atmospheric N<sub>2</sub>O plus any in situ N<sub>2</sub>O. For our study, we need to calculate the mixing ratio and isotopic composition of in situ N<sub>2</sub>O only. To calculate the in situ values from the measured values, we used the following mass balance approach for each sample:

$$[N_2O]_{in\ situ} = [N_2O]_{meas} - [N_2O]_{atm} \quad (3)$$

$$\delta_{in\ situ} = \frac{\delta_{meas} * [N_2O]_{meas} - \delta_{atm} * [N_2O]_{atm}}{[N_2O]_{in\ situ}} \quad (4)$$

where [N<sub>2</sub>O]<sub>meas</sub> is the N<sub>2</sub>O mixing ratio measured in the ice core sample, [N<sub>2</sub>O]<sub>in situ</sub> is the mixing ratio of in situ N<sub>2</sub>O in that sample, and [N<sub>2</sub>O]<sub>atm</sub> is the true atmospheric mixing ratio of N<sub>2</sub>O at the gas age of the sample; the same terminology applies for delta values.

One issue with this mass balance approach is the need to know [N<sub>2</sub>O]<sub>atm</sub> and δ<sub>atm</sub>, given that most N<sub>2</sub>O records are affected by in situ production. We used the N<sub>2</sub>O record from the dust-poor TALDICE ice core, which is the best estimate of an atmospheric baseline. TALDICE is not significantly impacted by in situ N<sub>2</sub>O production but is limited in time reconstruction (~150 ka). Low in situ contribution is supported by the observation that the TALDICE N<sub>2</sub>O mixing ratios during the dust-rich LGM and MIS4 periods generally align with the NGRIP N<sub>2</sub>O mixing ratios, after in situ N<sub>2</sub>O outliers are removed from the NGRIP record (Fig. A1 in Appendix A). Previous studies identified the high-resolution NGRIP record as representative of atmospheric N<sub>2</sub>O variations (Flückiger et al., 2004; Schilt et al., 2010a, 2013). As atmospheric N<sub>2</sub>O mixing ratios are globally homogeneous while in situ N<sub>2</sub>O production is ice-core dependent, the agreement between the TALDICE and NGRIP records supports the atmospheric nature of the TALDICE record. This is particularly significant because the NGRIP and TALDICE ice cores, drilled in Greenland and Antarctica, respectively, have very different chemical compositions that would lead to different in situ production features. To associate each sample with the atmospheric values matching its gas

age, we applied a cubic smoothing spline interpolation with a 2000-year smoothing window to the measured TALDICE data, which has a temporal resolution of approximately 300 years over the LGM and 600 years over MIS4. ~~Only the samples with a mixing ratio difference of more than 15 ppb from the TALDICE spline were used in the mass balance calculation.~~

~~There are several sources of error in our approach, including measurement uncertainties in N<sub>2</sub>O mixing ratios and isotopic composition, uncertainties in the TALDICE N<sub>2</sub>O spline interpolation, and uncertainties in gas age estimates, which in turn impact the chronological alignment between ice cores. We used a Monte Carlo method to assess the uncertainty of reported values, and ran 1000 simulations to determine the mixing ratio and isotopic composition of in situ N<sub>2</sub>O. We varied the variables of Eq. (3) and (4) within their uncertainty ranges (Table B1). The derived uncertainties were calculated as the standard deviation of the results of the 1000 simulations.~~

We acknowledge that there could be a small in situ production of N<sub>2</sub>O in the TALDICE ice core, isotopically undetectable if the isotopic signature of in situ N<sub>2</sub>O is close to the atmospheric one. We conducted a sensitivity study to evaluate the impact of this possibility (Fig. C1 and C2 [in Appendix C](#)). Assuming that N<sub>2</sub>O production is proportional to dust content, we estimated the in situ N<sub>2</sub>O mixing ratios by multiplying the calcium concentrations – used as a dust proxy – by a constant N<sub>2</sub>O production factor. These in situ N<sub>2</sub>O mixing ratios were subtracted from the TALDICE N<sub>2</sub>O mixing ratios to obtain a corrected record that was used in the mass balance approach as an atmospheric baseline. This approach assumes a constant total air content (TAC) across all samples. While variations in TAC affect the conversion from Ca<sup>2+</sup>-based N<sub>2</sub>O estimates (in ng.g<sup>-1</sup>) to mixing ratios (ppb), this effect is relatively minor (within ±10 %) and does not dominate the overall uncertainty in our mass balance calculation. Our sensitivity study varied the production factor from 0 to 1 ppb-N<sub>2</sub>O/ng.g<sup>-1</sup>-Ca<sup>2+</sup> (Fig. C1 and C2 [in Appendix C](#)). A production factor above 0.5 ppb-N<sub>2</sub>O/ng.g<sup>-1</sup>-Ca<sup>2+</sup> is unlikely, as it would result in significantly lower N<sub>2</sub>O mixing ratios in TALDICE compared to NGRIP. Increasing production factors in TALDICE result in isotopic signatures of in situ N<sub>2</sub>O in the other ice cores that are closer to atmospheric values. Importantly, [assuming small production factors even with a small production factor](#) of 0.1 to 0.2 ppb-N<sub>2</sub>O/ng.g<sup>-1</sup>-Ca<sup>2+</sup>, [which represents the upper range of expected values for TALDICE, results in only our findings remain consistent, with](#) minimal changes in regression slopes when comparing the isotopic compositions of in situ N<sub>2</sub>O and NO<sub>3</sub><sup>-</sup>. Thus, we conclude that the interpretations that follow remain valid even if the assumption that TALDICE represents the true atmospheric N<sub>2</sub>O baseline is not entirely [fulfilled accurate](#).

### 3.2.3 Calculation of the position-specific isotopic composition of the in situ N<sub>2</sub>O fraction

We used the same mass balance approach as in Sect. 3.2.3 to calculate the in situ δ<sup>15</sup>N<sup>α</sup> values in the Vostok and TG samples, with Eq. (3) and (4) in which the δ values are substituted with δ<sup>15</sup>N<sup>α</sup>. The in situ δ<sup>15</sup>N<sup>β</sup> values were calculated with Eq. (1) (δ<sup>15</sup>N<sup>β</sup><sub>in situ</sub> = 2 δ<sup>15</sup>N<sub>bulk in situ</sub> - δ<sup>15</sup>N<sup>α</sup><sub>in situ</sub>) and in situ SP values with Eq. (2) (SP<sub>in situ</sub> = δ<sup>15</sup>N<sup>α</sup><sub>in situ</sub> - δ<sup>15</sup>N<sup>β</sup><sub>in situ</sub>). One problem with this approach is that the TALDICE record does not include position-specific information. As the atmospheric reference δ<sup>15</sup>N<sup>α</sup><sub>atm</sub>, we therefore used the average of the values measured by Menking et al. (2025) in samples from the TG

330 ice core during the period 16 to 21 ka, as these values vary little over time during the last glacial period and because t. These TGspecific samples were shown to be unaffected by in situ production by comparison with TALDICE and NGRIP.

### 3.2.4 Uncertainties

335 There are several sources of error in our approach, including measurement uncertainties in N<sub>2</sub>O mixing ratios and isotopic composition, uncertainties in the TALDICE N<sub>2</sub>O spline interpolation, and uncertainties in gas-age estimates – which in turn impact the chronological alignment between ice cores – and potential small in situ production in TALDICE. We used a Monte Carlo method for error propagation by running to assess the uncertainty of reported values, and ran 1000 simulations to determine the mixing ratio and isotopic composition of in situ N<sub>2</sub>O. We varied the variables of Eq. (3) and (4) within their uncertainty ranges (Table B1 in Appendix B). The derived uncertainties were calculated as the standard deviation of the results of the 1000 simulations.

340 As expected, the uncertainty increases for low in situ N<sub>2</sub>O mixing ratios (see Eq. 4). To avoid too large uncertainties, we excluded samples with calculated in situ N<sub>2</sub>O mixing ratios below 20 ppb. This threshold was chosen because a large part of the dataset exhibits in situ mixing ratios below 50 ppb. Applying a higher cutoff would remove a substantial number of samples and significantly limit our ability to investigate in situ N<sub>2</sub>O production processes. For samples with in situ N<sub>2</sub>O mixing ratios close to 20 ppb, the propagated uncertainties are large (up to several tens of per mil). Nevertheless, these samples were included in this study because in situ N<sub>2</sub>O production in ice, although small in absolute mixing ratio, can significantly alter the measured N<sub>2</sub>O isotopic composition (Fig. 3a) and these isotopic deviations should be documented. Characterizing the isotopic signatures of in situ N<sub>2</sub>O across different ice cores is therefore a key objective of this study. Keeping a large number of data points across multiple ice cores, even with uncertainties of a few tens of per mil, provides valuable information on the potential production mechanisms. For Taylor Glacier, in particular, all affected samples exhibit low in situ N<sub>2</sub>O mixing ratios (~20 ppb), so excluding them would prevent us from characterizing this site.

350

### 3.3 Measurement of NO<sub>3</sub><sup>-</sup> concentration and isotopic composition

After wet extraction and dry extraction of N<sub>2</sub>O at the University of Bern and Oregon State University, respectively, the meltwater and melted ice chips from ice-core samples were used for nitrate isotope analysis. To avoid any chemical reaction and hence production or consumption of NO<sub>3</sub><sup>-</sup>, the collected samples were refrozen and stored at -25 °C.

355

To assess the potential contamination impact of the gas extraction techniques on NO<sub>3</sub><sup>-</sup>, we measured the concentration and isotopic composition of NO<sub>3</sub><sup>-</sup> in ultrapure ice samples spiked with a controlled amount of NO<sub>3</sub><sup>-</sup> isotope standard after gas extraction as described above. Additionally, we compared the concentration and isotopic composition of NO<sub>3</sub><sup>-</sup> in duplicate ice core samples, one analyzed directly and the other analyzed after gas extraction (Table D1 in Appendix D). These tests show that the gas extraction techniques do not lead to measurable contamination, loss, or δ<sup>15</sup>N isotopic fractionation of NO<sub>3</sub><sup>-</sup>

360

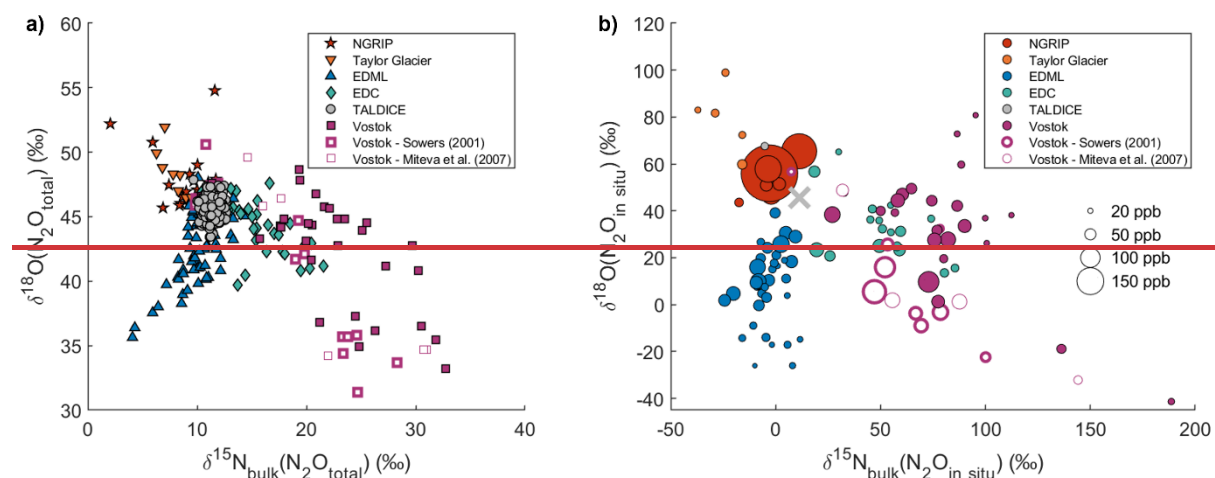
in the collected samples. Although  $\delta^{18}\text{O}(\text{NO}_3^-)$  values are slightly affected, the impact is negligible relative to their typical variability observed in ice cores.

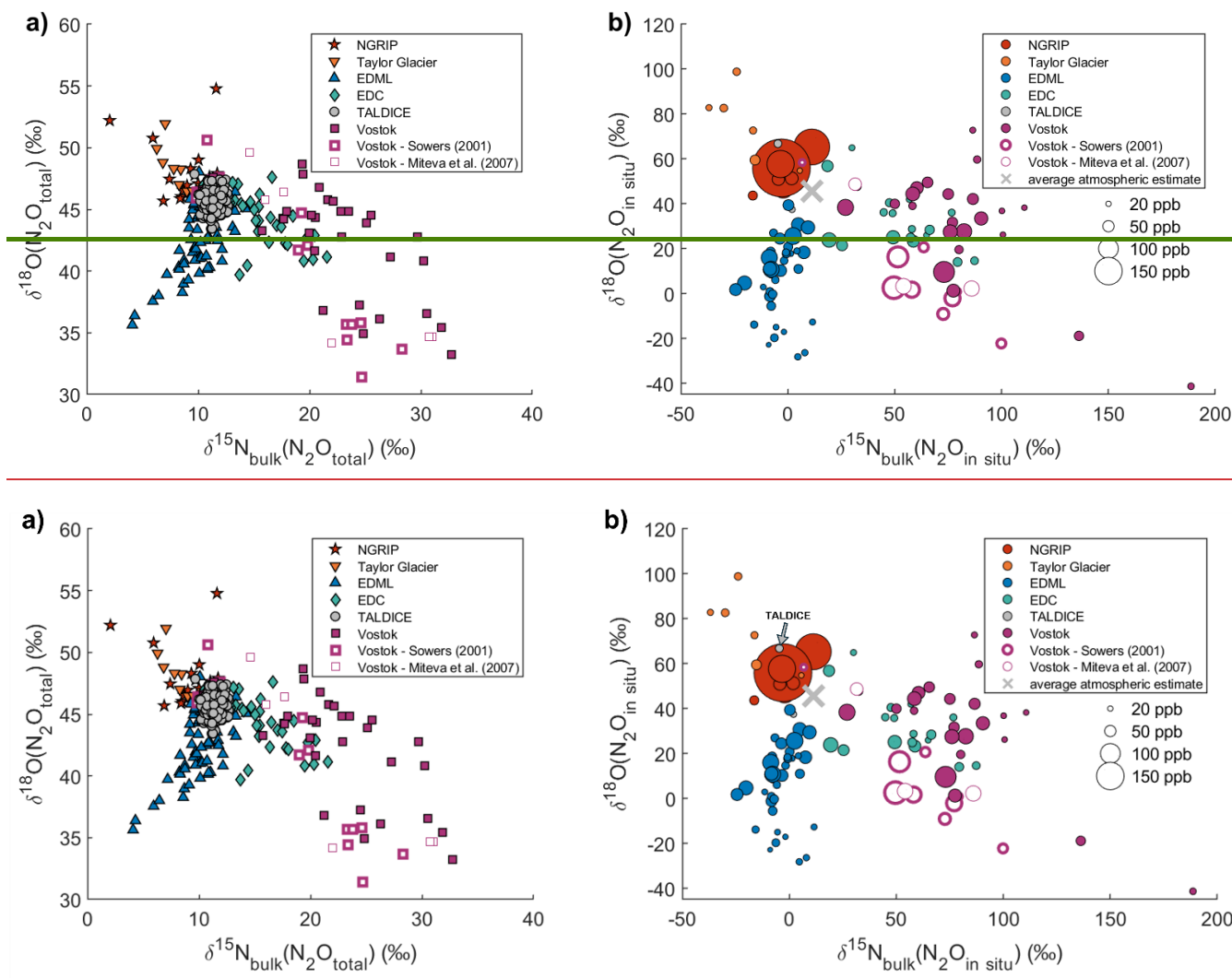
The method used for nitrate isotope analysis is described in detail in previous publications (Erland et al., 2013; Kaiser et al., 2007; Morin et al., 2009).

365 Briefly, the  $\text{NO}_3^-$  concentration was measured by ion chromatography using a Dionex Integriion  
ThermoFischer Scientific IRMS system;  $\text{NO}_3^-$  in the samples was preconcentrated using an AG 1-X8 anion exchange resin in  
the chloride form. After the sample was drained and the  $\text{NO}_3^-$  ions were quantitatively trapped onto the resin,  $\text{NO}_3^-$  was  
eluted from the resin with 6 mL of 1M NaCl solution in three portions of 2 mL.  $\text{NO}_3^-$  was then converted to  $\text{N}_2\text{O}$  through  
bacterial denitrification, using a strain of *Pseudomonas aureofaciens*. The bacteria were injected in 2 mL aliquots into 20 mL  
headspace vials. To remove air and dissolved  $\text{N}_2\text{O}$ , the vials were purged for 3 h with pure helium. The concentrated  $\text{NO}_3^-$   
370 samples were added to the vials in volumes adjusted to obtain 100 nmol of  $\text{NO}_3^-$ , and were allowed to denitrify overnight.  
For isotope analysis, a continuous He flow was used to transfer the produced  $\text{N}_2\text{O}$  from the headspace vial and carry it  
through a purification line. The  $\text{N}_2\text{O}$  sample was passed through columns of perchlorate, Ascarite, and Supelco Purge Trap  
type F to remove water,  $\text{CO}_2$ , and VOCs, respectively. Following this purification step, the purified  $\text{N}_2\text{O}$  was decomposed to  
 $\text{N}_2$  and  $\text{O}_2$  on a gold catalyst kept at 850 °C, and the isotopic compositions of the obtained  $\text{N}_2$  and  $\text{O}_2$  were measured with a  
375 Thermo Fischer MAT 253 IRMS. Briefly,  $\text{NO}_3^-$  in the samples was preconcentrated using an ion exchange resin, then  
converted to  $\text{N}_2\text{O}$  through bacterial denitrification, using a strain of *Pseudomonas aureofaciens*. The resulting  $\text{N}_2\text{O}$  was then  
decomposed to  $\text{N}_2$  and  $\text{O}_2$  on a gold catalyst kept at 850 °C, and the isotopic compositions of the obtained  $\text{N}_2$  and  $\text{O}_2$  were  
measured by IRMS.The results were corrected for blank contribution and calibrated on international scales following the  
procedure described in Erland et al. (2013). Measurement errors are  $\pm 0.8$  ‰ for  $\delta^{15}\text{N}$  and  $\pm 1.0$  ‰ for  $\delta^{18}\text{O}$ .

## 380 4 Results

### 4.1 Bulk isotopic signatures of total $\text{N}_2\text{O}$ and in situ $\text{N}_2\text{O}$





385 **Figure 3. Nitrogen and oxygen isotopic composition of total  $\text{N}_2\text{O}$  measured in samples from different ice cores (a) and nitrogen and oxygen isotopic composition calculated for in situ  $\text{N}_2\text{O}$  in the same samples (b). The mixing ratio of in situ  $\text{N}_2\text{O}$  is represented by the size of the markers. The grey cross represents the average isotopic signature of the TALDICE samples and reflects the isotopic composition of atmospheric  $\text{N}_2\text{O}$ . In panel (b), one TALDICE sample shows in situ  $\text{N}_2\text{O}$  production associated with an exceptionally high dust peak (see Text). Note that the scale of the axes is different for panel (a) and (b).**

390

Figure 3a illustrates the measured isotopic signatures of total  $\text{N}_2\text{O}$  from various ice cores. The TALDICE data, representing atmospheric  $\text{N}_2\text{O}$ , clusters around a mean  $\delta^{15}\text{N}_{\text{bulk}}$  value of  $+11.3 \pm 0.7$  ‰ ( $1\sigma$  standard deviation) and a mean  $\delta^{18}\text{O}$  value of  $+45.7 \pm 0.9$  ‰. These data cover the last 140-kyr interval and their standard deviation is only about two times the measurement error, hence the detectable temporal variability of the isotopic signature of  $\text{N}_2\text{O}$  is small. In contrast, other ice

395 cores show wider ranges, both in  $\delta^{15}\text{N}_{\text{bulk}}$  and  $\delta^{18}\text{O}$ : the deviations from the atmospheric range and relationship with elevated  $\text{N}_2\text{O}$  mixing ratios indicate that these samples are substantially affected by in situ production.

Importantly, the magnitude and direction of deviations from the atmospheric signature are ice core specific. Because the in situ  $\text{N}_2\text{O}$  fraction shapes the observed isotopic deviations, we closely examine the isotopic signature of in situ  $\text{N}_2\text{O}$  in Fig. 3b, which presents the results of our mass balance calculation. Individual samples in the NGRIP ice core in Greenland show the highest in situ  $\text{N}_2\text{O}$  production, up to 380 ppb, while Antarctic ice cores like Vostok, EDML, EDC, and TG show in situ production in the order of 40 ppb, which corresponds to 20 % of the atmospheric  $\text{N}_2\text{O}$  mixing ratios during glacial periods. The isotopic signature of in situ  $\text{N}_2\text{O}$  is highly variable, ranging from -37 ‰ to +189 ‰ for  $\delta^{15}\text{N}_{\text{bulk}}$  and from -41 ‰ to +100 ‰ for  $\delta^{18}\text{O}$ . Not only does in situ  $\text{N}_2\text{O}$  have a distinct isotopic signature in each ice core, it also exhibits a variable isotopic signature within a given ice core. This suggests that the isotopic signature of the precursor(s) varies. Interestingly, all the ice cores except EDML show a negative correlation between  $\delta^{15}\text{N}_{\text{bulk}}(\text{N}_2\text{O}_{\text{in situ}})$  and  $\delta^{18}\text{O}(\text{N}_2\text{O}_{\text{in situ}})$  (Fig. 3b) while EDML shows a positive correlation. ~~This~~

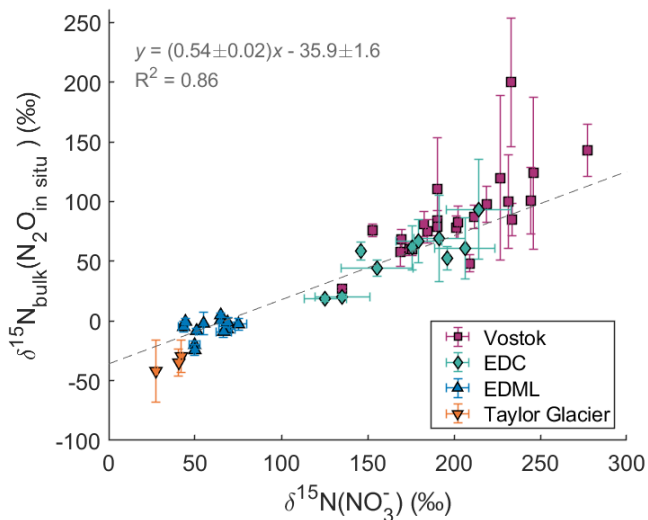
While we used the TALDICE  $\text{N}_2\text{O}$  record to represent atmospheric  $\text{N}_2\text{O}$ , it is important to note that one sample within this ice core record is affected by in situ production (Fig. 3b). By comparison with the TALDICE spline, this particular sample contains 31 ppb of in situ  $\text{N}_2\text{O}$  with a  $\delta^{15}\text{N}_{\text{bulk}}(\text{N}_2\text{O}_{\text{in situ}})$  value of -5 ‰ and a  $\delta^{18}\text{O}(\text{N}_2\text{O}_{\text{in situ}})$  value of +67 ‰. Despite this anomaly, there are compelling reasons to use TALDICE as a reliable record for atmospheric values. Firstly, only one sample out of the 192 measured was found to be affected by in situ production, indicating that such occurrences are rare. Indeed, this sample is characterized by an exceptionally high dust content of 188  $\text{ng}\cdot\text{g}^{-1}$  of  $\text{Ca}^{2+}$ , which is 280 % higher than typical dust peaks observed in the TALDICE ice core during the LGM. Secondly, the amount of in situ  $\text{N}_2\text{O}$  in the affected sample is relatively small compared to this high dust content: it corresponds to a production factor of 0.16 ppb of  $\text{N}_2\text{O}$  per  $\text{ng}\cdot\text{g}^{-1}$  of  $\text{Ca}^{2+}$ , which has little influence on our results, as shown by our sensitivity study (Fig. C2 in Appendix C).

We stress that the mass balance approach used to calculate the isotopic signature of in situ  $\text{N}_2\text{O}$  leads to substantial uncertainties due to error propagation from atmospheric  $\text{N}_2\text{O}$  estimates and analytical precision. These uncertainties are not shown in Fig. 3 for readability but are reported in Figs. 4 – 7 and are explicitly taken into account in the following comparisons between  $\delta^{15}\text{N}(\text{N}_2\text{O}_{\text{in situ}})$  and  $\delta^{15}\text{N}(\text{NO}_3^-)$ , including the regression analyses.

#### 4.2 Comparison of isotopic compositions of $\text{NO}_3^-$ and in situ $\text{N}_2\text{O}$

In this section, we compare the measured isotopic composition of  $\text{NO}_3^-$  and the calculated isotopic composition of in situ  $\text{N}_2\text{O}$  to test our hypothesis that  $\text{NO}_3^-$  is a precursor for in situ produced  $\text{N}_2\text{O}$ . ~~We compare the isotopic composition of  $\text{N}_2\text{O}$  and  $\text{NO}_3^-$  measured in the same ice samples, with  $\text{N}_2\text{O}$  analyzed in the extracted air and  $\text{NO}_3^-$  in the meltwater collected after air extraction. The analyses come from the same ice samples:  $\text{N}_2\text{O}$  was measured in the extracted air and subsequently used to calculate the in situ  $\text{N}_2\text{O}$  isotopic signature, while  $\text{NO}_3^-$  was measured in the sample meltwater collected after air~~

extraction. -To compare the data, we used the regression method by York et al. (2004) that accounts for errors in both the x and y variables and their potential correlation.



430 **Figure 4. Relation between  $\delta^{15}\text{N}_{\text{bulk}}(\text{N}_2\text{O}_{\text{in situ}})$  and  $\delta^{15}\text{N}(\text{NO}_3^-)$ . The dashed line represents the linear regression.**

Figure 4 shows the bulk nitrogen isotopic composition of in situ  $\text{N}_2\text{O}$  and the nitrogen isotopic composition of  $\text{NO}_3^-$  measured in the EDML, EDC, TG and Vostok ice cores. There is a clear positive correlation between  $\delta^{15}\text{N}_{\text{bulk}}(\text{N}_2\text{O}_{\text{in situ}})$  and  $\delta^{15}\text{N}(\text{NO}_3^-)$  with a  $R^2$  value of 0.86 which points to nitrate being a key precursor for the in situ produced  $\text{N}_2\text{O}$ . However, the slope is significantly different from 1, and in fact close to one half ( $0.54 \pm 0.02$ ), i.e., roughly one of the two N atoms of the in situ produced  $\text{N}_2\text{O}$  originates from  $\text{NO}_3^-$ .

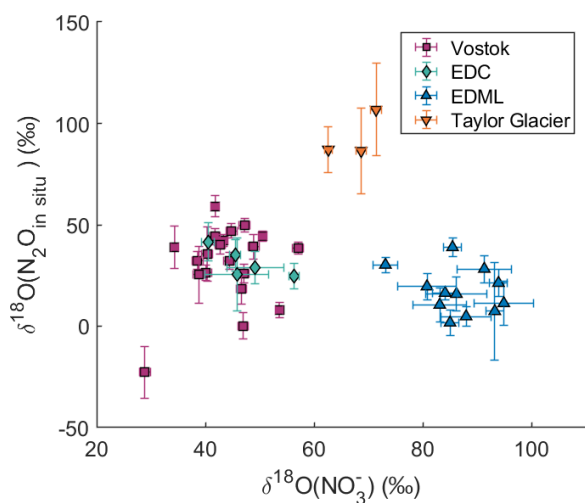


**Figure 5. Relation between  $\delta^{18}\text{O}(\text{N}_2\text{O}_{\text{in situ}})$  and  $\delta^{18}\text{O}(\text{NO}_3^-)$ .**

440

Figure 5 shows the comparison between the  $\delta^{18}\text{O}$  values of  $\text{NO}_3^-$  and in situ  $\text{N}_2\text{O}$ . There is no correlation between these two variables across or within sites, and no general trend towards  $^{18}\text{O}$  enrichment or depletion of in situ  $\text{N}_2\text{O}$  relative to  $\text{NO}_3^-$ . At Vostok and EDC,  $\delta^{18}\text{O}(\text{NO}_3^-)$  values are around  $+45 \pm 6 \text{ ‰}$  ( $1\sigma$ ), while  $\delta^{18}\text{O}(\text{N}_2\text{O}_{\text{in situ}})$  values are approximately  $+31 \pm 17 \text{ ‰}$ . At TG,  $\delta^{18}\text{O}(\text{NO}_3^-)$  values are higher at  $+68 \pm 4 \text{ ‰}$ , and  $\delta^{18}\text{O}(\text{N}_2\text{O}_{\text{in situ}})$  values reach  $+93 \pm 11 \text{ ‰}$ . At EDML,  $\delta^{18}\text{O}(\text{NO}_3^-)$  values are the highest at  $+87 \pm 6 \text{ ‰}$ , whereas  $\delta^{18}\text{O}(\text{N}_2\text{O}_{\text{in situ}})$  values are the lowest, at  $+17 \pm 11 \text{ ‰}$ .

445

The very high  $\delta^{18}\text{O}(\text{N}_2\text{O}_{\text{in situ}})$  values observed at TG may appear anomalous compared to other sites, but we are confident that they do not result from a bias in the measurements or calculation. Even without applying the mass balance calculation, the measured  $\text{N}_2\text{O}$  at TG already shows  $\delta^{18}\text{O}$  values higher than the atmospheric signature in samples affected by in situ production (Fig. 3a). This indicates that the in situ  $\text{N}_2\text{O}$  at TG is indeed enriched in  $\delta^{18}\text{O}$ . A similar enrichment is observed in

450

the NGRIP ice core. Importantly, these elevated  $\delta^{18}\text{O}$  values were measured using two different extraction methods and two different IRMS instruments at the University of Bern and Oregon State University, which strengthens our confidence that the signal is robust and not an artefact of a specific analytical setup.

In summary, despite the clear correlation between  $\delta^{15}\text{N}_{\text{bulk}}(\text{N}_2\text{O}_{\text{in situ}})$  and  $\delta^{15}\text{N}(\text{NO}_3^-)$  values suggesting  $\text{NO}_3^-$  as a precursor, the incomplete transfer of both its nitrogen and oxygen isotopic compositions to in situ  $\text{N}_2\text{O}$  indicates that  $\text{NO}_3^-$  alone does not fully account for the nitrogen and oxygen sources of in situ  $\text{N}_2\text{O}$ . To gain deeper insights into the reaction mechanisms, we turn our focus to the position-specific isotopic composition of in situ  $\text{N}_2\text{O}$ .

455

### 4.3 Site preference of $^{15}\text{N}$ in in situ $\text{N}_2\text{O}$

Figure 6 shows clear correlations of  $\delta^{15}\text{N}^{\alpha}$ ,  $\delta^{15}\text{N}^{\beta}$ , and SP values versus  $\delta^{15}\text{N}_{\text{bulk}}$  of total  $\text{N}_2\text{O}$  (a, c) and in-situ  $\text{N}_2\text{O}$  (b, d) measured in the TG and Vostok.

460

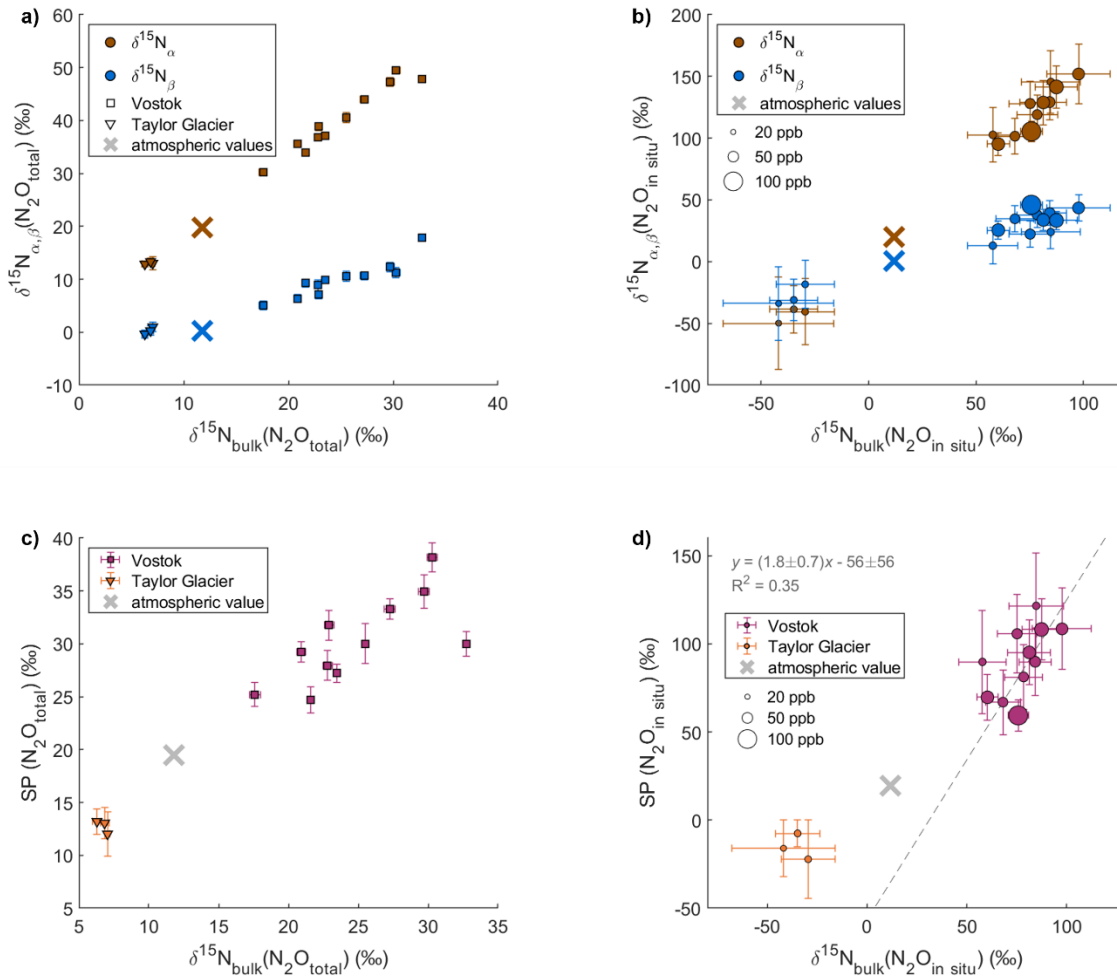


**Figure 6. Position-specific isotopic composition measured for total (atmospheric + in situ)  $N_2O$  and calculated for in situ  $N_2O$  in the Vostok and TG ice cores. The panels show the relation between  $\delta^{15}N^\alpha$ ,  $\delta^{15}N^\beta$  and  $\delta^{15}N_{\text{bulk}}$  of total  $N_2O$  (atmospheric + in situ) (a) and in situ  $N_2O$  (b), and between site preference (SP) and  $\delta^{15}N_{\text{bulk}}$  of total  $N_2O$  (atmospheric + in situ) (c) and in situ  $N_2O$  (d). The size of the markers on panel (b) and (d) are scaled to the amount of in situ  $N_2O$  in the sample. In panel (b), TG samples are in the bottom-left corner. The crosses represent the unaffected atmospheric values measured by Menking et al. (2025) in dust-poor Taylor Glacier samples from the period 16 to 21 ka.**

In situ  $N_2O$  at Vostok exhibits high  $\delta^{15}N^\alpha$  values from +95 ‰ to +152 ‰ and much lower  $\delta^{15}N^\beta$  values from +13 ‰ to +43 ‰. In contrast, in situ  $N_2O$  at TG has low  $\delta^{15}N^\alpha$  values from -50 ‰ to -39 ‰ and low  $\delta^{15}N^\beta$  values from -34 ‰ to -18 ‰, with  $\delta^{15}N^\alpha$  being lower than the  $\delta^{15}N^\beta$  values. The Vostok and TG samples exhibit very different  $SP(N_2O_{\text{in situ}})$  values; +59 ‰ to +122 ‰ and -22 ‰ to -8 ‰, respectively. These values differ significantly from those of atmospheric  $N_2O$  which range in SP from +17 ‰ to +24 ‰ across last glacial termination, as reconstructed from dust-poor sections of TG ice (Menking et al., 2025). The  $SP(N_2O_{\text{in situ}})$  values at Vostok are very high and variable, and are outside the range of typical reported values

475 from -11 ‰ to +37 ‰ (Toyoda et al., 2017; Zhu-Barker et al., 2015). Note that the  $\text{SP}(\text{N}_2\text{O}_{\text{in situ}})$  values at Vostok seem to be correlated to the  $\delta^{15}\text{N}_{\text{bulk}}(\text{N}_2\text{O}_{\text{in situ}})$  values with a slope of  $1.8 \pm 0.7$ , whereas SP values in field and culture studies have been shown to be generally independent of  $\delta^{15}\text{N}_{\text{bulk}}$  (Frame and Casciotti, 2010; Sutka et al., 2003, 2006; Toyoda et al., 2005). For TG, there is too little data to identify a potential correlation.

480 Interestingly, the  $\text{SP}(\text{N}_2\text{O}_{\text{in situ}})$  values at TG are negative. Although the low amounts of in situ  $\text{N}_2\text{O}$  at TG result in large uncertainties in the calculated in situ signatures, the low SP signal is already visible in the measured (total)  $\text{N}_2\text{O}$  data (Fig. 6c), independent of any mass-balance calculation. While Vostok samples affected by in situ production show total SP values higher than the atmospheric signature, TG samples show the opposite pattern, with total SP values lower than the atmospheric signature. This opposite deviation indicates that the low SP values observed at TG reflect a real feature of in situ  $\text{N}_2\text{O}$  production rather than an artefact of the calculation.

485

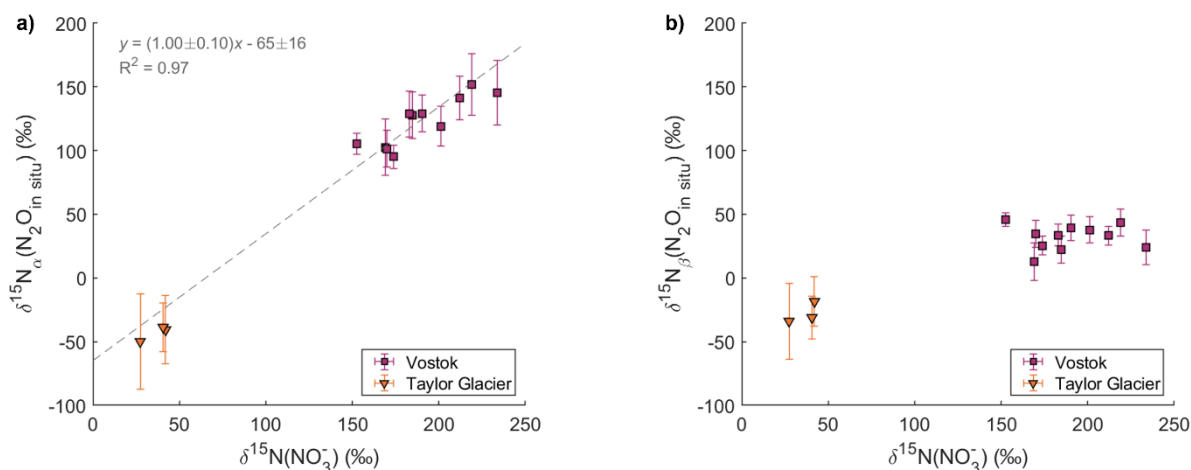


**Figure 7. Relation between  $\delta^{15}\text{N}_{\alpha}(\text{N}_2\text{O}_{\text{in situ}})$  and  $\delta^{15}\text{N}(\text{NO}_3^-)$  (a) and between  $\delta^{15}\text{N}_{\beta}(\text{N}_2\text{O}_{\text{in situ}})$  and  $\delta^{15}\text{N}(\text{NO}_3^-)$  (b).**

490 In Fig. 7, the  $\delta^{15}\text{N}_{\alpha}$  and  $\delta^{15}\text{N}_{\beta}$  values of in situ  $\text{N}_2\text{O}$  are compared with  $\delta^{15}\text{N}$  values of  $\text{NO}_3^-$  measured in the TG and Vostok ice cores. There is a clear positive correlation between  $\delta^{15}\text{N}_{\alpha}(\text{N}_2\text{O}_{\text{in situ}})$  and  $\delta^{15}\text{N}(\text{NO}_3^-)$  with a slope of  $1.0 \pm 0.1$  and an  $R^2$  value of 0.97. This correlation is robust when excluding the TG data. However, there is no statistically significant correlation between  $\delta^{15}\text{N}_{\beta}(\text{N}_2\text{O}_{\text{in situ}})$  and  $\delta^{15}\text{N}(\text{NO}_3^-)$  for the individual sites. In Fig. 7, the  $\delta^{15}\text{N}_{\alpha}$  and  $\delta^{15}\text{N}_{\beta}$  values of in situ  $\text{N}_2\text{O}$  are compared with  $\delta^{15}\text{N}$  values of  $\text{NO}_3^-$  measured in the TG and Vostok ice cores on the same samples. When considering both

495 TG and Vostok samples,  $\delta^{15}\text{N}_{\alpha}(\text{N}_2\text{O}_{\text{in situ}})$  shows a strong positive correlation with  $\delta^{15}\text{N}(\text{NO}_3^-)$  (slope =  $1.0 \pm 0.1$ ,  $R^2 = 0.97$ ). This relationship also holds when considering the Vostok data alone, indicating that the correlation is robust even within a single ice core. In contrast,  $\delta^{15}\text{N}_{\beta}(\text{N}_2\text{O}_{\text{in situ}})$  does not show a statistically significant correlation with  $\delta^{15}\text{N}(\text{NO}_3^-)$  for either site.

## 500 5 Discussion

### 5.1 Production of hybrid N<sub>2</sub>O

The strong correlation between  $\delta^{15}\text{N}_{\text{bulk}}(\text{N}_2\text{O}_{\text{in situ}})$  and  $\delta^{15}\text{N}(\text{NO}_3^-)$  indicates that  $\text{NO}_3^-$  is involved in the in situ N<sub>2</sub>O formation. However, the slope is  $(0.54 \pm 0.02)$  (Fig. 4), whereas a slope of 1 would be expected if both nitrogen atoms in N<sub>2</sub>O originate from  $\text{NO}_3^-$  in the ice. Therefore, our results suggest that in situ N<sub>2</sub>O is not derived from  $\text{NO}_3^-$  alone, and  
505 doesthus not originate from a single precursor (we use the term “single-precursor N<sub>2</sub>O” hereafter, see Fig. 8 Fig. 9). The strong correlation of  $\delta^{15}\text{N}^\alpha(\text{N}_2\text{O}_{\text{in situ}})$  and  $\delta^{15}\text{N}(\text{NO}_3^-)$  with a slope of  $1.0 \pm 0.1$  (Fig. 7a), implies that the central N atom in N<sub>2</sub>O (N<sup>α</sup>), originates exclusively from  $\text{NO}_3^-$  archived in the ice. At the same time, the  $\delta^{15}\text{N}^\beta(\text{N}_2\text{O}_{\text{in situ}})$  values are not correlated to  $\delta^{15}\text{N}(\text{NO}_3^-)$ , indicating that the terminal N atom (N<sup>β</sup>) originates from a different nitrogen source. The slope of the linear regression between  $\text{SP}(\text{N}_2\text{O}_{\text{in situ}})$  and  $\delta^{15}\text{N}_{\text{bulk}}(\text{N}_2\text{O}_{\text{in situ}})$  ( $1.8 \pm 0.7$ ) is consistent, within uncertainty, with transfer  
510 of a variable N isotopic composition from  $\text{NO}_3^-$  to N<sup>α</sup> and transfer of a constant N isotopic composition from another precursor to N<sup>β</sup>. Indeed, by substitution of equations Eq. (1) and (2), one would expect  $\text{SP} = 2 * \delta^{15}\text{N}_{\text{bulk}} - 2 * \delta^{15}\text{N}^\beta$ , where  $\delta^{15}\text{N}^\beta$  is relatively constant within each ice core, although its specific value differs between cores (Fig. 7b). Our results suggest that the N<sub>2</sub>O produced in situ is thus “hybrid N<sub>2</sub>O”, defined by its two nitrogen atoms originating from two distinct nitrogen precursors, one of them being  $\text{NO}_3^-$  in ice (Fig. 8 Fig. 9).

515 To assess whether microbial N<sub>2</sub>O reduction to N<sub>2</sub> could provide an alternative explanation for the observed isotopic patterns of in situ N<sub>2</sub>O – such as high SP values correlated with  $\delta^{15}\text{N}_{\text{bulk}}$  or high  $\delta^{18}\text{O}$  values – we examined the relationship between SP and  $\delta^{18}\text{O}$  in our samples (Fig. 8). Previous studies showed that N<sub>2</sub>O reduction produces a characteristic increase in both SP and  $\delta^{18}\text{O}$  in the residual N<sub>2</sub>O, with data falling along a “reduction line” defined by the ratio of the fractionation factors (median slope  $\approx 0.36$ ; Lewicka-Szczebak et al., 2015; Yu et al., 2020). In contrast, in both the Vostok and Taylor Glacier ice  
520 cores, SP increases while  $\delta^{18}\text{O}$  decreases, and the data clearly do not fall along the expected reduction line (Fig. 8). This dual isotope plot for in situ N<sub>2</sub>O is therefore incompatible with N<sub>2</sub>O reduction. We note that published reduction lines were derived from studies conducted at warmer temperatures than those in ice cores (Yu et al., 2020). Very low temperatures could modify the fractionation factors; however, colder conditions would be expected to increase the fractionation for both SP and  $\delta^{18}\text{O}$ , still resulting in a positive slope. The mismatch between our data and the reduction line therefore remains  
525 regardless of potential temperature effects. A second line of evidence comes from the correlation between  $\delta^{15}\text{N}(\text{NO}_3^-)$  and  $\delta^{15}\text{N}_\alpha(\text{N}_2\text{O}_{\text{in situ}})$ , which shows a slope of  $\sim 1$ . Because N<sub>2</sub>O reduction preferentially breaks N-O bonds of light isotopes, the residual N<sub>2</sub>O becomes enriched in <sup>15</sup>N at the α position, resulting in a steeper slope than observed here. Taken together, these observations show that microbial N<sub>2</sub>O reduction cannot explain the isotopic signatures in the ice cores, and that N<sub>2</sub>O consumption does not occur in the ice. The isotopic signature of in situ N<sub>2</sub>O is therefore explained by hybrid N<sub>2</sub>O  
530 production.

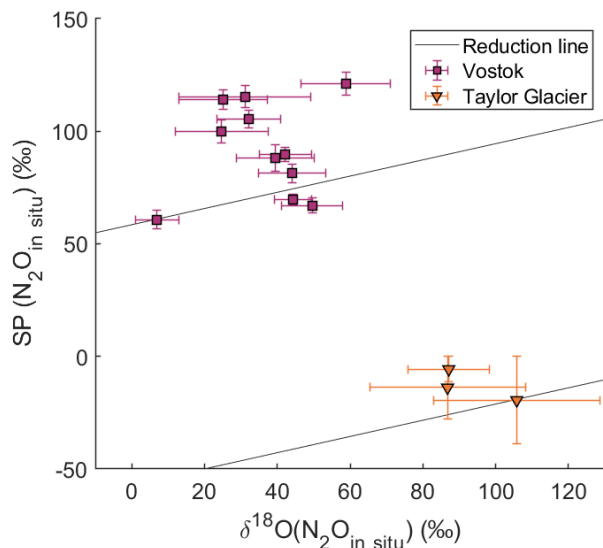


**Figure 8. Dual isotope plot of  $\delta^{18}\text{O}$  and site preference (SP) values of in situ  $\text{N}_2\text{O}$ . Theoretical  $\text{N}_2\text{O}$  reduction lines (thin black lines) are shown for comparison, with intercepts calculated assuming that samples with the lowest SP values are unaffected by  $\text{N}_2\text{O}$  reduction. The slope of the reduction line corresponds to the median of published fractionation ratios for SP versus  $\delta^{18}\text{O}$  during  $\text{N}_2\text{O}$  reduction, as reported by Yu et al. (2020).**

### 5.1.1 Potential reaction pathways

A large number of studies have reported the production of hybrid  $\text{N}_2\text{O}$  through various reaction pathways, including N-nitrosation reactions (Spott et al., 2011) and the decomposition of ammonium nitrate ( $\text{NH}_4\text{NO}_3$ ) (Rubasinghege et al., 2011). N-nitrosation reactions generally involve the replacement of a hydrogen atom on a nucleophilic precursor by a nitroso ( $-\text{N}=\text{O}$ ) group (Spott et al., 2011). Production of  $\text{N}_2\text{O}$  occurs during N-nitrosation under acidic conditions, when the nitrosating agent nitrite ( $\text{NO}_2^-$ ) reacts with the nucleophile hydroxylamine ( $\text{NH}_2\text{OH}$ ) to form nitroxyl (HNO). Two HNO molecules then dimerize to produce nitrous oxide ( $\text{N}_2\text{O}$ ) and water (Spott et al., 2011). This reaction can be abiotic or mediated by bacteria, archaea, or fungi. Other nucleophilic species can react with  $\text{NO}_2^-$  to produce  $\text{N}_2\text{O}$ , such as azide ( $\text{N}_3^-$ ), ammonium ( $\text{NH}_4^+$ ), hydrazine ( $\text{N}_2\text{H}_4$ ), or salicylhydroxamic acid ( $\text{C}_7\text{H}_7\text{NO}_3$ ) (Spott et al., 2011). ~~In the case of in situ  $\text{N}_2\text{O}$ , the central nitrogen  $\text{N}^\alpha$  may originate from  $\text{NO}_2^-$  after reduction of  $\text{NO}_3^-$ , and the terminal nitrogen  $\text{N}^\beta$  may come from one such nucleophilic precursor (Fig. 8). Our work does not yet allow us to identify the nucleophilic precursor for  $\text{N}^\beta$ , especially because the presence and concentration of most of the N-bearing compounds in ice have not yet been investigated.~~

Another pathway for hybrid  $\text{N}_2\text{O}$  production is the decomposition of ammonium nitrate ( $\text{NH}_4\text{NO}_3$ ), either by thermal decomposition or by a light-initiated reaction involving the photoreduction of  $\text{NO}_3^-$  to  $\text{NO}_2$  coupled with the oxidation of  $\text{NH}_4^+$  to  $\text{NH}_2$ , which react with each other to produce  $\text{N}_2\text{O}$  (Rubasinghege et al., 2011). However, several arguments challenge the feasibility of the  $\text{NH}_4\text{NO}_3$  decomposition in ice. Firstly, the ice environment lacks sufficient heat for thermal

decomposition, and light penetration is minimal within the deep firn and ice, raising questions about the availability of sufficient energy for these reactions. The high activation energy of the decomposition would make the reaction very slow at the ice temperature. Additionally, if  $\text{N}_2\text{O}$  were produced from  $\text{NH}_4\text{NO}_3$ , the oxygen atom in  $\text{N}_2\text{O}$  would originate from  $\text{NO}_3^-$  and inherit its isotopic composition, yet the  $\delta^{18}\text{O}$  values of in situ  $\text{N}_2\text{O}$  do not correlate with those of  $\text{NO}_3^-$  (Fig. 5). Finally,  $\text{NO}_3^-$  and  $\text{NH}_4^+$  are present in dust-poor polar ice as well, where no in situ  $\text{N}_2\text{O}$  production is observed, and similarly, there is not necessarily in situ  $\text{N}_2\text{O}$  production everywhere in dust-rich ice from Greenland despite sufficient  $\text{NO}_3^-$  and  $\text{NH}_4^+$ . In our view, an N-nitrosation reaction is more likely than a  $\text{NH}_4\text{NO}_3$  decomposition reaction for  $\text{N}_2\text{O}$  production in ice.

### 560 5.1.2 Source of central nitrogen atom $\text{N}^{\alpha}$

In the case of in situ  $\text{N}_2\text{O}$  produced by N-nitrosation, the central nitrogen atom ( $\text{N}^{\alpha}$ ) may originate from  $\text{NO}_2^-$  after reduction of  $\text{NO}_3^-$ . However, it is unlikely that this  $\text{NO}_2^-$  derives directly from  $\text{NO}_3^-$  photolysis in the near-surface snowpack.  $\text{NO}_3^-$  photolysis produces both gaseous  $\text{NO}_2$  and  $\text{NO}_2^-$  ion, with  $\text{NO}_2^-$  accounting for ~10% of the photolysis products (Meusinger et al., 2014; Warneck and Wurzinger, 1988). Photolysis occurs at the snow surface only, where sunlight penetrates and where air exchange with the atmosphere is still active. Any  $\text{N}_2\text{O}$  produced through photolysis-driven pathways in this zone would therefore be largely released to the atmosphere and not preserved in the ice core record. In addition, photolysis enriches the remaining  $\text{NO}_3^-$  in  $^{15}\text{N}$  while producing  $\text{NO}_2^-$  that is depleted in  $^{15}\text{N}$ , with its isotopic composition depending on the extent of photolysis. If photolysis-derived  $\text{NO}_2^-$  were a precursor of in situ  $\text{N}_2\text{O}$ , the  $\delta^{15}\text{N}^{\alpha}$  signature of in situ  $\text{N}_2\text{O}$  would reflect both the initial  $\delta^{15}\text{N}(\text{NO}_3^-)$  and the extent of photolysis, and would not be directly proportional to the  $\delta^{15}\text{N}$  values of  $\text{NO}_3^-$  archived in the ice. Instead, our data show a strong proportionality between  $\delta^{15}\text{N}(\text{NO}_3^-)$  and  $\delta^{15}\text{N}(\text{N}_2\text{O}_{\text{in situ}})$ , indicating that the  $\text{NO}_2^-$  precursor must form deeper in the ice from archived  $\text{NO}_3^-$  that already carries its final, post-photolysis isotopic signature, rather than from photolysis-derived  $\text{NO}_2^-$  produced in the surface snowpack. Therefore, the reduction of  $\text{NO}_3^-$  to  $\text{NO}_2^-$  occurring within the ice requires a reducing agent. Such a reducing agent is likely associated with mineral dust, which is consistent with the observation that in situ  $\text{N}_2\text{O}$  production occurs only in dust-rich ice. Iron II ( $\text{Fe}^{2+}$ ) is likely involved in this reduction step (see Sect. 5.2).

### 575 5.1.3. Source of terminal nitrogen atom $\text{N}^{\beta}$

Our work does not yet allow us to identify the nucleophilic precursor for  $\text{N}^{\beta}$ , especially because the presence and concentrations of most of the N-bearing compounds in ice have not yet been investigated.  
Nevertheless,  $\text{NH}_4^+$  represents a potential candidate for supplying could provide the terminal nitrogen ( $\text{N}^{\beta}$ ) in the case of N-nitrosation reactions. Atmospheric  $\text{NH}_4^+$  exhibits of in situ  $\text{N}_2\text{O}$  also in the case of N-nitrosation. The  $\delta^{15}\text{N}$  values of  $\text{NH}_4^+$  in the atmosphere ranging e from -20 ‰ to +25 ‰ (Chen et al., 2022), rather similar to the  $\delta^{15}\text{N}^{\beta}$  values of in situ  $\text{N}_2\text{O}$  in Vostok and TG with average  $\delta^{15}\text{N}^{\beta}$  values of -27 ‰ and +24 ‰, respectively. These site differences could be due to post-depositional processes altering the isotopic composition of  $\text{NH}_4^+$  differently at different drilling sites. The nitrogen isotopic composition of  $\text{NH}_4^+$  has been measured only in one alpine glacier ice core, with  $\delta^{15}\text{N}$  values ranging from -15 ‰ to +5 ‰

585 for the years 2013-2017 (Lamothe et al., 2023). To further investigate this hypothesis, we suggest measuring the nitrogen isotopic composition of  $\text{NH}_4^+$  in Antarctic ice cores, specifically from Vostok and Taylor Glacier, to compare with the  $\delta^{15}\text{N}^\beta$  values of in situ  $\text{N}_2\text{O}$ .

## 5.2 Limiting factor of the reaction

590 One key observation is that the elevated  $\text{N}_2\text{O}$  mixing ratios during glacial periods are of similar magnitude over the last 800 kyr in the EDC ice core with no increase with depth/age (Schilt et al., 2010b). This observation suggests that  $\text{N}_2\text{O}$  in situ production does not increase further over time and is essentially finished at the LGM (20 to 26.5 ka). Therefore, we hypothesize a mechanism that is limited by the concentration or transport/diffusion of a reactant. The limiting factor cannot be  $\text{NO}_3^-$  as the concentrations remain high over time. Thus, it could be the precursor of the terminal N atom ( $\text{N}^\beta$ ) or the agent reducing  $\text{NO}_3^-$  to  $\text{NO}_2^-$ .

595 Indeed, because N-nitrosation reactions typically involve  $\text{NO}_2^-$  rather than  $\text{NO}_3^-$  (Spott et al., 2011), a prior conversion of  $\text{NO}_3^-$  to  $\text{NO}_2^-$  is required. While this step can be carried out by denitrifying organisms, the extremely low temperatures and acidic conditions in Antarctic ice make an abiotic process more likely (see Sect. 5.5).  $\text{NO}_3^-$  can be abiotically reduced to  $\text{NO}_2^-$  by redox-active metal ions such as  $\text{Fe}^{2+}$  or  $\text{Mn}^{2+}$  (Zhu-Barker et al., 2015). This hypothesis is supported by the presence of  $\text{Fe}^{2+}$  in ice cores (Spolaor et al., 2012, 2013). Baccolo et al. (2021) found decreasing  $\text{Fe}^{2+}$  concentrations with depth in the TALDICE core, and below 1500 m only  $\text{Fe}^{3+}$  is present in the form of jarosite ( $\text{KFe}^{3+}_3(\text{SO}_4)_2(\text{OH})_6$ ), a mineral that forms through ~~the chemical weathering of aeolian dust under acidic conditions in deep ice. -oxidation of aeolian dust under acidic conditions.~~ These findings indicate that  $\text{Fe}^{2+}$  undergoes slow post-depositional oxidation in the ice. One possible explanation is that  $\text{NO}_3^-$  oxidizes dust-derived  $\text{Fe}^{2+}$ , which could explain the observed link between dust content and in situ  $\text{N}_2\text{O}$  production. In this scenario,  $\text{Fe}^{2+}$  is the limiting factor for  $\text{N}_2\text{O}$  production, as it is progressively consumed during the  
605 conversion from  $\text{NO}_3^-$  to  $\text{NO}_2^-$ .

## 5.3 Site preference constraints on the $\text{N}_2\text{O}$ production mechanism

**Table 2.** ~~Site preference (SP) ranges measured for different  $\text{N}_2\text{O}$  production pathways compared to site preference ranges calculated for in situ  $\text{N}_2\text{O}$  in the Vostok and TG ice cores.~~ Comparison of the site preference (SP) range measured for hybrid  $\text{N}_2\text{O}$  in a previous study with SP ranges calculated for in situ  $\text{N}_2\text{O}$  in the Vostok and TG ice cores.

Reaction pathway	SP range (‰)	Suspected intermediate species	Reference
Abiotic oxidation of $\text{NH}_2\text{OH}$ by $\text{NO}_2^-$ ( <u>production of hybrid <math>\text{N}_2\text{O}</math></u> )	[+34 ; +35]	<u>Symmetric intermediate: cis-hyponitrite (<math>^-\text{ONNO}^-</math>)</u>	(Heil et al., 2014)
<u><math>\text{N}_2\text{O}</math></u> in situ production at Vostok	[+57.2 ; +187.4]	Asymmetric intermediate (unknown)	This study
<u><math>\text{N}_2\text{O}</math></u> in situ production at TG	[-17.3 ; -6.9]	Asymmetric intermediate (unknown)	This study

Since many reaction pathways have specific SP values, the SP signature is commonly used to attribute N<sub>2</sub>O production pathway to a specific pathway. High SP values ranging from +22 ‰ to +37 ‰ are reported for nitrification (Toyoda et al., 2002, 2017), fungal denitrification (Toyoda et al., 2017), and abiotic reactions such as NO<sub>2</sub><sup>-</sup> reduction and NH<sub>2</sub>OH oxidation (Heil et al., 2015; Toyoda et al., 2005) (Table 3). Several studies suggested that the similarity of the SP signatures for these distinct formation pathways is attributable to a common intermediate species – hyponitrous acid HONNOH<sub>cis</sub> (Heil et al., 2015; Toyoda et al., 2002, 2005, 2017). During decomposition, this intermediate preferentially breaks at the <sup>14</sup>N-O bond over the <sup>15</sup>N-O bond, enriching the central N atom (N<sup>α</sup>) in <sup>15</sup>N and explaining high SP values (Toyoda et al., 2002) (Fig. 8Fig. 9a). In contrast, bacterial and nitrifier denitrification produce N<sub>2</sub>O with low SP values from -11 ‰ to 0 ‰ (Toyoda et al., 2017), which are thought to derive from a different intermediate. Modeling work suggested a trans-hyponitrous structure that decomposes preferentially into <sup>15</sup>N<sup>14</sup>NO due to kinetic isotope effects, thus explaining the low SP values of these formation pathways (Fehling, 2012) (Fig. 8Fig. 9a). Overall, in these cases, SP values are therefore determined by the decomposition step of the last intermediate into N<sub>2</sub>O and are independent of the δ<sup>15</sup>N values of the precursor (Fig. 8Fig. 9). ~~REFERENCE !!!~~

For in situ N<sub>2</sub>O, however, the SP values for the Vostok and TG ice cores do not fall into either typical low or high SP range and are highly variable (Table 2). The constant-SP pathways discussed above produce single-precursor N<sub>2</sub>O, but in the case of hybrid N<sub>2</sub>O production, one would expect a priori that the SP would no longer be a unique mechanism-dependent signature. Instead, for hybrid reactions the SP should be influenced by the difference between the δ<sup>15</sup>N signatures of the two precursors, if the central N atom (N<sup>α</sup>) is derived from one precursor and the terminal N atom (N<sup>β</sup>) from the other. However, Heil et al. (2014) demonstrated that hybrid N<sub>2</sub>O from the nitrosation of NH<sub>2</sub>OH by NO<sub>2</sub><sup>-</sup> is also characterized by a constant SP value of +34 ‰ (Table 2) regardless of the precursor signatures. The authors concluded that the NH<sub>2</sub>OH-nitrosation mechanism also involves the symmetric hyponitrous intermediate (Fig. 8Fig. 9b). In fact, since this intermediate is symmetrical, the N atoms from each precursor can either take the α-position or the β-position in the final N<sub>2</sub>O molecule; the difference in their δ<sup>15</sup>N values then has no influence on the SP value (Fig. 8Fig. 9b).

Because of the variability of the SP(N<sub>2</sub>O<sub>in situ</sub>) values and their dependence on the δ<sup>15</sup>N(NO<sub>3</sub><sup>-</sup>) signature, we therefore deduce that the production mechanism of in situ N<sub>2</sub>O does not involve the hyponitrous symmetrical intermediate. In Fig. 8Fig. 9c, we propose a new reaction mechanism that involves an asymmetric intermediate, resulting in a hybrid N<sub>2</sub>O molecule in which the N atoms at the α and β positions are derived from a specific precursor. N<sup>α</sup> and N<sup>β</sup> retain the two individual signatures of the precursors rather than losing them as discussed above. The high variability of SP values is then attributable to the variability of δ<sup>15</sup>N<sup>α</sup> values (Fig. 6), which originates from the wide range of δ<sup>15</sup>N(NO<sub>3</sub><sup>-</sup>) values (Fig. 7).

We note that all published SP datasets used for comparison were obtained at ambient temperatures, whereas in situ N<sub>2</sub>O production in Antarctic ice occurs at very low temperatures. Such low temperatures imply extremely slow reaction rates, which may alter the magnitude of isotope fractionation and make direct comparison of absolute SP values with ambient-temperature experiments difficult. To our knowledge, no SP measurements exist under such cold conditions. However, our

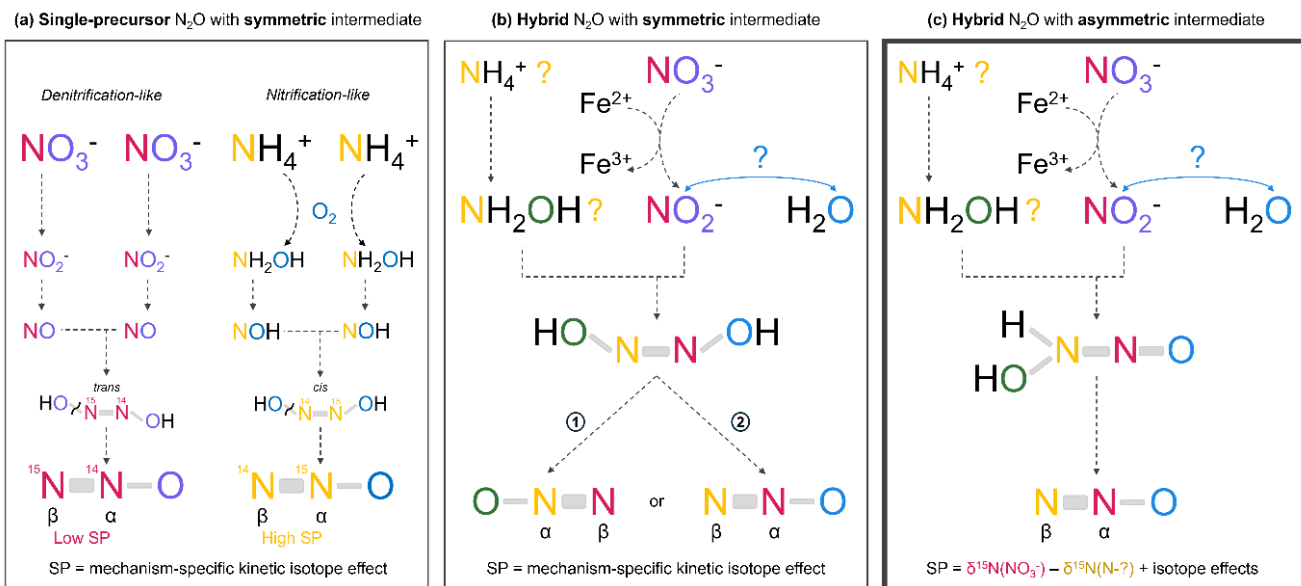
645 interpretation does not rely on comparing absolute SP values. Instead, we focus on whether SP is constant or variable with respect to the  $\delta^{15}\text{N}$  signature of the precursor: this property should be independent of the absolute magnitude of isotope fractionation. Although lower temperatures may increase kinetic isotope effects and shift absolute SP values, they do not change whether SP remains constant (as in reactions involving symmetrical intermediates) or varies with the precursor isotopic composition (as expected when an asymmetrical intermediate forms). Thus, the comparison of the mechanisms remains valid even without low-temperature experimental data from previous studies.

650 Several mechanisms could potentially explain why the intermediate of in situ  $\text{N}_2\text{O}$  production is asymmetric, even though its exact chemical structure remains unknown. ~~Two options could then be considered to justify the asymmetric nature of the intermediate whose exact chemical formula is unknown.~~ Firstly, the precursor of the  $\beta$ -position N atom could be different from  $\text{NH}_2\text{OH}$ . Although most studies on hybrid  $\text{N}_2\text{O}$  production report a reaction between  $\text{NH}_2\text{OH}$  and  $\text{NO}_2^-$  (Frame et al., 2017; Spott et al., 2011; Stieglmeier et al., 2014; Terada et al., 2017), other nucleophilic precursors have been reported as

655 precursors of hybrid  $\text{N}_2\text{O}$ . Hydrazine ( $\text{N}_2\text{H}_4$ ), for example, forms the asymmetrical intermediate  $\text{HO-N=N-NH}_2$  (Perron et al., 1976). ~~The second alternative is that hybrid  $\text{N}_2\text{O}$  is indeed produced from  $\text{NH}_2\text{OH}$  and  $\text{NO}_2^-$ , but the very low temperatures modify the intermediate species.~~ A second possibility is that very low temperatures modify the structure or stability of the intermediate normally formed from  $\text{NH}_2\text{OH}$  and  $\text{NO}_2^-$  at ambient temperature conditions, favoring an asymmetrical species and thereby generating the observed dependence of SP on the precursor  $\delta^{15}\text{N}$  values.

660 The same hybrid production mechanism proposed for in situ  $\text{N}_2\text{O}$  production in Antarctic ice may occur at Don Juan Pond (DJP), Antarctica. Like in ice cores,  $\text{N}_2\text{O}$  formation at DJP reported by Samarkin et al. (2010) occurs under very low temperatures and involves  $\text{NO}_3^-$  and especially  $\text{NO}_2^-$ , with higher production rates for  $\text{NO}_2^-$  as precursor. The authors demonstrated that  $\text{N}_2\text{O}$  extracted from DJP soil is abiotically produced. Moreover, they measured very low and highly variable SP values at DJP, down to -45 ‰, which also fall outside the typical SP range. This variability in SP values and

665 similar environmental conditions support the possibility of a shared, likely abiotic, mechanism of hybrid  $\text{N}_2\text{O}$  production in Antarctic ice and at DJP.



670 **Figure 98.** Production mechanisms for single-precursor  $N_2O$  (a) and hybrid  $N_2O$  (b), (c). Two mechanisms for hybrid  $N_2O$   
 675 production are proposed: panel (b) explains constant SP values, while panel (c), which explains the observed SP dependence on the  $\delta^{15}N$  values of the precursor, is more likely to represents the in situ production pathway. (b) Mechanism with a symmetric  
 680 intermediate, here the *cis*-hyponitrous acid HONNOH. Depending on which N-O bond of the symmetric intermediate breaks, the  $NO_2$ -derived and  $NH_2OH$ -derived N atoms can each end up either in the central position ( $\alpha$ ) or in the terminal position ( $\beta$ ) in  $N_2O$ . The percentage of molecules 1 and 2, and consequently the site preference, only reflects the preferential cleavage of the  $^{14}N$ -O bond over the  $^{15}N$ -O bond during the last step of  $N_2O$  formation. Therefore, hybrid  $N_2O$  exhibits a consistent site preference that is independent of the  $\delta^{15}N$  values of the precursors (Heil et al., 2014). In this case the O atom is derived from one precursor or the other. (c) Mechanism with an asymmetric intermediate. In this case, the O atom and the central N atom ( $N^\alpha$ ) are always derived from  $NO_2^-$  and the terminal N atom ( $N^\beta$ ) from  $NH_2OH$ . The two N atoms retain the  $\delta^{15}N$  signatures of their individual precursors. The site preference is therefore variable, as it depends on the difference between the  $\delta^{15}N$  values of the two precursors. This mechanism matches our observations but to our knowledge has not yet been reported in the literature. Note that the precursors and intermediates shown in this figure are only examples used to illustrate our point about SP values. It is one hypothesis among others for the mechanism of in situ  $N_2O$  production as the nitrogen source of the terminal nitrogen  $N^\beta$  in  $N_2O$  (in yellow) remains unknown. During in situ production,  $Fe^{2+}$  carried by dust may reduce  $NO_3^-$  to  $NO_2^-$  and act as the limiting factor once fully oxidized to  $Fe^{3+}$ .

#### 685 5.4 Source of oxygen in in situ $N_2O$

The  $\delta^{18}O$  signature of in situ  $N_2O$  does not reflect the  $\delta^{18}O$  of  $NO_3^-$ , indicating that additional processes modify the oxygen isotopic composition during or prior to  $N_2O$  formation; below, we therefore discuss possible mechanisms that could explain this decoupling, while noting that the dominant process remains uncertain.

690 Considering an N-nitrosation pathway, the observed  $\delta^{18}O(N_2O_{in\ situ})$  values might be explained by the combined processes of  $NO_3^-$  reduction and  $NO_2^-$  isotopic equilibration with  $H_2O$  (Casciotti et al., 2007). Since N-nitrosation typically involves  $NO_2^-$  rather than  $NO_3^-$ , it is likely that  $NO_3^-$  is first reduced to  $NO_2^-$ . Several studies have shown that  $NO_2^-$  is prone to exchange its O atoms with the O atoms of water molecules in aqueous solution (Bunton et al., 1959). The water from Antarctic ice is strongly depleted in  $^{18}O$ , with  $\delta^{18}O(H_2O)$  values of approximately -62 ‰ at Vostok (Lorius et al., 1985), -56 ‰ at EDC (Landais and Stenni, 2021), -42 ‰ at EDML (EPICA Community Members, 2010) and -42 ‰ as well as TG (Baggenstos et

695 al., 2018). Thus, incorporation of O atoms from H<sub>2</sub>O into N<sub>2</sub>O through exchange with NO<sub>2</sub><sup>-</sup> could explain the <sup>18</sup>O depletion observed in in situ N<sub>2</sub>O compared to NO<sub>3</sub><sup>-</sup> in the EDML, EDC, and Vostok ice cores (Fig. 5). However, the δ<sup>18</sup>O(N<sub>2</sub>O<sub>in situ</sub>) values are not correlated to δ<sup>18</sup>O(H<sub>2</sub>O) values and the difference between δ<sup>18</sup>O(N<sub>2</sub>O<sub>in situ</sub>) and δ<sup>18</sup>O(NO<sub>3</sub><sup>-</sup>) is significantly larger at EDML than at EDC and Vostok. This may indicate an incomplete exchange of O atoms between NO<sub>2</sub><sup>-</sup> and H<sub>2</sub>O, with a larger fraction of exchanged O atoms at EDML than EDC and Vostok.

700 In contrast, δ<sup>18</sup>O(N<sub>2</sub>O<sub>in situ</sub>) values at TG are unexpectedly higher than δ<sup>18</sup>O(NO<sub>3</sub><sup>-</sup>), suggesting that oxygen exchange with water alone cannot explain the δ<sup>18</sup>O(N<sub>2</sub>O<sub>in situ</sub>) values. In this case, the observed enrichment in <sup>18</sup>O compared to NO<sub>3</sub><sup>-</sup> might be due to the “branching effect” associated with NO<sub>3</sub><sup>-</sup> reduction. This effect results from the incomplete incorporation of the oxygen pool from NO<sub>3</sub><sup>-</sup> to N<sub>2</sub>O (Casciotti et al., 2007). Indeed, only two out of three O atoms from NO<sub>3</sub><sup>-</sup> are transferred into NO<sub>2</sub><sup>-</sup>, then one out of two from NO<sub>2</sub><sup>-</sup> to N<sub>2</sub>O. Since <sup>16</sup>O atoms are preferentially lost, NO<sub>2</sub><sup>-</sup> and N<sub>2</sub>O become enriched in <sup>18</sup>O.  
705 For the abiotic reduction of NO<sub>2</sub><sup>-</sup> to N<sub>2</sub>O by Fe<sup>2+</sup>, the branching effect results in positive isotope effect of about +30 ‰ at 25 °C (Buchwald et al., 2016) which is likely even larger at very low temperatures. Although the same branching effect probably occurs at EDC, Vostok, and EDML, the fraction of exchanged O atoms might be smaller at TG, making the branching effect relatively more pronounced in the final δ<sup>18</sup>O(N<sub>2</sub>O<sub>in situ</sub>) values.

The reason why the fraction of exchanged O atoms would vary among ice cores is not fully understood. It likely depends on  
710 the relative rates of oxygen isotope equilibration and the N-nitrosation reaction, both of which are temperature- and pH-dependent. Casciotti et al. (2007) showed that oxygen exchange is faster under acidic conditions, and Su et al. (2019) reported that low pH also accelerates abiotic nitrosation reactions. ~~Therefore, the combination of different ice chemical compositions and environmental conditions during the reaction could influence the fraction of O atoms exchanged between NO<sub>2</sub><sup>-</sup> and H<sub>2</sub>O.~~ However, measurement constraints of pH remain limited. Although glacial Antarctic ice is generally acidic and Greenland ice is typically more alkaline, pH measurements are not available for the specific samples investigated here, making it difficult to interpret the differences in δ<sup>18</sup>O(N<sub>2</sub>O<sub>in situ</sub>) among Antarctic sites in terms of pH effects. Moreover, even if pH were measured in the liquid phase (meltwater), it would be difficult to directly infer the pH of the solid ice matrix, as pH is formally defined only for liquid solutions. In addition, the relevant reactions likely occur at the surfaces of dust particles (where the reduction of NO<sub>3</sub><sup>-</sup> to NO<sub>2</sub><sup>-</sup> may take place) rather than in the bulk ice, and the chemical conditions ~~in~~  
715 these micro-environments may differ from those of the surrounding ice.

To conclude, ~~Therefore, the combination of different ice chemical compositions and environmental conditions during the reaction could influence the fraction of O atoms exchanged between NO<sub>2</sub><sup>-</sup> and H<sub>2</sub>O.~~

720 While the relative contributions of oxygen exchange and branching effect to the δ<sup>18</sup>O(N<sub>2</sub>O<sub>in situ</sub>) values remain unclear, overall, these processes may mask the transfer of the original δ<sup>18</sup>O(NO<sub>3</sub><sup>-</sup>) signature into in situ N<sub>2</sub>O.

## 725 5.5 Likelihood of an abiotic production of N<sub>2</sub>O

In situ N<sub>2</sub>O production in polar ice has often been attributed to microbial activity. Sowers (2001) reported two N<sub>2</sub>O maxima in the Vostok ice core at around 150 ka that coincided with elevated bacterial counts. Similarly, Rohde et al. (2008) found

that in the GISP2 Greenland ice core, most of the samples affected by in situ production were associated with large cell counts.

730 However, several observations challenge the hypothesis of a microbial in situ production. First, the correlation between microbial counts and N<sub>2</sub>O maxima may not be causal, as the dust content could be a confounding variable: mineral particles are the main carriers of microbial cells to the ice sheet (Miteva, 2008; Miteva et al., 2016), so both microbial concentrations and in situ N<sub>2</sub>O are positively correlated with dust content in Antarctic ice cores. Second, because the low temperatures affect microbial metabolism and thus limit the reaction, one would expect the increase in ice temperature with depth to result  
735 in an increase in excess N<sub>2</sub>O as well. However, such an increase is not observed (Schilt et al., 2010b). Third, microbial activity generally requires the presence of liquid water. Although thin water channels called “liquid veins” can form during ice crystal growth due to concentration of acidic impurities at crystal interfaces (Barletta et al., 2012; Dani et al., 2012), the upper hundreds of meters where N<sub>2</sub>O is produced are too cold for such features to exist at sites like Vostok (Dani et al., 2012). Fourth, our SP and δ<sup>18</sup>O data indicate the absence of microbial N<sub>2</sub>O reduction in the ice (Sect. 5.1). While absence of  
740 N<sub>2</sub>O reduction alone does not rule out microbial N<sub>2</sub>O production, these two processes are generally linked in terrestrial and aquatic environments, where N<sub>2</sub>O produced by bacterial denitrification is typically at least partly reduced to N<sub>2</sub>. ~~Fourth~~Fifth, no functional genes involved in bacterial and archaeal nitrification and denitrification were detected by PCR amplification in the NEEM Greenland ice core during the last glacial period (Miteva et al., 2016). Finally, Antarctic ice is an acidic environment (EPICA community members, 2004; Wolff et al., 1997), but the review by Spott et al. (2011) indicates that  
745 hybrid N<sub>2</sub>O production by biotic nitrosation generally occurs under neutral pH conditions, within a range of 6 to 7.5. Only one study reported ~~AOA~~ production of hybrid N<sub>2</sub>O by ammonia-oxidizing archaea at a moderately low pH of 5.5 (Jung et al., 2019). In contrast, Su et al. (2019) showed that abiotic production of hybrid N<sub>2</sub>O is enhanced at pH ≤ 5. Given the above constraints, an abiotic mechanism is the most plausible explanation for in situ N<sub>2</sub>O production.

An abiotic reaction triggered by low pH could also explain the differences in N<sub>2</sub>O production observed between Antarctic  
750 and Greenland ice. In Antarctic ice cores, N<sub>2</sub>O production occurs consistently throughout dust-rich depths and the amount of in situ N<sub>2</sub>O is roughly correlated with the amount of dust (Schilt et al., 2010b, a). In contrast, Greenland ice shows erratic N<sub>2</sub>O production with a finite number of outliers of very high N<sub>2</sub>O mixing ratio (Flückiger et al., 2004). In Greenland ice  
cores it occurs in specific depth intervals with moderate dust concentrations, while sections with very high dust concentrations rarely show in situ production. This very dusty Greenland ice is alkaline due to the deposition of alkaline dust  
755 (calcium carbonates), which can neutralize acids in the ice (Biscaye et al., 1997; Mayewski et al., 1994; Wolff et al., 1997), a phenomenon not observed in Antarctic ice which is acidic (EPICA community members, 2004; Wolff et al., 1997). The generally higher pH of Greenland ice (Rasmussen et al., 2023) may inhibit in situ N<sub>2</sub>O production, potentially explaining the absence of widespread production in these cores. Isolated outliers with elevated N<sub>2</sub>O mixing ratios occur at depths where the ice is more acidic, for instance near volcanic horizons, as they are often found close to sulfate peaks.

## 760 6 Conclusion

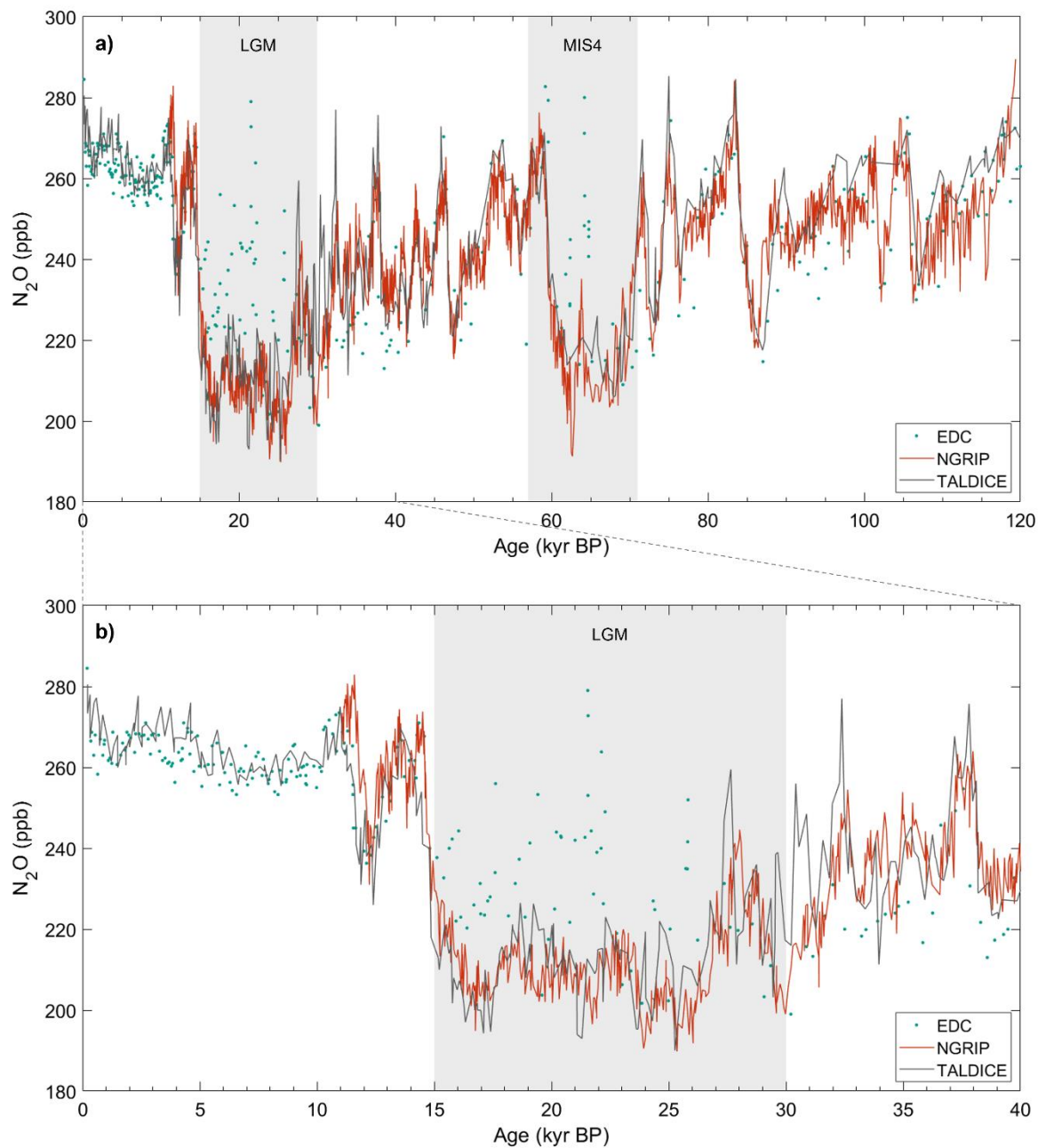
Using bulk and position-specific isotope analyses, we have improved the understanding of N<sub>2</sub>O production in Antarctic ice while also raising new questions about its nature. Our results show that N<sub>2</sub>O produced in ice is hybrid N<sub>2</sub>O, with its central N atom (N<sup>α</sup>) derived from NO<sub>3</sub><sup>-</sup> and its terminal N atom (N<sup>β</sup>) from a different precursor. This hybrid N<sub>2</sub>O is likely produced abiotically through an N-nitrosation reaction, in which NO<sub>3</sub><sup>-</sup> is first reduced to NO<sub>2</sub><sup>-</sup> that then reacts with a nucleophilic  
765 compound that supplies N<sup>β</sup> in N<sub>2</sub>O. Fe<sup>2+</sup> contained in dust particles may be the agent that reduces NO<sub>3</sub><sup>-</sup> to NO<sub>2</sub><sup>-</sup>. In addition to the precursor of the terminal N atom, this reducing agent could be a limiting factor in the reaction. Low pH may also be a necessary condition for this process. To better understand the pH control on N<sub>2</sub>O production, future work should investigate the isolated in situ N<sub>2</sub>O outliers in Greenland ice. The sources of the terminal N atom (N<sup>β</sup>) and the O atom in in situ N<sub>2</sub>O remain uncertain. One possibility is that N<sup>β</sup> originates from NH<sub>4</sub><sup>+</sup>, potentially converted to NH<sub>2</sub>OH; measuring the isotopic  
770 composition of NH<sub>4</sub><sup>+</sup> in Antarctic ice cores could help testing this hypothesis. For the O atom, it may be derived from two different oxygen pools – either from NO<sub>3</sub><sup>-</sup> or from H<sub>2</sub>O through oxygen exchange with NO<sub>2</sub><sup>-</sup>.

Our work revealed that the isotopic composition of in situ N<sub>2</sub>O is highly variable even within a single ice core. As a result, N<sub>2</sub>O records from ice cores cannot be accurately corrected for in situ production using a fixed isotopic signature in a mass balance approach. A more robust correction method would be to measure NO<sub>3</sub><sup>-</sup> isotopic composition alongside total N<sub>2</sub>O in  
775 the same samples, as we did in this study. Since the in situ N<sub>2</sub>O signature reflects the variability of NO<sub>3</sub><sup>-</sup> isotopes, this method would help estimate the isotopic signature of in situ N<sub>2</sub>O in affected samples. We could not apply this method to the existing N<sub>2</sub>O records because the meltwater at that time was not collected after N<sub>2</sub>O analysis, thus the NO<sub>3</sub><sup>-</sup> isotopic composition cannot be measured in these specific samples.

This study also highlights the importance of accounting for in situ N<sub>2</sub>O production when using N<sub>2</sub>O isotopes for source  
780 attribution. In some ice cores, the isotopic signature of in situ N<sub>2</sub>O deviates drastically from the atmospheric signal. Even small amounts of in situ N<sub>2</sub>O can significantly impact the measured isotopic composition and thus alter paleoclimatic interpretations. For example, for atmospheric N<sub>2</sub>O at a mixing ratio of 200 ppb and in situ N<sub>2</sub>O at 5 ppb, with  $\delta^{15}\text{N}_{\text{bulk}}(\text{N}_2\text{O}_{\text{in situ}})$  as high as +70 ‰ as we observed in the Vostok ice core, this small in situ contribution would shift the  $\delta^{15}\text{N}_{\text{bulk}}(\text{N}_2\text{O}_{\text{total}})$  by +1.5 ‰. Such a shift would result in a 16 % increase in estimated marine N<sub>2</sub>O emissions and a change in marine-to-  
785 terrestrial emission ratio from 0.39 to 0.45, which is close to the entire change observed over the last 21 kyr (Fischer et al., 2019). Therefore, identifying and excluding all samples affected by in situ production is essential to avoid misinterpretation. Our results reveal a previously unidentified N<sub>2</sub>O production pathway likely involving an asymmetric reaction intermediate. This process may not be limited to ice but could also occur in other environments such as soils or aquatic systems, suggesting it may contribute to atmospheric N<sub>2</sub>O more broadly. This has important implications for the interpretation of SP  
790 values. The SP(N<sub>2</sub>O<sub>in situ</sub>) values observed in this study show unusual variability and strong dependence on the isotopic composition of the precursors, compared to SP values reported in previous studies (Heil et al., 2014; Toyoda et al., 2017). These results may reflect the production of hybrid N<sub>2</sub>O via an asymmetric intermediate, where N<sup>α</sup> and N<sup>β</sup> originate from

distinct precursors and retain the isotopic signature of their respective sources. In this case, the SP values depend on the difference between the isotopic signatures of the two sources. This mechanism complicates the use of SP to trace N<sub>2</sub>O pathways, as they are not always characterized by a constant SP value. We therefore recommend further investigation of SP values in hybrid N<sub>2</sub>O under different environmental conditions and reaction mechanisms.

## Appendix A – Can the TALDICE data be used as an atmospheric reference?



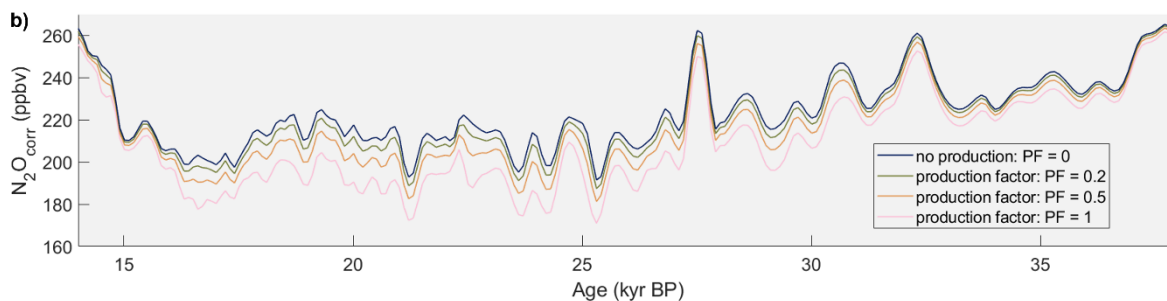
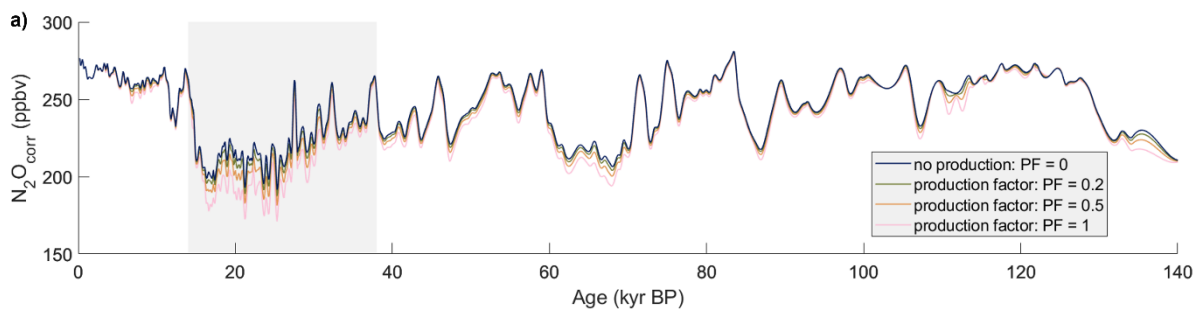
800 **Figure A1.** N<sub>2</sub>O concentrations measured in the TALDICE (Schilt et al., 2010a), NGRIP (Flückiger et al., 2004; Schilt et al., 2010a, 2013), and EDC (Schilt et al., 2010b) ice cores over the last 120 kyr (a) and over the last 40 kyr (b). In situ N<sub>2</sub>O outliers have been removed from the NGRIP record. The EDC ice core is affected by in situ production of N<sub>2</sub>O during the LGM and MIS4.

## Appendix B – Uncertainties in the mass balance calculation

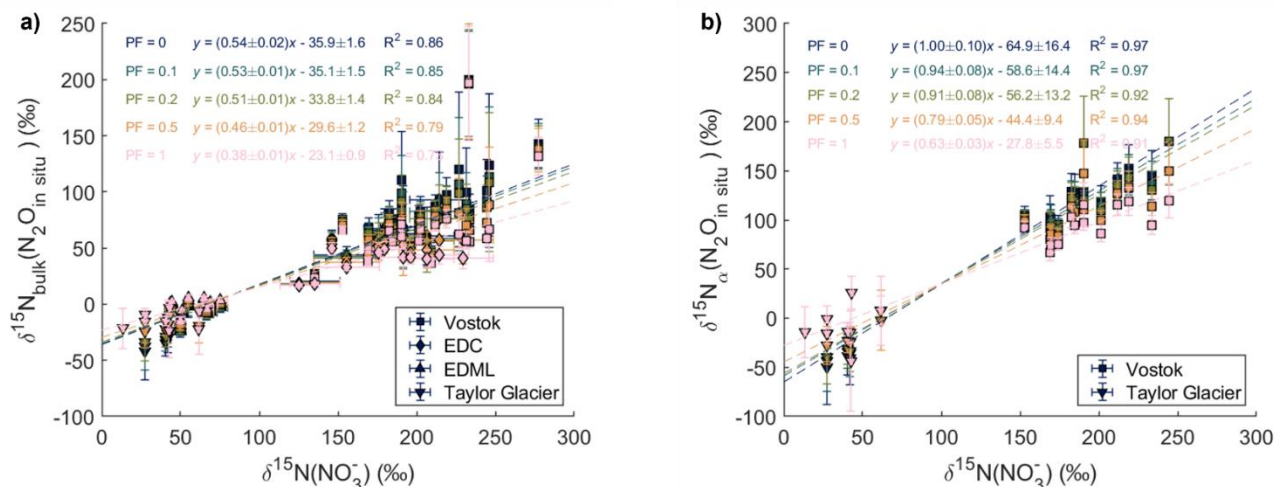
805 **Table B1.** Uncertainty ranges used in the Monte-Carlo calculation of the uncertainty of in situ  $N_2O$  isotopic signature. Here we report the uncertainties due to differences in gas age scales of TALDICE and other ice cores, as the atmospheric values in the mass balance calculation are defined as the spline values matching the age of the measured sample.

Variable	Uncertainty range
Gas age	0.7 kyr
$N_2O$ concentration of the atmospheric spline	4 ppb
$\delta^{15}N$ values of the $N_2O$ atmospheric spline	0.3 ‰
$\delta^{15}N^a$ value of atmospheric $N_2O$ (Menking et al., 2025)	1.7 ‰
$\delta^{18}O$ values of the $N_2O$ atmospheric spline	0.6 ‰
Measured $N_2O$ concentration	4 ppb
Measured $\delta^{15}N(N_2O)$ values	0.3 ‰
Measured $\delta^{15}N^a(N_2O)$ values	0.6 ‰
Measured $\delta^{18}O(N_2O)$ values	0.6 ‰

## Appendix C – Sensitivity study: potential in situ contribution in TALDICE $N_2O$



- 810 **Figure C1. Spline interpolation of TALDICE N<sub>2</sub>O concentrations, corrected for potential in situ production proportional to dust content. The different curves correspond to varying production factors, which link dust concentration to the amount of in situ N<sub>2</sub>O produced. (a): 0 to 140 kyr BP, (b): 14 to 38 kyr BP.**



- 815 **Figure C2. Sensitivity study testing the impact of in situ N<sub>2</sub>O production in TALDICE proportional to Ca<sup>2+</sup> concentrations, with production factors (PF) ranging from 0 to 1. PF = 0 means no N<sub>2</sub>O production. (a) Relation between δ<sup>15</sup>N<sub>bulk</sub>(N<sub>2</sub>O<sub>in situ</sub>) and δ<sup>15</sup>N(NO<sub>3</sub><sup>-</sup>). (b) Relation between δ<sup>15</sup>N<sup>α</sup>(N<sub>2</sub>O<sub>in situ</sub>) and δ<sup>15</sup>N(NO<sub>3</sub><sup>-</sup>).**

#### Appendix D – Assessment of potential NO<sub>3</sub><sup>-</sup> contamination, loss, or isotopic fractionation during N<sub>2</sub>O extraction from ice core samples

- 820 **Table D1. NO<sub>3</sub><sup>-</sup> concentration and isotopic composition of the same samples with and without N<sub>2</sub>O extraction.**

		NO <sub>3</sub> <sup>-</sup> concentration (ng.g <sup>-1</sup> )		NO <sub>3</sub> <sup>-</sup> isotopic composition			
				δ <sup>15</sup> N (‰)		δ <sup>18</sup> O (‰)	
		No N <sub>2</sub> O extraction	After N <sub>2</sub> O extraction	No N <sub>2</sub> O extraction	After N <sub>2</sub> O extraction	No N <sub>2</sub> O extraction	After N <sub>2</sub> O extraction
Ultrapure water with NO <sub>3</sub> <sup>-</sup> isotopic standard USGS32 (Bohlke et al., 1993)		80	75.2	+180 (reference value)	+175.7 ± 0.5	+25.4 ± 0.2 (reference value)	+34.7 ± 1.7
Duplicate ice core samples	B37 108	55.7	53.0	51.9 ± 0.4	54.8 ± 0.4	48.4 ± 2.3	59.2 ± 2.3
	EDC 1841	35.6	35.1	175.8 ± 0.5	176.0 ± 0.4	38.2 ± 1.7	40.5 ± 2.3

	EDML 1768	93.0	90.3	46.9 ± 0.4	50.9 ± 0.4	76.1 ± 2.3	84.1 ± 2.3
	EDML 976	64.8	64.6	63.3 ± 0.5	65.0 ± 0.5	78.5 ± 1.7	93.9 ± 1.7

### Data Availability.

The data presented in this study ~~are will be~~ available on PANGAEA at: <https://doi.pangaea.de/10.1594/PANGAEA.986638> -

825

### Author Contribution.

The concept of the study was developed by JSc, HF, and LS. The bulk isotope analyses of N<sub>2</sub>O were carried out by LS and BS. LS performed the position-specific isotope analyses of N<sub>2</sub>O under the guidance of JM and EB and the NO<sub>3</sub><sup>-</sup> isotope analyses under the guidance of JSa. JSa, VL, and EB provided ice core samples. LS and JSc analyzed the data. TR, JM, and EB provided input on SP measurements. HF managed and supervised the project. LS wrote the manuscript with contributions from all authors.

830

### Competing interests.

The contact author has declared that none of the authors has any competing interests.

### Acknowledgements.

This publication was generated in the frame of the DEEPICE project. The project has received funding from the European Union's Horizon 2020 research and innovation programme under the Marie Skłodowska-Curie grant agreement no. 955750

835

### Financial support.

This research has been supported by the Horizon 2020 research and innovation programme (grant no. 955750) and by the Swiss National Science Foundation (grant no. 200020\_200328).

- Aarons, S. M., Aciego, S. M., Arendt, C. A., Blakowski, M. A., Steigmeyer, A., Gabrielli, P., Sierra-Hernández, M. R., Beaudon, E., Delmonte, B., Baccolo, G., May, N. W., and Pratt, K. A.: Dust composition changes from Taylor Glacier (East Antarctica) during the last glacial-interglacial transition: A multi-proxy approach, *Quaternary Science Reviews*, 162, 60–71, <https://doi.org/10.1016/j.quascirev.2017.03.011>, 2017.
- 845 Anklin, M., Barnola, J.-M., Schwander, J., Stauffer, B., and Raynaud, D.: Processes affecting the CO<sub>2</sub> concentrations measured in Greenland ice, *Tellus B*, 47, 461–470, <https://doi.org/10.1034/j.1600-0889.47.issue4.6.x>, 1995.
- Baccolo, G., Delmonte, B., Niles, P. B., Cibin, G., Di Stefano, E., Hampai, D., Keller, L., Maggi, V., Marcelli, A., Michalski, J., Snead, C., and Frezzotti, M.: Jarosite formation in deep Antarctic ice provides a window into acidic, water-limited weathering on Mars, *Nat Commun*, 12, 436, <https://doi.org/10.1038/s41467-020-20705-z>, 2021.
- 850 Baggenstos, D., Severinghaus, J. P., Mulvaney, R., McConnell, J. R., Sigl, M., Maselli, O., Petit, J., Grente, B., and Steig, E. J.: A Horizontal Ice Core From Taylor Glacier, Its Implications for Antarctic Climate History, and an Improved Taylor Dome Ice Core Time Scale, *Paleoceanog and Paleoclimatol*, 33, 778–794, <https://doi.org/10.1029/2017PA003297>, 2018.
- Baggs, E. M.: Soil microbial sources of nitrous oxide: recent advances in knowledge, emerging challenges and future direction, *Current Opinion in Environmental Sustainability*, 3, 321–327, <https://doi.org/10.1016/j.cosust.2011.08.011>, 2011.
- 855 Bange, H. W.: Gaseous Nitrogen Compounds (NO, N<sub>2</sub>O, N<sub>2</sub>, NH<sub>3</sub>) in the Ocean, in: *Nitrogen in the Marine Environment*, Elsevier, 51–94, <https://doi.org/10.1016/B978-0-12-372522-6.00002-5>, 2008.
- Barletta, R. E., Priscu, J. C., Mader, H. M., Jones, W. L., and Roe, C. H.: Chemical analysis of ice vein microenvironments: II. Analysis of glacial samples from Greenland and Antarctica, *J. Glaciol.*, 58, 1109–1118, <https://doi.org/10.3189/2012JoG12J112>, 2012.
- 860 Battle, M., Bender, M., Sowers, T., Tans, P. P., Butler, J. H., Elkins, J. W., Ellis, J. T., Conway, T., Zhang, N., Lang, P., and Clark, A. D.: Atmospheric gas concentrations over the past century measured in air from firn at the South Pole, *Nature*, 383, 231–235, <https://doi.org/10.1038/383231a0>, 1996.
- Bauska, T. K., Baggenstos, D., Brook, E. J., Mix, A. C., Marcott, S. A., Petrenko, V. V., Schaefer, H., Severinghaus, J. P., and Lee, J. E.: Carbon isotopes characterize rapid changes in atmospheric carbon dioxide during the last deglaciation, *Proc. Natl. Acad. Sci. U.S.A.*, 113, 3465–3470, <https://doi.org/10.1073/pnas.1513868113>, 2016.
- 865 Bigler, M.: Hochauflösende Spurenstoffmessungen an polaren Eisbohrkernen: Glazio-chemische und klimatische Prozessstudien, <https://doi.org/10.57694/7211>, 2004.
- Biscaye, P. E., Grousset, F. E., Revel, M., Van Der Gaast, S., Zielinski, G. A., Vaars, A., and Kukla, G.: Asian provenance of glacial dust (stage 2) in the Greenland Ice Sheet Project 2 Ice Core, Summit, Greenland, *J. Geophys. Res.*, 102, 26765–26781, <https://doi.org/10.1029/97JC01249>, 1997.
- 870 Blunier, T., Floch, G. L., Jacobi, H., and Quansah, E.: Isotopic view on nitrate loss in Antarctic surface snow, *Geophysical Research Letters*, 32, 2005GL023011, <https://doi.org/10.1029/2005GL023011>, 2005.

- Bohlke, J. K., Gwinn, C. J., and Coplen, T. B.: NEW REFERENCE MATERIALS FOR NITROGEN-ISOTOPE-RATIO MEASUREMENTS, *Geostandards and Geoanalytical Research*, 17, 159–164, <https://doi.org/10.1111/j.1751-908X.1993.tb00131.x>, 1993.
- Bouchet, M., Landais, A., Grisart, A., Parrenin, F., Prié, F., Jacob, R., Fourré, E., Capron, E., Raynaud, D., Lipenkov, V. Y., Loutre, M.-F., Extier, T., Svensson, A. M., Martinerie, P., Leuenberger, M. C., Jiang, W., Ritterbusch, F., Lu, Z.-T., and Yang, G.-M.: The Antarctic ice core chronology (AICC2023), <https://doi.org/10.1594/PANGAEA.961017>, 2023.
- Buchwald, C., Grabb, K., Hansel, C. M., and Wankel, S. D.: Constraining the role of iron in environmental nitrogen transformations: Dual stable isotope systematics of abiotic NO<sub>2</sub><sup>-</sup> reduction by Fe(II) and its production of N<sub>2</sub>O, *Geochimica et Cosmochimica Acta*, 186, 1–12, <https://doi.org/10.1016/j.gca.2016.04.041>, 2016.
- Buiron, D., Chappellaz, J., Stenni, B., Frezzotti, M., Baumgartner, M., Capron, E., Landais, A., Lemieux-Dudon, B., Masson-Delmotte, V., Montagnat, M., Parrenin, F., and Schilt, A.: TALDICE-1 age scale of the Talos Dome deep ice core, East Antarctica, *Clim. Past*, 7, 1–16, <https://doi.org/10.5194/cp-7-1-2011>, 2011.
- Bunton, C. A., Llewellyn, D. R., and Stedman, G.: Oxygen exchange between nitrous acid and water, *J. Chem. Soc.*, 568, <https://doi.org/10.1039/jr9590000568>, 1959.
- Casciotti, K. L., Böhlke, J. K., McIlvin, M. R., Mroczkowski, S. J., and Hannon, J. E.: Oxygen Isotopes in Nitrite: Analysis, Calibration, and Equilibration, *Anal. Chem.*, 79, 2427–2436, <https://doi.org/10.1021/ac061598h>, 2007.
- Chen, Z.-L., Song, W., Hu, C.-C., Liu, X.-J., Chen, G.-Y., Walters, W. W., Michalski, G., Liu, C.-Q., Fowler, D., and Liu, X.-Y.: Significant contributions of combustion-related sources to ammonia emissions, *Nat Commun*, 13, 7710, <https://doi.org/10.1038/s41467-022-35381-4>, 2022.
- Crotti, I., Landais, A., Stenni, B., Bazin, L., Parrenin, F., Frezzotti, M., Ritterbusch, F., Lu, Z.-T., Jiang, W., Yang, G.-M., Fourré, E., Orsi, A., Jacob, R., Minster, B., Prié, F., Dreossi, G., and Barbante, C.: An extension of the TALDICE ice core age scale reaching back to MIS 10.1, *Quaternary Science Reviews*, 266, 107078, <https://doi.org/10.1016/j.quascirev.2021.107078>, 2021.
- Dani, K. G. S., Mader, H. M., Wolff, E. W., and Wadham, J. L.: Modelling the liquid-water vein system within polar ice sheets as a potential microbial habitat, *Earth and Planetary Science Letters*, 333–334, 238–249, <https://doi.org/10.1016/j.epsl.2012.04.009>, 2012.
- Delmas, R. J.: A natural artefact in Greenland ice-core CO<sub>2</sub> measurements, *Tellus B*, 45, 391–396, <https://doi.org/10.1034/j.1600-0889.1993.t01-3-00006.x>, 1993.
- Delmonte, B., Basile-Doelsch, I., Petit, J.-R., Maggi, V., Revel-Rolland, M., Michard, A., Jagoutz, E., and Grousset, F.: Comparing the Epica and Vostok dust records during the last 220,000 years: stratigraphical correlation and provenance in glacial periods, *Earth-Science Reviews*, 66, 63–87, <https://doi.org/10.1016/j.earscirev.2003.10.004>, 2004.
- Delmonte, B., Baroni, C., Andersson, P. S., Schoberg, H., Hansson, M., Aciego, S., Petit, J., Albani, S., Mazzola, C., Maggi, V., and Frezzotti, M.: Aeolian dust in the Talos Dome ice core (East Antarctica, Pacific/Ross Sea sector): Victoria Land

- versus* remote sources over the last two climate cycles, *J Quaternary Science*, 25, 1327–1337, <https://doi.org/10.1002/jqs.1418>, 2010.
- EPICA community members: Eight glacial cycles from an Antarctic ice core, *Nature*, 429, 623–628, <https://doi.org/10.1038/nature02599>, 2004.
- 910 EPICA Community Members: Stable oxygen isotopes of ice core EDML, <https://doi.org/10.1594/PANGAEA.754444>, 2010.
- Erbland, J.: Contraintes isotopiques sur l'interprétation de l'enregistrement en nitrate dans la carotte de glace de Vostok, Université de Grenoble, 2011.
- Erbland, J., Vicars, W. C., Savarino, J., Morin, S., Frey, M. M., Frosini, D., Vince, E., and Martins, J. M. F.: Air–snow transfer of nitrate on the East Antarctic Plateau – Part 1: Isotopic evidence for a photolytically driven dynamic equilibrium in summer, *Atmos. Chem. Phys.*, 13, 6403–6419, <https://doi.org/10.5194/acp-13-6403-2013>, 2013.
- 915 Fehling, C.: Mechanistic Insights from the  $^{15}\text{N}$ -Site Preference of Nitrous Oxide utilizing High Resolution Near-Infrared cw Cavity Ringdown Spectroscopy and Density Functional Theory Calculations, PhD Thesis, Kiel University, 130 pp., 2012.
- Fischer, H., Fundel, F., Ruth, U., Twarloh, B., Wegner, A., Udisti, R., Becagli, S., Castellano, E., Morganti, A., Severi, M., Wolff, E., Littot, G., Röthlisberger, R., Mulvaney, R., Hutterli, M. A., Kaufmann, P., Federer, U., Lambert, F., Bigler, M.,
- 920 Hansson, M., Jonsell, U., De Angelis, M., Boutron, C., Siggaard-Andersen, M.-L., Steffensen, J. P., Barbante, C., Gaspari, V., Gabrielli, P., and Wagenbach, D.: Reconstruction of millennial changes in dust emission, transport and regional sea ice coverage using the deep EPICA ice cores from the Atlantic and Indian Ocean sector of Antarctica, *Earth and Planetary Science Letters*, 260, 340–354, <https://doi.org/10.1016/j.epsl.2007.06.014>, 2007.
- Fischer, H., Schmitt, J., Bock, M., Seth, B., Joos, F., Spahni, R., Lienert, S., Battaglia, G., Stocker, B. D., Schilt, A., and
- 925 Brook, E. J.:  $\text{N}_2\text{O}$  changes from the Last Glacial Maximum to the preindustrial – Part 1: Quantitative reconstruction of terrestrial and marine emissions using  $\text{N}_2\text{O}$  stable isotopes in ice cores, *Biogeosciences*, 16, 3997–4021, <https://doi.org/10.5194/bg-16-3997-2019>, 2019.
- Flückiger, J., Monnin, E., Stauffer, B., Schwander, J., Stocker, T. F., Chappellaz, J., Raynaud, D., and Barnola, J.-M.: High-resolution Holocene  $\text{N}_2\text{O}$  ice core record and its relationship with  $\text{CH}_4$  and  $\text{CO}_2$ : High-resolution Holocene  $\text{N}_2\text{O}$  ice core
- 930 record, *Global Biogeochem. Cycles*, 16, 10-1-10–8, <https://doi.org/10.1029/2001GB001417>, 2002.
- Flückiger, J., Blunier, T., Stauffer, B., Chappellaz, J., Spahni, R., Kawamura, K., Schwander, J., Stocker, T. F., and Dahl-Jensen, D.:  $\text{N}_2\text{O}$  and  $\text{CH}_4$  variations during the last glacial epoch: Insight into global processes., *Global Biogeochem. Cycles*, 18, n/a-n/a, <https://doi.org/10.1029/2003GB002122>, 2004.
- Frame, C. H. and Casciotti, K. L.: Biogeochemical controls and isotopic signatures of nitrous oxide production by a marine ammonia-oxidizing bacterium, *Biogeosciences*, 7, 2695–2709, <https://doi.org/10.5194/bg-7-2695-2010>, 2010.
- 935 Frame, C. H., Lau, E., Nolan, E. J., Goepfert, T. J., and Lehmann, M. F.: Acidification Enhances Hybrid  $\text{N}_2\text{O}$  Production Associated with Aquatic Ammonia-Oxidizing Microorganisms, *Front. Microbiol.*, 7, <https://doi.org/10.3389/fmicb.2016.02104>, 2017.

- 940 Frey, M. M., Savarino, J., Morin, S., Erbland, J., and Martins, J. M. F.: Photolysis imprint in the nitrate stable isotope signal  
in snow and atmosphere of East Antarctica and implications for reactive nitrogen cycling, *Atmos. Chem. Phys.*, 9, 8681–  
8696, <https://doi.org/10.5194/acp-9-8681-2009>, 2009.
- Fuhrer, K., Wolff, E., and Johnsen, S. J.: Timescales for dust variability in the Greenland Ice Core Project (GRIP) ice core in  
the last 100,000 years, *J. Geophys. Res.*, 104, 31043–31052, <https://doi.org/10.1029/1999JD900929>, 1999.
- 945 Gruber, N. and Galloway, J. N.: An Earth-system perspective of the global nitrogen cycle, *Nature*, 451, 293–296,  
<https://doi.org/10.1038/nature06592>, 2008.
- Heil, J., Wolf, B., Brüggemann, N., Emmenegger, L., Tuzson, B., Vereecken, H., and Mohn, J.: Site-specific <sup>15</sup>N isotopic  
signatures of abiotically produced N<sub>2</sub>O, *Geochimica et Cosmochimica Acta*, 139, 72–82,  
<https://doi.org/10.1016/j.gca.2014.04.037>, 2014.
- 950 Heil, J., Liu, S., Vereecken, H., and Brüggemann, N.: Abiotic nitrous oxide production from hydroxylamine in soils and their  
dependence on soil properties, *Soil Biology and Biochemistry*, 84, 107–115, <https://doi.org/10.1016/j.soilbio.2015.02.022>,  
2015.
- Herron, M. M. and Langway, C. C.: Firm Densification: An Empirical Model, *J. Glaciol.*, 25, 373–385,  
<https://doi.org/10.3189/S0022143000015239>, 1980.
- 955 IPCC: Climate Change 2021: The Physical Science Basis. Contribution of Working Group I to the Sixth Assessment Report  
of the Intergovernmental Panel on Climate Change, , In Press, <https://doi.org/10.1017/9781009157896>, 2021.
- Jones, L. C., Peters, B., Lezama Pacheco, J. S., Casciotti, K. L., and Fendorf, S.: Stable Isotopes and Iron Oxide Mineral  
Products as Markers of Chemodenitrification., *Environ. Sci. Technol.*, 49, 3444–3452, <https://doi.org/10.1021/es504862x>,  
2015.
- 960 Jung, M.-Y., Gwak, J.-H., Rohe, L., Giesemann, A., Kim, J.-G., Well, R., Madsen, E. L., Herbold, C. W., Wagner, M., and  
Rhee, S.-K.: Indications for enzymatic denitrification to N<sub>2</sub>O at low pH in an ammonia-oxidizing archaeon, *The ISME  
Journal*, 13, 2633–2638, <https://doi.org/10.1038/s41396-019-0460-6>, 2019.
- Kaiser, J., Hastings, M. G., Houlton, B. Z., Röckmann, T., and Sigman, D. M.: Triple Oxygen Isotope Analysis of Nitrate  
Using the Denitrifier Method and Thermal Decomposition of N<sub>2</sub>O, *Anal. Chem.*, 79, 599–607,  
<https://doi.org/10.1021/ac061022s>, 2007.
- 965 Kaufmann, P., Fundel, F., Fischer, H., Bigler, M., Ruth, U., Udisti, R., Hansson, M., de Angelis, M., Barbante, C., Wolff, E.  
W., Hutterli, M., and Wagenbach, D.: Ammonium and non-sea salt sulfate in the EPICA ice cores as indicator of biological  
activity in the Southern Ocean, *Quaternary Science Reviews*, 29, 313–323, <https://doi.org/10.1016/j.quascirev.2009.11.009>,  
2010.
- 970 Kindler, P., Guillevic, M., Baumgartner, M., Schwander, J., Landais, A., and Leuenberger, M.: Temperature reconstruction  
from 10 to 120 kyr b2k from the NGRIP ice core, *Clim. Past*, 10, 887–902, <https://doi.org/10.5194/cp-10-887-2014>, 2014.
- Lambert, F., Bigler, M., Steffensen, J. P., Hutterli, M., and Fischer, H.: Centennial mineral dust variability in high-resolution  
ice core data from Dome C, Antarctica, *Clim. Past*, 8, 609–623, <https://doi.org/10.5194/cp-8-609-2012>, 2012.

- Lamothe, A., Savarino, J., Ginot, P., Soussaintjean, L., Gautier, E., Akers, P. D., Caillon, N., and Erbland, J.: An extraction method for nitrogen isotope measurement of ammonium in a low-concentration environment, *Atmos. Meas. Tech.*, 16, 975 4015–4030, <https://doi.org/10.5194/amt-16-4015-2023>, 2023.
- Lan, X., Thoning, K., Dlugokencky, E., and NOAA Global Monitoring Laboratory: Trends in globally-averaged CH<sub>4</sub>, N<sub>2</sub>O, and SF<sub>6</sub> determined from NOAA Global Monitoring Laboratory measurements (Version 2025-04), <https://doi.org/10.15138/P8XG-AA10>, 2025.
- Landais, A. and Stenni, B.: Water stable isotopes (dD, d18O) from EPICA Dome C ice core (Antarctica) (0-800 ka), 980 <https://doi.org/10.1594/PANGAEA.934094>, 2021.
- Lee, J. E., Edwards, J. S., Schmitt, J., Fischer, H., Bock, M., and Brook, E. J.: Excess methane in Greenland ice cores associated with high dust concentrations, *Geochimica et Cosmochimica Acta*, 270, 409–430, <https://doi.org/10.1016/j.gca.2019.11.020>, 2020.
- Lewicka-Szczebak, D., Well, R., Bol, R., Gregory, A. S., Matthews, G. P., Misselbrook, T., Whalley, W. R., and Cardenas, 985 L. M.: Isotope fractionation factors controlling isotopocule signatures of soil-emitted N<sub>2</sub> O produced by denitrification processes of various rates, *Rapid Comm Mass Spectrometry*, 29, 269–282, <https://doi.org/10.1002/rcm.7102>, 2015.
- Lorius, C., Jouzel, J., Ritz, C., Merlivat, L., Barkov, N. I., Korotkevitch, Y. S., and Kotlyakov, V.: Delta 18O record versus age for 150 ka in ice core Vostok, <https://doi.org/10.1594/PANGAEA.860950>, 1985.
- Loulergue, L., Schilt, A., Spahni, R., Masson-Delmotte, V., Blunier, T., Lemieux, B., Barnola, J.-M., Raynaud, D., Stocker, 990 T. F., and Chappellaz, J.: Orbital and millennial-scale features of atmospheric CH<sub>4</sub> over the past 800,000 years, *Nature*, 453, 383–386, <https://doi.org/10.1038/nature06950>, 2008.
- Lüthi, D., Le Floch, M., Bereiter, B., Blunier, T., Barnola, J.-M., Siegenthaler, U., Raynaud, D., Jouzel, J., Fischer, H., Kawamura, K., and Stocker, T. F.: High-resolution carbon dioxide concentration record 650,000–800,000 years before present, *Nature*, 453, 379–382, <https://doi.org/10.1038/nature06949>, 2008.
- 995 Marino, F., Castellano, E., Nava, S., Chiari, M., Ruth, U., Wegner, A., Lucarelli, F., Udisti, R., Delmonte, B., and Maggi, V.: Coherent composition of glacial dust on opposite sides of the East Antarctic Plateau inferred from the deep EPICA ice cores, *Geophysical Research Letters*, 36, 2009GL040732, <https://doi.org/10.1029/2009GL040732>, 2009.
- Markle, B. R. and Steig, E. J.: Improving temperature reconstructions from ice-core water-isotope records, *Clim. Past*, 18, 1321–1368, <https://doi.org/10.5194/cp-18-1321-2022>, 2022.
- 1000 Mayewski, P. A., Meeker, L. D., Whitlow, S., Twickler, M. S., Morrison, M. C., Bloomfield, P., Bond, G. C., Alley, R. B., Gow, A. J., Meese, D. A., Grootes, P. M., Ram, M., Taylor, K. C., and Wumkes, W.: Changes in Atmospheric Circulation and Ocean Ice Cover over the North Atlantic During the Last 41,000 Years, *Science*, 263, 1747–1751, <https://doi.org/10.1126/science.263.5154.1747>, 1994.
- Menking, J. A., Brook, E. J., Schilt, A., Shackleton, S., Dyonisius, M., Severinghaus, J. P., and Petrenko, V. V.: Millennial- 1005 Scale Changes in Terrestrial and Marine Nitrous Oxide Emissions at the Onset and Termination of Marine Isotope Stage 4, *Geophysical Research Letters*, 47, <https://doi.org/10.1029/2020GL089110>, 2020.

- Menking, J. A., Lee, J. E., Brook, E. J., Schmitt, J., Soussaintjean, L., Fischer, H., Kaiser, J., and Rice, A.: Glacial-Interglacial and Millennial-Scale Changes in Nitrous Oxide Emissions Pathways and Source Regions, *Global Biogeochemical Cycles*, 39, e2024GB008287, <https://doi.org/10.1029/2024GB008287>, 2025.
- 1010 Meusinger, C., Berhanu, T. A., Erbland, J., Savarino, J., and Johnson, M. S.: Laboratory study of nitrate photolysis in Antarctic snow. I. Observed quantum yield, domain of photolysis, and secondary chemistry, *The Journal of Chemical Physics*, 140, 244305, <https://doi.org/10.1063/1.4882898>, 2014.
- Miteva, V.: Bacteria in Snow and Glacier Ice, in: *Psychrophiles: from Biodiversity to Biotechnology*, Springer Berlin Heidelberg, Berlin, Heidelberg, 31–50, [https://doi.org/10.1007/978-3-540-74335-4\\_3](https://doi.org/10.1007/978-3-540-74335-4_3), 2008.
- 1015 Miteva, V., Sowers, T., and Brenchley, J.: Production of N<sub>2</sub>O by Ammonia Oxidizing Bacteria at Subfreezing Temperatures as a Model for Assessing the N<sub>2</sub>O Anomalies in the Vostok Ice Core, *Geomicrobiology Journal*, 24, 451–459, <https://doi.org/10.1080/01490450701437693>, 2007.
- Miteva, V., Sowers, T., Schüpbach, S., Fischer, H., and Brenchley, J.: Geochemical and Microbiological Studies of Nitrous Oxide Variations within the New NEEM Greenland Ice Core during the Last Glacial Period, *Geomicrobiology Journal*, 33, 647–660, <https://doi.org/10.1080/01490451.2015.1074321>, 2016.
- 1020 Morin, S., Savarino, J., Frey, M. M., Domine, F., Jacobi, H.-W., Kaleschke, L., and Martins, J. M. F.: Comprehensive isotopic composition of atmospheric nitrate in the Atlantic Ocean boundary layer from 65°S to 79°N, *J. Geophys. Res.*, 114, D05303, <https://doi.org/10.1029/2008JD010696>, 2009.
- Mühl, M., Schmitt, J., Seth, B., Lee, J. E., Edwards, J. S., Brook, E. J., Blunier, T., and Fischer, H.: Methane, ethane, and propane production in Greenland ice core samples and a first isotopic characterization of excess methane, *Clim. Past*, 19, 999–1025, <https://doi.org/10.5194/cp-19-999-2023>, 2023.
- 1025 Perron, J. R., Stedman, G., and Uysal, N.: Kinetic and product study of the reaction between nitrous acid and hydrazine, *J. Chem. Soc., Dalton Trans.*, 2058, <https://doi.org/10.1039/dt9760002058>, 1976.
- Prather, M. J., Hsu, J., DeLuca, N. M., Jackman, C. H., Oman, L. D., Douglass, A. R., Fleming, E. L., Strahan, S. E., 1030 Steenrod, S. D., Søvde, O. A., Isaksen, I. S. A., Froidevaux, L., and Funke, B.: Measuring and modeling the lifetime of nitrous oxide including its variability, *J. Geophys. Res. Atmos.*, 120, 5693–5705, <https://doi.org/10.1002/2015JD023267>, 2015.
- Priscu, J. C., Christner, B. C., Dore, J. E., Popp, B. N., Casciotti, K. L., and Lyons, W. B.: Supersaturated N<sub>2</sub>O in a perennially ice-covered Antarctic lake: Molecular and stable isotopic evidence for a biogeochemical relict, *Limnology & Oceanography*, 53, 2439–2450, <https://doi.org/10.4319/lo.2008.53.6.2439>, 2008.
- 1035 Prokopiou, M., Sapart, C. J., Rosen, J., Sperlich, P., Blunier, T., Brook, E., Van De Wal, R. S. W., and Röckmann, T.: Changes in the Isotopic Signature of Atmospheric Nitrous Oxide and Its Global Average Source During the Last Three Millennia, *JGR Atmospheres*, 123, <https://doi.org/10.1029/2018JD029008>, 2018.
- Rasmussen, S. O., Dahl-Jensen, D., Fischer, H., Fuhrer, K., Hansen, S. B., Hansson, M., Hvidberg, C. S., Jonsell, U., 1040 Kipfstuhl, S., Ruth, U., Schwander, J., Siggaard-Andersen, M.-L., Sinnl, G., Steffensen, J. P., Svensson, A. M., and Vinther,

- B. M.: Ice-core data used for the construction of the Greenland Ice-Core Chronology 2005 and 2021 (GICC05 and GICC21), *Earth Syst. Sci. Data*, 15, 3351–3364, <https://doi.org/10.5194/essd-15-3351-2023>, 2023.
- Ravishankara, A. R., Daniel, J. S., and Portmann, R. W.: Nitrous Oxide (N<sub>2</sub>O): The Dominant Ozone-Depleting Substance Emitted in the 21st Century, *Science*, 326, 123–125, <https://doi.org/10.1126/science.1176985>, 2009.
- 1045 Ritz, C., Lliboutry, L., and Rado, C.: Analysis of a 870 m deep temperature profile at Dome C, *Annals of Glaciology*, 3, 284–289, 1982.
- Rohde, R. A., Price, P. B., Bay, R. C., and Bramall, N. E.: In situ microbial metabolism as a cause of gas anomalies in ice, *Proceedings of the National Academy of Sciences*, 105, 8667–8672, <https://doi.org/10.1073/pnas.0803763105>, 2008.
- Röthlisberger, R., Hutterli, M. A., Sommer, S., Wolff, E. W., and Mulvaney, R.: Factors controlling nitrate in ice cores: Evidence from the Dome C deep ice core, *J. Geophys. Res.*, 105, 20565–20572, <https://doi.org/10.1029/2000JD900264>, 2000a.
- Röthlisberger, R., Bigler, M., Hutterli, M., Sommer, S., Stauffer, B., Junghans, H. G., and Wagenbach, D.: Technique for Continuous High-Resolution Analysis of Trace Substances in Firn and Ice Cores, *Environ. Sci. Technol.*, 34, 338–342, <https://doi.org/10.1021/es9907055>, 2000b.
- 1055 Rubasinghege, G., Spak, S. N., Stanier, C. O., Carmichael, G. R., and Grassian, V. H.: Abiotic Mechanism for the Formation of Atmospheric Nitrous Oxide from Ammonium Nitrate, *Environ. Sci. Technol.*, 45, 2691–2697, <https://doi.org/10.1021/es103295v>, 2011.
- Rubino, M., Etheridge, D. M., Thornton, D. P., Howden, R., Allison, C. E., Francey, R. J., Langenfelds, R. L., Steele, L. P., Trudinger, C. M., Spencer, D. A., Curran, M. A. J., Van Ommen, T. D., and Smith, A. M.: Revised records of atmospheric trace gases CO<sub>2</sub>, CH<sub>4</sub>, N<sub>2</sub>O, and d<sup>13</sup>C-CO<sub>2</sub> over the last 2000 years from Law Dome, Antarctica, *Earth Syst. Sci. Data*, 11, 473–492, <https://doi.org/10.5194/essd-11-473-2019>, 2019.
- Ruth, U., Wagenbach, D., Bigler, M., Steffensen, J. P., Röthlisberger, R., and Miller, H.: High-resolution microparticle profiles at NorthGRIP, Greenland: case studies of the calcium–dust relationship, *Ann. Glaciol.*, 35, 237–242, <https://doi.org/10.3189/172756402781817347>, 2002.
- 1065 Ruth, U., Wagenbach, D., Steffensen, J. P., and Bigler, M.: Continuous record of microparticle concentration and size distribution in the central Greenland NGRIP ice core during the last glacial period, *J. Geophys. Res.*, 108, 2002JD002376, <https://doi.org/10.1029/2002JD002376>, 2003.
- Salamatin, A. N., Lipenkov, V. Y., and Blinov, K. V.: Vostok (Antarctica) climate record time-scale deduced from the analysis of a borehole-temperature profile, *Annals of Glaciology*, 20, 207–214, 1994.
- 1070 Samarkin, V. A., Madigan, M. T., Bowles, M. W., Casciotti, K. L., Priscu, J. C., McKay, C. P., and Joye, S. B.: Abiotic nitrous oxide emission from the hypersaline Don Juan Pond in Antarctica, *Nature Geosci*, 3, 341–344, <https://doi.org/10.1038/ngeo847>, 2010.

- Schilt, A., Baumgartner, M., Schwander, J., Buiron, D., Capron, E., Chappellaz, J., Loulergue, L., Schüpbach, S., Spahni, R., Fischer, H., and Stocker, T. F.: Atmospheric nitrous oxide during the last 140,000 years, *Earth and Planetary Science Letters*, 1075 300, 33–43, <https://doi.org/10.1016/j.epsl.2010.09.027>, 2010a.
- Schilt, A., Baumgartner, M., Blunier, T., Schwander, J., Spahni, R., Fischer, H., and Stocker, T. F.: Glacial–interglacial and millennial-scale variations in the atmospheric nitrous oxide concentration during the last 800,000 years, *Quaternary Science Reviews*, 29, 182–192, <https://doi.org/10.1016/j.quascirev.2009.03.011>, 2010b.
- Schilt, A., Baumgartner, M., Eicher, O., Chappellaz, J., Schwander, J., Fischer, H., and Stocker, T. F.: The response of atmospheric nitrous oxide to climate variations during the last glacial period, *Geophysical Research Letters*, 1080 40, 1888–1893, <https://doi.org/10.1002/grl.50380>, 2013.
- Schilt, A., Brook, E. J., Bauska, T. K., Baggenstos, D., Fischer, H., Joos, F., Petrenko, V. V., Schaefer, H., Schmitt, J., Severinghaus, J. P., Spahni, R., and Stocker, T. F.: Isotopic constraints on marine and terrestrial N<sub>2</sub>O emissions during the last deglaciation, *Nature*, 516, 234–237, <https://doi.org/10.1038/nature13971>, 2014.
- Schmitt, J., Seth, B., Bock, M., and Fischer, H.: Online technique for isotope and mixing ratios of CH<sub>4</sub>, N<sub>2</sub>O, Xe and mixing ratios of organic trace gases on a single ice core sample, *Atmos. Meas. Tech.*, 7, 2645–2665, <https://doi.org/10.5194/amt-7-2645-2014>, 2014.
- Schüpbach, S., Federer, U., Kaufmann, P. R., Albani, S., Barbante, C., Stocker, T. F., and Fischer, H.: Calcium and sodium concentrations of the Talos Dome ice core, *Antarctica*, <https://doi.org/10.1594/PANGAEA.833044>, 2014.
- Sowers, T.: N<sub>2</sub>O record spanning the penultimate deglaciation from the Vostok ice core, *J. Geophys. Res.*, 106, 31903–31914, <https://doi.org/10.1029/2000JD900707>, 2001.
- Spahni, R., Chappellaz, J., Stocker, T. F., Loulergue, L., Hausammann, G., Kawamura, K., Flückiger, J., Schwander, J., Raynaud, D., Masson-Delmotte, V., and Jouzel, J.: Atmospheric Methane and Nitrous Oxide of the Late Pleistocene from Antarctic Ice Cores, *Science*, 310, 1317–1321, <https://doi.org/10.1126/science.1120132>, 2005.
- Spolaor, A., Vallelonga, P., Gabrieli, J., Cozzi, G., Boutron, C., and Barbante, C.: Determination of Fe<sup>2+</sup> and Fe<sup>3+</sup> species by FIA-CRC-ICP-MS in Antarctic ice samples, *J. Anal. At. Spectrom.*, 27, 310–317, <https://doi.org/10.1039/C1JA10276A>, 2012.
- Spolaor, A., Vallelonga, P., Cozzi, G., Gabrieli, J., Varin, C., Kehrwald, N., Zennaro, P., Boutron, C., and Barbante, C.: Iron speciation in aerosol dust influences iron bioavailability over glacial-interglacial timescales, *Geophysical Research Letters*, 1100 40, 1618–1623, <https://doi.org/10.1002/grl.50296>, 2013.
- Spott, O., Russow, R., and Stange, C. F.: Formation of hybrid N<sub>2</sub>O and hybrid N<sub>2</sub> due to codenitrification: First review of a barely considered process of microbially mediated N-nitrosation, *Soil Biology and Biochemistry*, 43, 1995–2011, <https://doi.org/10.1016/j.soilbio.2011.06.014>, 2011.
- Stauffer, B., Flückiger, J., Monnin, E., Nakazawa, T., and Aoki, S.: Discussion of the reliability of CO<sub>2</sub>, CH<sub>4</sub> and N<sub>2</sub>O records from polar ice cores, *Mem. Natl Inst. Polar Res.*, 139–152, 2003.

- Stieglmeier, M., Mooshammer, M., Kitzler, B., Wanek, W., Zechmeister-Boltenstern, S., Richter, A., and Schleper, C.: Aerobic nitrous oxide production through N-nitrosating hybrid formation in ammonia-oxidizing archaea, *The ISME Journal*, 8, 1135–1146, <https://doi.org/10.1038/ismej.2013.220>, 2014.
- 1110 Su, Q., Domingo-Félez, C., Jensen, M. M., and Smets, B. F.: Abiotic Nitrous Oxide (N<sub>2</sub>O) Production Is Strongly pH Dependent, but Contributes Little to Overall N<sub>2</sub>O Emissions in Biological Nitrogen Removal Systems, *Environ. Sci. Technol.*, 53, 3508–3516, <https://doi.org/10.1021/acs.est.8b06193>, 2019.
- Sutka, R. L., Ostrom, N. E., Ostrom, P. H., Gandhi, H., and Breznak, J. A.: Nitrogen isotopomer site preference of N<sub>2</sub>O produced by *Nitrosomonas europaea* and *Methylococcus capsulatus* Bath, *Rapid Comm Mass Spectrometry*, 17, 738–745, <https://doi.org/10.1002/rcm.968>, 2003.
- 1115 Sutka, R. L., Ostrom, N. E., Ostrom, P. H., Breznak, J. A., Gandhi, H., Pitt, A. J., and Li, F.: Distinguishing Nitrous Oxide Production from Nitrification and Denitrification on the Basis of Isotopomer Abundances, *Appl Environ Microbiol*, 72, 638–644, <https://doi.org/10.1128/AEM.72.1.638-644.2006>, 2006.
- Tarasov, L. and Peltier, W. R.: Greenland glacial history, borehole constraints, and Eemian extent, *J. Geophys. Res.*, 108, 2001JB001731, <https://doi.org/10.1029/2001JB001731>, 2003.
- 1120 Terada, A., Sugawara, S., Hojo, K., Takeuchi, Y., Riya, S., Harper, W. F., Yamamoto, T., Kuroiwa, M., Isobe, K., Katsuyama, C., Suwa, Y., Koba, K., and Hosomi, M.: Hybrid Nitrous Oxide Production from a Partial Nitrifying Bioreactor: Hydroxylamine Interactions with Nitrite, *Environ. Sci. Technol.*, 51, 2748–2756, <https://doi.org/10.1021/acs.est.6b05521>, 2017.
- Tian, H., Xu, R., Canadell, J. G., Thompson, R. L., Winiwarter, W., Suntharalingam, P., Davidson, E. A., Ciais, P., Jackson, 1125 R. B., Janssens-Maenhout, G., Prather, M. J., Regnier, P., Pan, N., Pan, S., Peters, G. P., Shi, H., Tubiello, F. N., Zaehle, S., Zhou, F., Arneeth, A., Battaglia, G., Berthet, S., Bopp, L., Bouwman, A. F., Buitenhuis, E. T., Chang, J., Chipperfield, M. P., Dangal, S. R. S., Dlugokencky, E., Elkins, J. W., Eyre, B. D., Fu, B., Hall, B., Ito, A., Joos, F., Krummel, P. B., Landolfi, A., Laruelle, G. G., Lauerwald, R., Li, W., Lienert, S., Maavara, T., MacLeod, M., Millet, D. B., Olin, S., Patra, P. K., Prinn, R. G., Raymond, P. A., Ruiz, D. J., van der Werf, G. R., Vuichard, N., Wang, J., Weiss, R. F., Wells, K. C., Wilson, C., Yang, 1130 J., and Yao, Y.: A comprehensive quantification of global nitrous oxide sources and sinks, *Nature*, 586, 248–256, <https://doi.org/10.1038/s41586-020-2780-0>, 2020.
- Tischer, J., Zopfi, J., Frey, C., Magyar, P. M., Brand, A., Oswald, K., Jegge, C., Frame, C. H., Miracle, M. R., Sòria-Perpinyà, X., Vicente, E., and Lehmann, M. F.: Isotopic signatures of biotic and abiotic N<sub>2</sub>O production and consumption in the water column of meromictic, ferruginous Lake La Cruz (Spain), *Limnology & Oceanography*, 67, 1760–1775, 1135 <https://doi.org/10.1002/lno.12165>, 2022.
- Toyoda, S., Yoshida, N., Miwa, T., Matsui, Y., Yamagishi, H., Tsunogai, U., Nojiri, Y., and Tsurushima, N.: Production mechanism and global budget of N<sub>2</sub>O inferred from its isotopomers in the western North Pacific, *Geophysical Research Letters*, 29, <https://doi.org/10.1029/2001GL014311>, 2002.

- Toyoda, S., Mutobe, H., Yamagishi, H., Yoshida, N., and Tanji, Y.: Fractionation of N<sub>2</sub>O isotopomers during production by denitrifier, *Soil Biology and Biochemistry*, 37, 1535–1545, <https://doi.org/10.1016/j.soilbio.2005.01.009>, 2005.
- 1140 Toyoda, S., Yoshida, N., and Koba, K.: Isotopocule analysis of biologically produced nitrous oxide in various environments, *Mass Spectrometry Reviews*, 36, 135–160, <https://doi.org/10.1002/mas.21459>, 2017.
- Traversi, R., Barbante, C., Gaspari, V., Fattori, I., Largiuni, O., Magaldi, L., and Udisti, R.: Aluminium and iron record for the last 28 kyr derived from the Antarctic EDC96 ice core using new CFA methods, *Ann. Glaciol.*, 39, 300–306, 1145 <https://doi.org/10.3189/172756404781814438>, 2004.
- Warneck, P. and Wurzinger, C.: Product quantum yields for the 305-nm photodecomposition of nitrate in aqueous solution, *J. Phys. Chem.*, 92, 6278–6283, <https://doi.org/10.1021/j100333a022>, 1988.
- Wilhelms, F., Sheldon, S. G., Hamann, I., and Kipfstuhl, S.: Implications for and findings from deep ice core drillings an example: The ultimate tensile strength of ice at high strain rates, *Physics and Chemistry of Ice (The proceedings of the International Conference on the Physics and Chemistry of Ice held at Bremerhaven, Germany on 23-28 July 2006)* The Royal Society of Chemistry Special Publication No. 311, 635–639, 2007.
- 1150 Wolff, E. W., Moore, J. C., Clausen, H. B., and Hammer, C. U.: Climatic implications of background acidity and other chemistry derived from electrical studies of the Greenland Ice Core Project ice core, *J. Geophys. Res.*, 102, 26325–26332, <https://doi.org/10.1029/96JC02223>, 1997.
- 1155 Wrage-Mönnig, N., Horn, M. A., Well, R., Müller, C., Velthof, G., and Oenema, O.: The role of nitrifier denitrification in the production of nitrous oxide revisited, *Soil Biology and Biochemistry*, 123, A3–A16, <https://doi.org/10.1016/j.soilbio.2018.03.020>, 2018.
- York, D., Evensen, N. M., Martínez, M. L., and De Basabe Delgado, J.: Unified equations for the slope, intercept, and standard errors of the best straight line, *American Journal of Physics*, 72, 367–375, <https://doi.org/10.1119/1.1632486>, 2004.
- 1160 Yu, L., Harris, E., Lewicka-Szczebak, D., Barthel, M., Blomberg, M. R. A., Harris, S. J., Johnson, M. S., Lehmann, M. F., Liisberg, J., Müller, C., Ostrom, N. E., Six, J., Toyoda, S., Yoshida, N., and Mohn, J.: What can we learn from N<sub>2</sub>O isotope data? – Analytics, processes and modelling, *Rapid Comm Mass Spectrometry*, 34, e8858, <https://doi.org/10.1002/rcm.8858>, 2020.
- Zhu-Barker, X., Cavazos, A. R., Ostrom, N. E., Horwath, W. R., and Glass, J. B.: The importance of abiotic reactions for nitrous oxide production, *Biogeochemistry*, 126, 251–267, <https://doi.org/10.1007/s10533-015-0166-4>, 2015.

- 1170 ~~Aarons, S. M., Aciego, S. M., Arendt, C. A., Blakowski, M. A., Steigmeyer, A., Gabrielli, P., Sierra Hernández, M. R., Beaudon, E., Delmonte, B., Baccolo, G., May, N. W., and Pratt, K. A.: Dust composition changes from Taylor Glacier (East Antarctica) during the last glacial interglacial transition: A multi proxy approach, *Quaternary Science Reviews*, 162, 60–71, <https://doi.org/10.1016/j.quaseirev.2017.03.011>, 2017.~~
- ~~Anklin, M., Barnola, J. M., Schwander, J., Stauffer, B., and Raynaud, D.: Processes affecting the CO<sub>2</sub> concentrations measured in Greenland ice, *Tellus B*, 47, 461–470, <https://doi.org/10.1034/j.1600-0889.47.issue4.6.x>, 1995.~~

- 175 Baccolo, G., Delmonte, B., Niles, P. B., Cibin, G., Di Stefano, E., Hampai, D., Keller, L., Maggi, V., Marcelli, A., Michalski, J., Snead, C., and Frezzotti, M.: Jarosite formation in deep Antarctic ice provides a window into acidic, water-limited weathering on Mars, *Nat Commun*, 12, 436, <https://doi.org/10.1038/s41467-020-20705-z>, 2021.
- Baggenstos, D., Severinghaus, J. P., Mulvaney, R., McConnell, J. R., Sigl, M., Maselli, O., Petit, J., Grente, B., and Steig, E. J.: A Horizontal Ice Core From Taylor Glacier, Its Implications for Antarctic Climate History, and an Improved Taylor Dome Ice Core Time Scale, *Paleoceanog and Paleoclimatol*, 33, 778–794, <https://doi.org/10.1029/2017PA003297>, 2018.
- 180 Baggs, E. M.: Soil microbial sources of nitrous oxide: recent advances in knowledge, emerging challenges and future direction, *Current Opinion in Environmental Sustainability*, 3, 321–327, <https://doi.org/10.1016/j.cosust.2011.08.011>, 2011.
- Bange, H. W.: Gaseous Nitrogen Compounds (NO, N<sub>2</sub>O, N<sub>2</sub>, NH<sub>3</sub>) in the Ocean, in: *Nitrogen in the Marine Environment*, Elsevier, 51–94, <https://doi.org/10.1016/B978-0-12-372522-6.00002-5>, 2008.
- Barletta, R. E., Priscu, J. C., Mader, H. M., Jones, W. L., and Roe, C. H.: Chemical analysis of ice vein microenvironments: H. Analysis of glacial samples from Greenland and Antarctica, *J. Glaciol.*, 58, 1109–1118, <https://doi.org/10.3189/2012JG12J112>, 2012.
- 185 Battle, M., Bender, M., Sowers, T., Tans, P. P., Butler, J. H., Elkins, J. W., Ellis, J. T., Conway, T., Zhang, N., Lang, P., and Clarket, A. D.: Atmospheric gas concentrations over the past century measured in air from firn at the South Pole, *Nature*, 383, 231–235, <https://doi.org/10.1038/383231a0>, 1996.
- Bernard, S., Röckmann, T., Kaiser, J., Barnola, J. M., Fischer, H., Blunier, T., and Chappellaz, J.: Constraints on N<sub>2</sub>O budget changes since pre-industrial time from new firn air and ice core isotope measurements, *Atmos. Chem. Phys.*, 6, 493–503, <https://doi.org/10.5194/aep-6-493-2006>, 2006.
- Bigler, M.: Hochauflösende Spurenstoffmessungen an polaren Eisbohrkernen: Glazio-chemische und klimatische Prozessstudien, <https://doi.org/10.57694/7211>, 2024.
- 195 Biscaye, P. E., Grousset, F. E., Revel, M., Van Der Gaast, S., Zielinski, G. A., Vaars, A., and Kukla, G.: Asian provenance of glacial dust (stage 2) in the Greenland Ice Sheet Project 2 Ice Core, Summit, Greenland, *J. Geophys. Res.*, 102, 26765–26781, <https://doi.org/10.1029/97JC01249>, 1997.
- Blunier, T., Floch, G. L., Jacobi, H., and Quansah, E.: Isotopic view on nitrate loss in Antarctic surface snow, *Geophysical Research Letters*, 32, 2005GL023011, <https://doi.org/10.1029/2005GL023011>, 2005.
- Bohlke, J. K., Gwinn, C. J., and Coplen, T. B.: New reference materials for nitrogen isotope ratio measurements, *Geostandards and Geoanalytical Research*, 17, 159–164, <https://doi.org/10.1111/j.1751-908X.1993.tb00131.x>, 1993.
- 200 Bouchet, M., Landais, A., Grisart, A., Parrenin, F., Prié, F., Jacob, R., Fourré, E., Capron, E., Raynaud, D., Lipenkov, V. Y., Loutre, M. F., Extier, T., Svensson, A. M., Martinerie, P., Leuenberger, M. C., Jiang, W., Ritterbusch, F., Lu, Z. T., and Yang, G. M.: The Antarctic ice core chronology (AICC2023), <https://doi.org/10.1594/PANGAEA.961017>, 2023.
- Buchwald, C., Grabb, K., Hansel, C. M., and Wankel, S. D.: Constraining the role of iron in environmental nitrogen transformations: Dual stable isotope systematics of abiotic NO<sub>2</sub><sup>-</sup> reduction by Fe(II) and its production of N<sub>2</sub>O, *Geochimica et Cosmochimica Acta*, 186, 1–12, <https://doi.org/10.1016/j.gca.2016.04.041>, 2016.
- 205

- Buiron, D., Chappellaz, J., Stenni, B., Frezzotti, M., Baumgartner, M., Capron, E., Landais, A., Lemieux-Dudon, B., Masson Delmotte, V., Montagnat, M., Parrenin, F., and Schilt, A.: TALDICE 1 age scale of the Talos Dome deep ice core, East Antarctica, *Clim. Past*, 7, 1–16, <https://doi.org/10.5194/ep-7-1-2011>, 2011.
- 1210 Bunton, C. A., Llewellyn, D. R., and Stedman, G.: Oxygen exchange between nitrous acid and water, *J. Chem. Soc.*, 568, <https://doi.org/10.1039/jr9590000568>, 1959.
- Casciotti, K. L., Böhlke, J. K., McIlvin, M. R., Mroczkowski, S. J., and Hannon, J. E.: Oxygen Isotopes in Nitrite: Analysis, Calibration, and Equilibration, *Anal. Chem.*, 79, 2427–2436, <https://doi.org/10.1021/ac061598h>, 2007.
- Chen, Z. L., Song, W., Hu, C. C., Liu, X. J., Chen, G. Y., Walters, W. W., Michalski, G., Liu, C. Q., Fowler, D., and Liu, X. Y.: Significant contributions of combustion related sources to ammonia emissions, *Nat Commun*, 13, 7710, <https://doi.org/10.1038/s41467-022-35381-4>, 2022.
- 1215 Crotti, I., Landais, A., Stenni, B., Bazin, L., Parrenin, F., Frezzotti, M., Ritterbusch, F., Lu, Z. T., Jiang, W., Yang, G. M., Fourré, E., Orsi, A., Jacob, R., Minster, B., Prié, F., Dreossi, G., and Barbante, C.: An extension of the TALDICE ice core age scale reaching back to MIS 10.1, *Quaternary Science Reviews*, 266, 107078, <https://doi.org/10.1016/j.quaseirev.2021.107078>, 2021.
- 1220 Dani, K. G. S., Mader, H. M., Wolff, E. W., and Wadham, J. L.: Modelling the liquid water vein system within polar ice sheets as a potential microbial habitat, *Earth and Planetary Science Letters*, 333–334, 238–249, <https://doi.org/10.1016/j.epsl.2012.04.009>, 2012.
- Delmas, R. J.: A natural artefact in Greenland ice core CO<sub>2</sub> measurements, *Tellus B*, 45, 391–396, <https://doi.org/10.1034/j.1600-0889.1993.t013-00006.x>, 1993.
- 1225 Delmonte, B., Basile-Doelsch, I., Petit, J. R., Maggi, V., Revel-Rolland, M., Michard, A., Jagoutz, E., and Grousset, F.: Comparing the Epica and Vostok dust records during the last 220,000 years: stratigraphical correlation and provenance in glacial periods, *Earth Science Reviews*, 66, 63–87, <https://doi.org/10.1016/j.earscirev.2003.10.004>, 2004.
- Delmonte, B., Baroni, C., Andersson, P. S., Schoberg, H., Hansson, M., Aciego, S., Petit, J., Albani, S., Mazzola, C., Maggi, V., and Frezzotti, M.: Aeolian dust in the Talos Dome ice core (East Antarctica, Pacific/Ross Sea sector): Victoria Land *versus* remote sources over the last two climate cycles, *J Quaternary Science*, 25, 1327–1337, <https://doi.org/10.1002/jqs.1418>, 2010.
- 1230 EPICA community members: Eight glacial cycles from an Antarctic ice core, *Nature*, 429, 623–628, <https://doi.org/10.1038/nature02599>, 2004.
- 1235 EPICA Community Members: Stable oxygen isotopes of ice core EDML, <https://doi.org/10.1594/PANGAEA.754444>, 2010.
- Erbland, J.: Contraintes isotopiques sur l'interprétation de l'enregistrement en nitrate dans la carotte de glace de Vostok, Université de Grenoble, 2011.
- Erbland, J., Vicars, W. C., Savarino, J., Morin, S., Frey, M. M., Frosini, D., Vince, E., and Martins, J. M. F.: Air–snow transfer of nitrate on the East Antarctic Plateau—Part 1: Isotopic evidence for a photolytically driven dynamic equilibrium in summer, *Atmos. Chem. Phys.*, 13, 6403–6419, <https://doi.org/10.5194/acp-13-6403-2013>, 2013.
- 1240

- 1245 Fischer, H., Fundel, F., Ruth, U., Twarloh, B., Wegner, A., Udisti, R., Becagli, S., Castellano, E., Morganti, A., Severi, M., Wolff, E., Littot, G., Röthlisberger, R., Mulvaney, R., Hutterli, M. A., Kaufmann, P., Federer, U., Lambert, F., Bigler, M., Hansson, M., Jonsell, U., De Angelis, M., Boutron, C., Siggaard Andersen, M. L., Steffensen, J. P., Barbante, C., Gaspari, V., Gabrielli, P., and Wagenbach, D.: Reconstruction of millennial changes in dust emission, transport and regional sea ice coverage using the deep EPICA ice cores from the Atlantic and Indian Ocean sector of Antarctica, *Earth and Planetary Science Letters*, 260, 340–354, <https://doi.org/10.1016/j.epsl.2007.06.014>, 2007.
- 1250 Fischer, H., Schmitt, J., Bock, M., Seth, B., Joos, F., Spahni, R., Lienert, S., Battaglia, G., Stocker, B. D., Schilt, A., and Brook, E. J.: N<sub>2</sub>O changes from the Last Glacial Maximum to the preindustrial—Part 1: Quantitative reconstruction of terrestrial and marine emissions using N<sub>2</sub>O stable isotopes in ice cores, *Biogeosciences*, 16, 3997–4021, <https://doi.org/10.5194/bg-16-3997-2019>, 2019.
- Flückiger, J., Monnin, E., Stauffer, B., Schwander, J., Stocker, T. F., Chappellaz, J., Raynaud, D., and Barnola, J. M.: High-resolution Holocene N<sub>2</sub>O ice core record and its relationship with CH<sub>4</sub> and CO<sub>2</sub>: High resolution Holocene N<sub>2</sub>O ice core record, *Global Biogeochem. Cycles*, 16, 10–1–10–8, <https://doi.org/10.1029/2001GB001417>, 2002.
- 1255 Flückiger, J., Blunier, T., Stauffer, B., Chappellaz, J., Spahni, R., Kawamura, K., Schwander, J., Stocker, T. F., and Dahl-Jensen, D.: N<sub>2</sub>O and CH<sub>4</sub> variations during the last glacial epoch: Insight into global processes., *Global Biogeochem. Cycles*, 18, n/a–n/a, <https://doi.org/10.1029/2003GB002122>, 2004.
- Frame, C. H. and Casciotti, K. L.: Biogeochemical controls and isotopic signatures of nitrous oxide production by a marine ammonia oxidizing bacterium, *Biogeosciences*, 7, 2695–2709, <https://doi.org/10.5194/bg-7-2695-2010>, 2010.
- 1260 Frey, M. M., Savarino, J., Morin, S., Erbland, J., and Martins, J. M. F.: Photolysis imprint in the nitrate stable isotope signal in snow and atmosphere of East Antarctica and implications for reactive nitrogen cycling, *Atmos. Chem. Phys.*, 9, 8681–8696, <https://doi.org/10.5194/acp-9-8681-2009>, 2009.
- Fuhrer, K., Wolff, E., and Johnsen, S. J.: Timescales for dust variability in the Greenland Ice Core Project (GRIP) ice core in the last 100,000 years, *J. Geophys. Res.*, 104, 31043–31052, <https://doi.org/10.1029/1999JD900929>, 1999.
- 1265 Gruber, N. and Galloway, J. N.: An Earth system perspective of the global nitrogen cycle, *Nature*, 451, 293–296, <https://doi.org/10.1038/nature06592>, 2008.
- Heil, J., Wolf, B., Brüggemann, N., Emmenegger, L., Tuzson, B., Vereecken, H., and Mohn, J.: Site-specific <sup>15</sup>N isotopic signatures of abiotically produced N<sub>2</sub>O, *Geochimica et Cosmochimica Acta*, 139, 72–82, <https://doi.org/10.1016/j.gea.2014.04.037>, 2014.
- 1270 Heil, J., Liu, S., Vereecken, H., and Brüggemann, N.: Abiotic nitrous oxide production from hydroxylamine in soils and their dependence on soil properties, *Soil Biology and Biochemistry*, 84, 107–115, <https://doi.org/10.1016/j.soilbio.2015.02.022>, 2015.
- Herron, M. M. and Langway, C. C.: Firn Densification: An Empirical Model, *J. Glaciol.*, 25, 373–385, <https://doi.org/10.3189/S0022143000015239>, 1980.

1275 IPCC: Climate Change 2021: The Physical Science Basis. Contribution of Working Group I to the Sixth Assessment Report of the Intergovernmental Panel on Climate Change, In Press, <https://doi.org/10.1017/9781009157896>, 2021.

Jones, L. C., Peters, B., Lezama Pacheco, J. S., Casciotti, K. L., and Fendorf, S.: Stable Isotopes and Iron Oxide Mineral Products as Markers of Chemodenitrification., *Environ. Sci. Technol.*, 49, 3444–3452, <https://doi.org/10.1021/es504862x>, 2015.

1280 Jung, M. Y., Gwak, J. H., Rohe, L., Giesemann, A., Kim, J. G., Well, R., Madsen, E. L., Herbold, C. W., Wagner, M., and Rhee, S. K.: Indications for enzymatic denitrification to N<sub>2</sub>O at low pH in an ammonia oxidizing archaeon, *The ISME Journal*, 13, 2633–2638, <https://doi.org/10.1038/s41396-019-0460-6>, 2019.

Kaiser, J., Hastings, M. G., Houlton, B. Z., Röckmann, T., and Sigman, D. M.: Triple Oxygen Isotope Analysis of Nitrate Using the Denitrifier Method and Thermal Decomposition of N<sub>2</sub>O, *Anal. Chem.*, 79, 599–607, <https://doi.org/10.1021/ac061022s>, 2007.

1285 Kaufmann, P., Fundel, F., Fischer, H., Bigler, M., Ruth, U., Udisti, R., Hansson, M., de Angelis, M., Barbante, C., Wolff, E. W., Hutterli, M., and Wagenbach, D.: Ammonium and non-sea salt sulfate in the EPICA ice cores as indicator of biological activity in the Southern Ocean, *Quaternary Science Reviews*, 29, 313–323, <https://doi.org/10.1016/j.quascirev.2009.11.009>, 2010.

Kindler, P., Guillevie, M., Baumgartner, M., Schwander, J., Landais, A., and Leuenberger, M.: Temperature reconstruction from 10 to 120 kyr b2k from the NGRIP ice core, *Clim. Past*, 10, 887–902, <https://doi.org/10.5194/ep-10-887-2014>, 2014.

1290 Lambert, F., Bigler, M., Steffensen, J. P., Hutterli, M., and Fischer, H.: Centennial mineral dust variability in high-resolution ice core data from Dome C, Antarctica, *Clim. Past*, 8, 609–623, <https://doi.org/10.5194/ep-8-609-2012>, 2012.

Lamothe, A., Savarino, J., Ginot, P., Soussaintjean, L., Gautier, E., Akers, P. D., Caillon, N., and Erbland, J.: An extraction method for nitrogen isotope measurement of ammonium in a low concentration environment, *Atmos. Meas. Tech.*, 16, 4015–4030, <https://doi.org/10.5194/amt-16-4015-2023>, 2023.

1295 Lan, X., Thoning, K., Dlugokencky, E., and NOAA Global Monitoring Laboratory: Trends in globally averaged CH<sub>4</sub>, N<sub>2</sub>O, and SF<sub>6</sub> determined from NOAA Global Monitoring Laboratory measurements (Version 2025-04), <https://doi.org/10.15138/P8XG-AA10>, 2025.

Landais, Amaelle and Stenni, Barbara: Water stable isotopes (dD, d18O) from EPICA Dome C ice core (Antarctica) (0–800 ka), <https://doi.org/10.1594/PANGAEA.934094>, 2021.

1300 Lee, J. E., Edwards, J. S., Schmitt, J., Fischer, H., Bock, M., and Brook, E. J.: Excess methane in Greenland ice cores associated with high dust concentrations, *Geochimica et Cosmochimica Acta*, 270, 409–430, <https://doi.org/10.1016/j.gea.2019.11.020>, 2020.

Lorius, C., Jouzel, J., Ritz, C., Merlivat, L., Barkov, N. I., Korotkevitch, Y. S., and Kotlyakov, V.: Delta 18O record versus age for 150 ka in ice core Vostok, <https://doi.org/10.1594/PANGAEA.860950>, 1985.

1305

- Loulergue, L., Schilt, A., Spahni, R., Masson-Delmotte, V., Blunier, T., Lemieux, B., Barnola, J.-M., Raynaud, D., Stocker, T. F., and Chappellaz, J.: Orbital and millennial scale features of atmospheric CH<sub>4</sub> over the past 800,000 years, *Nature*, 453, 383–386, <https://doi.org/10.1038/nature06950>, 2008.
- 1310 Lüthi, D., Le Floch, M., Bereiter, B., Blunier, T., Barnola, J.-M., Siegenthaler, U., Raynaud, D., Jouzel, J., Fischer, H., Kawamura, K., and Stocker, T. F.: High resolution carbon dioxide concentration record 650,000–800,000 years before present, *Nature*, 453, 379–382, <https://doi.org/10.1038/nature06949>, 2008.
- Marino, F., Castellano, E., Nava, S., Chiari, M., Ruth, U., Wegner, A., Lucarelli, F., Udisti, R., Delmonte, B., and Maggi, V.: Coherent composition of glacial dust on opposite sides of the East Antarctic Plateau inferred from the deep EPICA ice cores, *Geophysical Research Letters*, 36, 2009GL040732, <https://doi.org/10.1029/2009GL040732>, 2009.
- 1315 Markle, B. R. and Steig, E. J.: Improving temperature reconstructions from ice core water isotope records, *Clim. Past*, 18, 1321–1368, <https://doi.org/10.5194/ep-18-1321-2022>, 2022.
- Mayewski, P. A., Meeker, L. D., Whitlow, S., Twickler, M. S., Morrison, M. C., Bloomfield, P., Bond, G. C., Alley, R. B., Gow, A. J., Meese, D. A., Grootes, P. M., Ram, M., Taylor, K. C., and Wumkes, W.: Changes in Atmospheric Circulation and Ocean Ice Cover over the North Atlantic During the Last 41,000 Years, *Science*, 263, 1747–1751, <https://doi.org/10.1126/science.263.5154.1747>, 1994.
- 1320 Menking, J. A., Brook, E. J., Schilt, A., Shackleton, S., Dyonisius, M., Severinghaus, J. P., and Petrenko, V. V.: Millennial Scale Changes in Terrestrial and Marine Nitrous Oxide Emissions at the Onset and Termination of Marine Isotope Stage 4, *Geophysical Research Letters*, 47, <https://doi.org/10.1029/2020GL089110>, 2020.
- Menking, J. A., Lee, J. E., Brook, E. J., Schmitt, J., Soussaintjean, L., Fischer, H., Kaiser, J., and Rice, A.: Glacial-Interglacial and Millennial Scale Changes in Nitrous Oxide Emissions Pathways and Source Regions, *Global Biogeochemical Cycles*, 39, e2024GB008287, <https://doi.org/10.1029/2024GB008287>, 2025.
- Miteva, V.: Bacteria in Snow and Glacier Ice, in: *Psychrophiles: from Biodiversity to Biotechnology*, edited by: Margesin, R., Schinner, F., Marx, J. C., and Gerday, C., Springer Berlin Heidelberg, Berlin, Heidelberg, 31–50, [https://doi.org/10.1007/978-3-540-74335-4\\_3](https://doi.org/10.1007/978-3-540-74335-4_3), 2008.
- 1330 Miteva, V., Sowers, T., and Brenchley, J.: Production of N<sub>2</sub>O by Ammonia Oxidizing Bacteria at Subfreezing Temperatures as a Model for Assessing the N<sub>2</sub>O Anomalies in the Vostok Ice Core, *Geomicrobiology Journal*, 24, 451–459, <https://doi.org/10.1080/01490450701437693>, 2007.
- Miteva, V., Sowers, T., Schüpbach, S., Fischer, H., and Brenchley, J.: Geochemical and Microbiological Studies of Nitrous Oxide Variations within the New NEEM Greenland Ice Core during the Last Glacial Period, *Geomicrobiology Journal*, 33, <https://doi.org/10.1080/01490451.2015.1074321>, 2016.
- 1335 Morin, S., Savarino, J., Frey, M. M., Domine, F., Jacobi, H. W., Kaleschke, L., and Martins, J. M. F.: Comprehensive isotopic composition of atmospheric nitrate in the Atlantic Ocean boundary layer from 65°S to 79°N, *J. Geophys. Res.*, 114, D05303, <https://doi.org/10.1029/2008JD010696>, 2009.

- Mühl, M., Schmitt, J., Seth, B., Lee, J. E., Edwards, J. S., Brook, E. J., Blunier, T., and Fischer, H.: Methane, ethane, and propane production in Greenland ice core samples and a first isotopic characterization of excess methane, *Clim. Past*, 19, 999–1025, <https://doi.org/10.5194/ep-19-999-2023>, 2023.
- Perron, J. R., Stedman, G., and Uysal, N.: Kinetic and product study of the reaction between nitrous acid and hydrazine, *J. Chem. Soc., Dalton Trans.*, 2058, <https://doi.org/10.1039/dt9760002058>, 1976.
- Prather, M. J., Hsu, J., DeLuca, N. M., Jackman, C. H., Oman, L. D., Douglass, A. R., Fleming, E. L., Strahan, S. E., Steenrod, S. D., Søvde, O. A., Isaksen, I. S. A., Froidevaux, L., and Funke, B.: Measuring and modeling the lifetime of nitrous oxide including its variability, *J. Geophys. Res. Atmos.*, 120, 5693–5705, <https://doi.org/10.1002/2015JD023267>, 2015.
- Priseu, J. C., Christner, B. C., Dore, J. E., Popp, B. N., Casciotti, K. L., and Lyons, W. B.: Supersaturated N<sub>2</sub>O in a perennially ice covered Antarctic lake: Molecular and stable isotopic evidence for a biogeochemical relict, *Limnology & Oceanography*, 53, 2439–2450, <https://doi.org/10.4319/lo.2008.53.6.2439>, 2008.
- Prokopiou, M., Martinerie, P., Sapart, C. J., Witrant, E., Monteil, G., Ishijima, K., Bernard, S., Kaiser, J., Levin, I., Blunier, T., Etheridge, D., Dlugokencky, E., Van De Wal, R. S. W., and Röckmann, T.: Constraining N<sub>2</sub>O emissions since 1940 using firn air isotope measurements in both hemispheres, *Atmos. Chem. Phys.*, 17, 4539–4564, <https://doi.org/10.5194/acp-17-4539-2017>, 2017.
- Prokopiou, M., Sapart, C. J., Rosen, J., Sperlich, P., Blunier, T., Brook, E., Van De Wal, R. S. W., and Röckmann, T.: Changes in the Isotopic Signature of Atmospheric Nitrous Oxide and Its Global Average Source During the Last Three Millennia, *JGR Atmospheres*, 123, <https://doi.org/10.1029/2018JD029008>, 2018.
- Rasmussen, S. O., Dahl Jensen, D., Fischer, H., Fuhrer, K., Hansen, S. B., Hansson, M., Hvidberg, C. S., Jonsell, U., Kipfstuhl, S., Ruth, U., Schwander, J., Siggaard Andersen, M. L., Sinnl, G., Steffensen, J. P., Svensson, A. M., and Vinther, B. M.: Ice core data used for the construction of the Greenland Ice Core Chronology 2005 and 2021 (GICC05 and GICC21), *Earth Syst. Sci. Data*, 15, 3351–3364, <https://doi.org/10.5194/essd-15-3351-2023>, 2023.
- Ravishankara, A. R., Daniel, J. S., and Portmann, R. W.: Nitrous Oxide (N<sub>2</sub>O): The Dominant Ozone Depleting Substance Emitted in the 21st Century, *Science*, 326, 123–125, <https://doi.org/10.1126/science.1176985>, 2009.
- Ritz, C., Lliboutry, L., and Rado, C.: Analysis of a 870 m deep temperature profile at Dome C, *Annals of Glaciology*, 3, 284–289, 1982.
- Rohde, R. A., Price, P. B., Bay, R. C., and Bramall, N. E.: In situ microbial metabolism as a cause of gas anomalies in ice, *Proceedings of the National Academy of Sciences*, 105, 8667–8672, <https://doi.org/10.1073/pnas.0803763105>, 2008.
- Röthlisberger, R., Hutterli, M. A., Sommer, S., Wolff, E. W., and Mulvaney, R.: Factors controlling nitrate in ice cores: Evidence from the Dome C deep ice core, *J. Geophys. Res.*, 105, 20565–20572, <https://doi.org/10.1029/2000JD900264>, 2000.

- Rubasinghege, G., Spak, S. N., Stanier, C. O., Carmichael, G. R., and Grassian, V. H.: Abiotic Mechanism for the Formation of Atmospheric Nitrous Oxide from Ammonium Nitrate, *Environ. Sci. Technol.*, **45**, 2691–2697, <https://doi.org/10.1021/es103295v>, 2011.
- 1375 Rubino, M., Etheridge, D. M., Thornton, D. P., Howden, R., Allison, C. E., Francey, R. J., Langenfelds, R. L., Steele, L. P., Trudinger, C. M., Spencer, D. A., Curran, M. A. J., Van Ommen, T. D., and Smith, A. M.: Revised records of atmospheric trace gases CO<sub>2</sub>, CH<sub>4</sub>, N<sub>2</sub>O, and δ<sup>13</sup>C CO<sub>2</sub> over the last 2000 years from Law Dome, Antarctica, *Earth Syst. Sci. Data*, **11**, 473–492, <https://doi.org/10.5194/essd-11-473-2019>, 2019.
- 1380 Ruth, U., Wagenbach, D., Bigler, M., Steffensen, J. P., Röthlisberger, R., and Miller, H.: High-resolution microparticle profiles at NorthGRIP, Greenland: case studies of the calcium dust relationship, *Ann. Glaciol.*, **35**, 237–242, <https://doi.org/10.3189/172756402781817347>, 2002.
- Ruth, U., Wagenbach, D., Steffensen, J. P., and Bigler, M.: Continuous record of microparticle concentration and size distribution in the central Greenland NGRIP ice core during the last glacial period, *J. Geophys. Res.*, **108**, 2002JD002376, <https://doi.org/10.1029/2002JD002376>, 2003.
- 1385 Salamatin, A. N., Lipenkov, V. Y., and Blinov, K. V.: Vostok (Antarctica) climate record time scale deduced from the analysis of a borehole temperature profile, *Annals of Glaciology*, **20**, 207–214, 1994.
- Samarkin, V. A., Madigan, M. T., Bowles, M. W., Casciotti, K. L., Priscu, J. C., McKay, C. P., and Joye, S. B.: Abiotic nitrous oxide emission from the hypersaline Don Juan Pond in Antarctica, *Nature Geosci.*, **3**, 341–344, <https://doi.org/10.1038/ngeo847>, 2010.
- 1390 Schilt, A., Baumgartner, M., Schwander, J., Buiron, D., Capron, E., Chappellaz, J., Loulergue, L., Schüpbach, S., Spahni, R., Fischer, H., and Stocker, T. F.: Atmospheric nitrous oxide during the last 140,000 years, *Earth and Planetary Science Letters*, **300**, 33–43, <https://doi.org/10.1016/j.epsl.2010.09.027>, 2010a.
- Schilt, A., Baumgartner, M., Blunier, T., Schwander, J., Spahni, R., Fischer, H., and Stocker, T. F.: Glacial-interglacial and millennial-scale variations in the atmospheric nitrous oxide concentration during the last 800,000 years, *Quaternary Science Reviews*, **29**, 182–192, <https://doi.org/10.1016/j.quascirev.2009.03.011>, 2010b.
- 1395 Schilt, A., Baumgartner, M., Eicher, O., Chappellaz, J., Schwander, J., Fischer, H., and Stocker, T. F.: The response of atmospheric nitrous oxide to climate variations during the last glacial period, *Geophysical Research Letters*, **40**, 1888–1893, <https://doi.org/10.1002/grl.50380>, 2013.
- 1400 Schilt, A., Brook, E. J., Bauska, T. K., Baggenstos, D., Fischer, H., Joos, F., Petrenko, V. V., Schaefer, H., Schmitt, J., Severinghaus, J. P., Spahni, R., and Stocker, T. F.: Isotopic constraints on marine and terrestrial N<sub>2</sub>O emissions during the last deglaciation, *Nature*, **516**, 234–237, <https://doi.org/10.1038/nature13971>, 2014.
- Schmitt, J., Seth, B., Bock, M., and Fischer, H.: Online technique for isotope and mixing ratios of CH<sub>4</sub>, N<sub>2</sub>O, Xe and mixing ratios of organic trace gases on a single ice core sample, *Atmos. Meas. Tech.*, **7**, 2645–2665, <https://doi.org/10.5194/amt-7-2645-2014>, 2014.

- 1405 Schüpbach, S., Federer, U., Kaufmann, P. R., Albani, S., Barbante, C., Stocker, T. F., and Fischer, H.: Calcium and sodium concentrations of the Talos Dome ice core, Antarctica, <https://doi.org/10.1594/PANGAEA.833044>, 2014.
- Sowers, T.: N<sub>2</sub>O record spanning the penultimate deglaciation from the Vostok ice core, *J. Geophys. Res.*, **106**, 31903–31914, <https://doi.org/10.1029/2000JD900707>, 2001.
- 1410 Spahni, R., Chappellaz, J., Stocker, T. F., Loulergue, L., Hausamann, G., Kawamura, K., Flückiger, J., Schwander, J., Raynaud, D., Masson-Delmotte, V., and Jouzel, J.: Atmospheric Methane and Nitrous Oxide of the Late Pleistocene from Antarctic Ice Cores, *Science*, **310**, 1317–1321, <https://doi.org/10.1126/science.1120132>, 2005.
- Spolaor, A., Vallelonga, P., Gabrieli, J., Cozzi, G., Boutron, C., and Barbante, C.: Determination of Fe<sup>2+</sup> and Fe<sup>3+</sup> species by FIA-CRC-ICP-MS in Antarctic ice samples, *J. Anal. At. Spectrom.*, **27**, 310–317, <https://doi.org/10.1039/C1JA10276A>, 2012.
- 1415 Spolaor, A., Vallelonga, P., Cozzi, G., Gabrieli, J., Varin, C., Kehrwald, N., Zennaro, P., Boutron, C., and Barbante, C.: Iron speciation in aerosol dust influences iron bioavailability over glacial interglacial timescales, *Geophysical Research Letters*, **40**, 1618–1623, <https://doi.org/10.1002/grl.50296>, 2013.
- Spott, O., Russow, R., and Stange, C. F.: Formation of hybrid N<sub>2</sub>O and hybrid N<sub>2</sub> due to codenitrification: First review of a barely considered process of microbially mediated N nitrosation, *Soil Biology and Biochemistry*, **43**, 1995–2011, <https://doi.org/10.1016/j.soilbio.2011.06.014>, 2011.
- 1420 Stauffer, B., Flückiger, J., Monnin, E., Nakazawa, T., and Aoki, S.: Discussion of the reliability of CO<sub>2</sub>, CH<sub>4</sub> and N<sub>2</sub>O records from polar ice cores, *Mem. Natl. Inst. Polar Res.*, **139**–152, 2003.
- Su, Q., Domingo-Félez, C., Jensen, M. M., and Smets, B. F.: Abiotic Nitrous Oxide (N<sub>2</sub>O) Production Is Strongly pH Dependent, but Contributes Little to Overall N<sub>2</sub>O Emissions in Biological Nitrogen Removal Systems, *Environ. Sci. Technol.*, **53**, 3508–3516, <https://doi.org/10.1021/acs.est.8b06193>, 2019.
- 1425 Sutka, R. L., Ostrom, N. E., Ostrom, P. H., Gandhi, H., and Breznak, J. A.: Nitrogen isotopomer site preference of N<sub>2</sub>O produced by *Nitrosomonas europaea* and *Methylococcus capsulatus* Bath, *Rapid Comm Mass Spectrometry*, **17**, 738–745, <https://doi.org/10.1002/rem.968>, 2003.
- Sutka, R. L., Ostrom, N. E., Ostrom, P. H., Breznak, J. A., Gandhi, H., Pitt, A. J., and Li, F.: Distinguishing Nitrous Oxide Production from Nitrification and Denitrification on the Basis of Isotopomer Abundances, *Appl Environ Microbiol*, **72**, 638–644, <https://doi.org/10.1128/AEM.72.1.638-644.2006>, 2006.
- 1430 Tarasov, L. and Peltier, W. R.: Greenland glacial history, borehole constraints, and Eemian extent, *J. Geophys. Res.*, **108**, 2001JB001731, <https://doi.org/10.1029/2001JB001731>, 2003.
- Tian, H., Xu, R., Canadell, J. G., Thompson, R. L., Winiwarter, W., Suntharalingam, P., Davidson, E. A., Ciais, P., Jackson, R. B., Janssens Maenhout, G., Prather, M. J., Regnier, P., Pan, N., Pan, S., Peters, G. P., Shi, H., Tubiello, F. N., Zaehle, S., Zhou, F., Arneeth, A., Battaglia, G., Berthet, S., Bopp, L., Bouwman, A. F., Buitenhuis, E. T., Chang, J., Chipperfield, M. P., Dangal, S. R. S., Dlugokenky, E., Elkins, J. W., Eyre, B. D., Fu, B., Hall, B., Ito, A., Joos, F., Krummel, P. B., Landolfi, A., Laruelle, G. G., Lauerwald, R., Li, W., Lienert, S., Maavara, T., MacLeod, M., Millet, D. B., Olin, S., Patra, P. K., Prinn, R.

- 1440 G., Raymond, P. A., Ruiz, D. J., van der Werf, G. R., Vuichard, N., Wang, J., Weiss, R. F., Wells, K. C., Wilson, C., Yang, J., and Yao, Y.: A comprehensive quantification of global nitrous oxide sources and sinks, *Nature*, 586, 248–256, <https://doi.org/10.1038/s41586-020-2780-0>, 2020.
- Tischer, J., Zopfi, J., Frey, C., Magyar, P. M., Brand, A., Oswald, K., Jegge, C., Frame, C. H., Mirale, M. R., Sòria-Perpinyà, X., Vicente, E., and Lehmann, M. F.: Isotopic signatures of biotic and abiotic  $\text{N}_2\text{O}$  production and consumption in the water column of meromictic, ferruginous Lake La Cruz (Spain), *Limnology & Oceanography*, 67, 1760–1775, <https://doi.org/10.1002/lno.12165>, 2022.
- 1445 Toyoda, S., Yoshida, N., Miwa, T., Matsui, Y., Yamagishi, H., Tsunogai, U., Nojiri, Y., and Tsurushima, N.: Production mechanism and global budget of  $\text{N}_2\text{O}$  inferred from its isotopomers in the western North Pacific, *Geophysical Research Letters*, 29, <https://doi.org/10.1029/2001GL014311>, 2002.
- Toyoda, S., Mutobe, H., Yamagishi, H., Yoshida, N., and Tanji, Y.: Fractionation of  $\text{N}_2\text{O}$  isotopomers during production by denitrifier, *Soil Biology and Biochemistry*, 37, 1535–1545, <https://doi.org/10.1016/j.soilbio.2005.01.009>, 2005.
- 1450 Toyoda, S., Yoshida, N., and Koba, K.: Isotopocule analysis of biologically produced nitrous oxide in various environments, *Mass Spectrometry Reviews*, 36, 135–160, <https://doi.org/10.1002/mas.21459>, 2017.
- Wilhelms, F., Sheldon, S. G., Hamann, I., and Kipfstuhl, S.: Implications for and findings from deep ice core drillings an example: The ultimate tensile strength of ice at high strain rates, *Physics and Chemistry of Ice (The proceedings of the International Conference on the Physics and Chemistry of Ice held at Bremerhaven, Germany on 23–28 July 2006)* The Royal Society of Chemistry Special Publication No. 311, 635–639, 2007.
- 1455 Wolff, E. W., Moore, J. C., Clausen, H. B., and Hammer, C. U.: Climatic implications of background acidity and other chemistry derived from electrical studies of the Greenland Ice Core Project ice core, *J. Geophys. Res.*, 102, 26325–26332, <https://doi.org/10.1029/96JC02223>, 1997.
- Wrage Mönning, N., Horn, M. A., Well, R., Müller, C., Velthof, G., and Oenema, O.: The role of nitrifier denitrification in the production of nitrous oxide revisited, *Soil Biology and Biochemistry*, 123, A3–A16, <https://doi.org/10.1016/j.soilbio.2018.03.020>, 2018.
- 1460 York, D., Evensen, N. M., Martínez, M. L., and De Basabe Delgado, J.: Unified equations for the slope, intercept, and standard errors of the best straight line, *American Journal of Physics*, 72, 367–375, <https://doi.org/10.1119/1.1632486>, 2004.
- Zhu Barker, X., Cavazos, A. R., Ostrom, N. E., Horwath, W. R., and Glass, J. B.: The importance of abiotic reactions for nitrous oxide production, *Biogeochemistry*, 126, 251–267, <https://doi.org/10.1007/s10533-015-0166-4>, 2015.
- 1465